Eur. Phys. J. C (2022) 82:717
https://doi.org/10.1140/epjc/s10052-022-10588-3

THE EUROPEAN PHYSICAL JOURNAL C

Regular Article - Experimental Physics

Direct constraint on the Higgs–charm coupling from a search for Higgs boson decays into charm quarks with the ATLAS detector

ATLAS Collaboration[⋆]

CERN, 1211 Geneva 23, Switzerland

Received: 28 January 2022 / Accepted: 6 July 2022

Abstract A search for the Higgs boson decaying into a pair of charm quarks is presented. The analysis uses proton–proton collisions to target the production of a Higgs boson in association with a leptonically decaying W or Z boson. The dataset delivered by the LHC at a centre-of-mass energy of $\sqrt{s} = 13$ TeV and recorded by the ATLAS detector corresponds to an integrated luminosity of 139 fb^{-1}. Flavour-tagging algorithms are used to identify jets originating from the hadronisation of charm quarks. The analysis method is validated with the simultaneous measurement of WW, WZ and ZZ production, with observed (expected) significances of 2.6 (2.2) standard deviations above the background-only prediction for the $(W/Z)Z(\to c\bar{c})$ process and 3.8 (4.6) standard deviations for the $(W/Z)W(\to cq)$ process. The $(W/Z)H(\to c\bar{c})$ search yields an observed (expected) upper limit of 26 (31) times the predicted Standard Model cross-section times branching fraction for a Higgs boson with a mass of 125 GeV, corresponding to an observed (expected) constraint on the charm Yukawa coupling modifier $|\kappa_c| < 8.5$ (12.4), at the 95% confidence level. A combination with the ATLAS $(W/Z)H$, $H \to b\bar{b}$ analysis is performed, allowing the ratio κ_c/κ_b to be constrained to less than 4.5 at the 95% confidence level, smaller than the ratio of the b- and c-quark masses, and therefore determines the Higgs-charm coupling to be weaker than the Higgs-bottom coupling at the 95% confidence level.

1 Introduction

Since the discovery of a new particle, H, with a mass of approximately 125 GeV by the ATLAS [1] and CMS [2] collaborations at the LHC [3], studies of its properties have indicated that it is consistent with the Standard Model (SM) Higgs boson [4–7]. The interactions between the Higgs boson and the charged fermions of the third generation have been observed by both the ATLAS [8–10] and CMS [11–13] collaborations, and CMS has reported evidence for the decay of the Higgs boson into a pair of muons [14], while ATLAS reported a 2σ excess over the background-only prediction [15]. Direct searches by the ATLAS and CMS collaborations for Higgs boson decays into a charm quark–antiquark pair, $H \to c\bar{c}$ [16,17], decays into an electron–positron pair [18,19], exclusive decays into mesons [20–25], and reinterpretations of the Higgs p_{T} spectrum [26,27], have not yet found experimental evidence for Higgs boson couplings to the first-generation fermions or second-generation quarks. Taken together, the results of these measurements and searches are consistent with the prediction that the coupling strength of the Higgs boson to each fermion scales proportionally to the fermion's mass.

In the SM the branching fraction of $H \to c\bar{c}$ is 2.89% [28], approximately 20 times smaller than the branching fraction of the Higgs boson to a bottom quark–antiquark pair, $H \to b\bar{b}$. Physics beyond the Standard Model can significantly enhance or reduce the coupling of the Higgs boson to the charm quark, and in turn the $H \to c\bar{c}$ branching fraction [29–35]. Direct searches for $H \to c\bar{c}$ in proton–proton (pp) collisions have set upper limits on the cross-section times branching fraction for the production of a W or Z boson in association with a Higgs boson decaying into $c\bar{c}$. The ATLAS Collaboration has performed a search in the $Z(\to \ell\ell)H(\to c\bar{c})$ channel, where $\ell = e, \mu$, using 36.1 fb^{-1} of pp collision data recorded at $\sqrt{s} = 13$ TeV [16], setting an observed (expected) upper limit at 110 (150) times the SM prediction, at 95% confidence level (CL). The CMS Collaboration has also performed a search using 35.9 fb^{-1} of pp collision data recorded at 13 TeV [17]; the search was conducted in three channels based on the number of charged leptons, namely the 0-, 1- and 2-lepton channels, targeting the $ZH \to \nu\nu c\bar{c}$, $WH \to \ell\nu c\bar{c}$ and $ZH \to \ell\ell c\bar{c}$ signatures, respectively. These were combined to set an observed (expected) upper limit of 70 (37) times the SM prediction, at 95% CL.

This paper presents a new search for $VH(\to c\bar{c})$, where $V = W$ or Z, using 139 fb^{-1} of pp collision data collected at a centre-of-mass energy of 13 TeV by the ATLAS detec-

⋆ e-mail: atlas.publications@cern.ch

Published online: 18 August 2022

tor from 2015 to 2018. Events are selected in the 0-, 1- and 2-lepton channels and are categorised according to the transverse momentum, p_{T}, of the vector boson and the number of jets.

Higgs boson candidates are constructed from the two jets with the highest p_{T}. One of the main challenges in searching for $H \to c\bar{c}$ is to recognise jets originating from the hadronisation of charm quarks. To identify these jets, a multivariate charm-jet tagging algorithm is used. Additionally, a bottom-jet identification algorithm is used to veto bottom jets, ensuring this analysis is orthogonal to the recent ATLAS $VH(\to b\bar{b})$ measurement [36]. Events are selected if one or both of the two highest-p_{T} jets are c-tagged.

In order to search for the $H \to c\bar{c}$ signal the distributions of the dijet invariant mass, m_{cc}, in all event categories are used simultaneously in a binned maximum-likelihood fit, which allows the signal yield and the main background normalisations to be extracted. The analysis strategy is validated by the simultaneous measurement of the diboson processes in which one of the bosons decays to at least one charm quark, $VW(\to cq)$ and $VZ(\to c\bar{c})$, where q is a down-type quark. The result is interpreted in the kappa framework [37,38] in terms of κ_c, the modifier of the coupling between the Higgs boson and the charm quark. The analysis is combined with the ATLAS VH, $H \to b\bar{b}$ measurement [36] and the results are interpreted in the kappa framework in terms of both κ_b and κ_c, and in terms of the ratio κ_c/κ_b.

2 ATLAS detector

The ATLAS experiment [39] at the LHC is a multipurpose particle detector with a forward–backward symmetric cylindrical geometry and a near 4π coverage in solid angle.[1] It consists of an inner tracking detector (ID) surrounded by a thin superconducting solenoid providing a 2T axial magnetic field, electromagnetic and hadron calorimeters, and a muon spectrometer. The inner tracking detector covers the pseudorapidity range $|\eta| < 2.5$. It consists of silicon pixel, silicon microstrip, and transition radiation tracking detectors. Lead/liquid-argon (LAr) sampling calorimeters provide electromagnetic (EM) energy measurements with high granularity. A steel/scintillator-tile hadron calorimeter covers the central pseudorapidity range ($|\eta| < 1.7$). The endcap and forward regions are instrumented with LAr calorimeters for both the EM and hadronic energy measurements up to $|\eta| = 4.9$. The muon spectrometer surrounds the calorimeters and is based on three large superconducting air-core toroidal magnets with eight coils each. The field integral of the toroids ranges between 2.0 and 6.0 T m across most of the detector. The muon spectrometer includes a system of precision chambers for tracking and fast detectors for triggering. A two-level trigger system is used to select events. The first-level trigger is implemented in hardware and uses a subset of the detector information to accept events at a rate below 100 kHz [40]. This is followed by a software-based trigger that reduces the accepted event rate to 1kHz on average depending on the data-taking conditions. An extensive software suite [41] is used in the reconstruction and analysis of real and simulated data, in detector operations, and in the trigger and data acquisition systems of the experiment.

[1] ATLAS uses a right-handed coordinate system with its origin at the nominal interaction point (IP) in the centre of the detector and the z-axis along the beam pipe. The x-axis points from the IP to the centre of the LHC ring, and the y-axis points upwards. Cylindrical coordinates (r, ϕ) are used in the transverse plane, ϕ being the azimuthal angle around the z-axis. The pseudorapidity is defined in terms of the polar angle θ as $\eta = -\ln\tan(\theta/2)$. Angular distance is measured in units of $\Delta R \equiv \sqrt{(\Delta\eta)^2 + (\Delta\phi)^2}$.

3 Dataset and simulated event samples

This analysis uses data recorded by the ATLAS detector during Run 2 of the LHC, which took place from 2015 to 2018 at a centre-of-mass energy of 13 TeV. Data were collected using a combination of missing transverse momentum triggers [42], in the 0- and 1-lepton channels, and single-lepton triggers [43,44], in the 1- and 2-lepton channels. Events are required to be of good quality and recorded while all relevant detector components were in operation [45]. The dataset corresponds to an integrated luminosity of 139.0 ± 2.4 fb^{-1} [46].

The Monte Carlo (MC) simulation samples used in this analysis are largely the same as those used in the ATLAS $VH(\to b\bar{b})$ analysis [36], and are summarised in Table 1. Samples of simulated events were generated for VH production with a Higgs boson mass, m_H, of 125 GeV, for both $H \to c\bar{c}$ and $H \to b\bar{b}$ decays, with branching fractions of 2.89% and 58.2%, respectively, and for the main background processes ($t\bar{t}$, single-top, $V+$jets and diboson). The samples are used to optimise the analysis and perform the statistical analysis of the data.

The background from multi-jet events is negligible in the 0- and 2-lepton channels after applying the selection criteria detailed in Sect. 4. In the 1-lepton channel, it is estimated using a data-driven method. All samples of simulated events are initially normalised to the most accurate theoretical cross-section predictions currently available. Samples produced using alternative event generators are used to assess systematic uncertainties in the modelling of the signal and background processes, and are discussed in Sect. 5.

All samples of MC events were passed through the ATLAS detector response simulation [47] based on GEANT4 [48] and were reconstructed with the same algorithms as used for data. The effect of multiple interactions in the same and neighbour-

Table 1 Signal and background processes and their corresponding MC generators used in this analysis. The acronyms ME and PS stand for matrix element and parton shower, respectively. The cross-section order refers to the order of the cross-section calculation used for process normalisation in QCD, unless otherwise stated, with ((N)NLO and ((N)NLL standing for ((next-to-)next-to-)leading order and ((next-to-)next-to-)leading log, respectively

Process	ME generator	ME PDF	PS and hadronisation	Tune	Cross-section order
$qq \to VH\ (H \to c\bar{c}/b\bar{b})$	Powheg Boxv2 [56,57] + GoSam[66] + MiNLO [67,68]	NNPDF3.0nlo [58]	PYTHIA8.212 [59]	AZNLO [60]	NNLO(QCD)+NLO(EW) [61–65]
$gg \to ZH$ $(H \to c\bar{c}/b\bar{b})$	Powheg Boxv2	NNPDF3.0nlo	PYTHIA8.212	AZNLO	NLO+NLL [69,70]
$t\bar{t}$	Powheg Boxv2 [71]	NNPDF3.0nlo	PYTHIA8.230	A14 [72]	NNLO +NNLL [73–79]
t/s-channel single top	Powheg Boxv2 [80]	NNPDF3.0nlo	PYTHIA8.230	A14	NLO [81,82]
Wt-channel single top	Powheg Boxv2 [83]	NNPDF3.0nlo	PYTHIA8.230	A14	Approx. NNLO [84,85]
V+jets	Sherpa2.2.1 [53–55]	NNPDF3.0nnlo [58]	Sherpa2.2.1	Default	NNLO [86]
$qq \to VV$	Sherpa2.2.1	NNPDF3.0nnlo	Sherpa2.2.1	Default	NLO
$gg \to VV$	Sherpa2.2.2	NNPDF3.0nnlo	Sherpa2.2.2	Default	NLO

ing bunch crossings (pile-up) was modelled by overlaying the simulated hard-scattering event with inelastic pp events generated with PYTHIA8.186 [49] using the NNPDF2.3lo set of parton distribution functions (PDF) [50] and the A3 set of tuned parameters (A3 tune) [51]. The simulated events were weighted to reproduce the distribution of the average number of interactions per bunch crossing seen in data. The EvtGen1.6.0 program [52] was used to describe the decays of bottom and charm hadrons in all samples, except those generated with Sherpa [53–55].

4 Object and event selection

4.1 Object selection

Interaction vertices are reconstructed from tracks in the ID. The vertex with the highest sum of squared transverse momenta of associated tracks is used as the primary vertex [87].

Electrons are reconstructed by matching ID tracks with energy clusters in the EM calorimeter [88]. Electrons are required to have $p_{\mathrm{T}} > 7$ GeV and $|\eta| < 2.47$. They must satisfy the *loose* identification criterion, based on a likelihood discriminant combining observables related to the shower shape in the calorimeter and to the track matching the energy cluster, and are required to be isolated in both the ID and calorimeter using p_{T}-dependent criteria. In the 1-lepton channel, more stringent requirements are placed on the identification and isolation of electrons. These electrons, called *tight* electrons, are required to satisfy the *tight* likelihood criterion and a stricter calorimeter-based isolation.

Muons are reconstructed within the acceptance of the muon spectrometer, $|\eta| < 2.7$ [89]. They are required to have $p_{\mathrm{T}} > 7$ GeV, to satisfy the *loose* identification criteria and to be isolated in the ID using p_{T}-dependent criteria. As with electrons, in the 1-lepton channel more stringent requirements are placed on the identification and isolation of muons. These muons, called *tight* muons, must satisfy the *medium* identification criteria and a stricter track-based isolation, and have $|\eta| < 2.5$.

Hadronically decaying τ-leptons [90,91], identified with a *medium* quality criterion [91], are required to have $p_{\mathrm{T}} > 20$ GeV and $|\eta| < 2.5$, excluding the transition region of $1.37 < |\eta| < 1.52$ between the barrel and endcap sections of the electromagnetic calorimeter. Reconstructed τ-leptons are not directly used in the event selection, but are used in the calculation of missing transverse momentum and to avoid double-counting reconstructed τ-leptons as other objects.

Jets are reconstructed from topological clusters of energy deposits in the calorimeter [92–94] by using the anti-k_t algorithm [95,96] with a radius parameter of $R = 0.4$. The jets are classified as *central* or *forward* jets depending on their

pseudorapidity. Jets are classified as forward jets if they have $2.5 < |\eta| < 4.5$ and $p_{\mathrm{T}} > 30$ GeV. Jets are classified as central jets if they have $p_{\mathrm{T}} > 20$ GeV and $|\eta| < 2.5$. Additionally, central jets with $p_{\mathrm{T}} < 120$ GeV are required to be identified as originating from the primary vertex using a jet-vertex tagging algorithm [97]. To improve the measurement of each jet's energy and direction, and consequently the measurement of m_{cc}, if any muons are found within a cone of jet-p_{T}-dependent size around the jet axis, the four-momentum of the muon closest to the jet is added to the jet four-momentum, following the procedure described in Ref. [36]. An overlap removal procedure is applied to avoid double-counting between electrons, muons, hadronically decaying τ-leptons and jets.

Central jets are tagged as containing either b- or c-hadrons using two discriminants resulting from multivariate tagging algorithms, MV2 and DL1 [98]. Jets are b-tagged using the MV2 discriminant, configured to select b-jets with 70% efficiency in simulated $t\bar{t}$ events. A c-tagging configuration of the DL1 discriminant, $\mathrm{DL1_c}$, was optimised for this analysis, and includes a veto on jets b-tagged by the MV2 algorithm. This configuration gives an average efficiency of 27% to tag c-jets in simulated $t\bar{t}$ events, and b- and light-jet misidentification rates of 8% and 1.6%, respectively. The efficiencies in simulation are calibrated to match those in data using control samples of $t\bar{t}$ and Z+jets events with a precision of 5%–10%, using methods identical to those applied to b-tagging algorithms [98–100]. Jets in simulated events are labelled using information from the MC generator's event 'truth' record, exclusively as b-, c-, or τ-jets, in this order, according to whether they contain a b-hadron, c-hadron, or τ-lepton with $p_{\mathrm{T}} > 5$ GeV within a cone of size $\Delta R = 0.3$ around their axis. Jets not labelled as b-, c- or τ-jets are labelled as light jets. Diboson, V+jets and top-quark backgrounds are classified according to the flavour labels of the jets that form the Higgs boson candidate in those selected events.

To maximise the statistical power of the available MC samples, the c-tagging requirement is not applied to the diboson, V+jets or top-quark samples. Instead, events are weighted by the probabilities for each jet to be c-tagged, based on its flavour label and as a function of the jet p_{T} and $|\eta|$, to obtain predictions for events with either one or two c-tagged jets. This is referred to as *truth-flavour tagging* since it uses information from the MC generator's event 'truth' record. In the V+jets samples, differences of up to 20% are observed between the two methods and are corrected for by weights assigned to each jet, dependent on the ΔR to the closest other jet and on the flavour labels of the jet and the closest other jet. Finally, to correct for any residual non-closure in the truth-flavour tagging procedure, small normalisation corrections are applied to the diboson, V+jets and top-quark predictions such that the number of events for each process in each analysis region (defined in Sect. 4.2) matches that obtained when directly applying c-tagging. These normalisation corrections vary between 0.9 and 1.05.

The missing transverse momentum, $\boldsymbol{E}_{\mathbf{T}}^{\mathbf{miss}}$ is reconstructed as the negative of the vector sum of the transverse momenta of electrons, muons, hadronically decaying τ-leptons, jets, and a 'soft term' which is constructed from tracks associated with the primary vertex but not with any reconstructed object [101]. The magnitude of the $\boldsymbol{E}_{\mathbf{T}}^{\mathbf{miss}}$ is referred to as $E_{\mathrm{T}}^{\mathrm{miss}}$. The track-based missing transverse momentum, $\boldsymbol{p}_{\mathbf{T}}^{\mathbf{miss}}$, is constructed using all ID tracks associated with the primary vertex and satisfying the quality criteria detailed in Ref. [102], with its magnitude denoted by $p_{\mathrm{T}}^{\mathrm{miss}}$.

4.2 Event selection and categorisation

Events are categorised into 0-, 1- and 2-lepton channels based on the number of *loose* electrons and muons they contain. Events with at least two central jets are selected, and they are further categorised as 2- or 3-jet events according to the total number of jets. Events with more than three jets are rejected in the 0- and 1-lepton channels to reduce the $t\bar{t}$ background. In the 2-lepton channel, events with more than three jets are included in the 3-jet category.

Since the signal-to-background ratio increases for large transverse momentum of the vector boson, p_{T}^{V}, events with reconstructed $p_{\mathrm{T}}^{V} > 75$ GeV are selected [103]. Two p_{T}^{V} regions are used: $75\ \mathrm{GeV} < p_{\mathrm{T}}^{V} < 150$ GeV (only in the 2-lepton channel) and $p_{\mathrm{T}}^{V} > 150$ GeV. The p_{T}^{V} corresponds to $E_{\mathrm{T}}^{\mathrm{miss}}$ in the 0-lepton channel, the magnitude of the vector sum of the $\boldsymbol{E}_{\mathbf{T}}^{\mathbf{miss}}$ and the lepton $\boldsymbol{p}_{\mathbf{T}}$ in the 1-lepton channel, and the magnitude of the vector sum of the two lepton transverse momenta in the 2-lepton channel.

The main discriminating variable in this analysis is the invariant mass, m_{cc}, of the two central jets with the highest p_{T}, hereafter referred to as *signal* jets. At least one signal jet must have $p_{\mathrm{T}} > 45$ GeV. *Signal regions* are composed of events in which one or both of these jets are c-tagged, with the two cases defining separate categories, referred to as 1-c-tag and 2-c-tag, respectively. Furthermore, any additional non-signal jet must *not* be b-tagged. This requirement means that events in the signal regions can contain at most one b-tagged jet. Combined with an identical jet selection, this ensures that selected events are orthogonal to those selected in the ATLAS $VH(\rightarrow b\bar{b})$ analysis [36]. Events selected in the control regions are not completely orthogonal with those selected in the $VH(\rightarrow b\bar{b})$ analysis, and the impact of this is discussed in Sect. 7. In total, 16 signal regions are defined, arising from the combination of three lepton channels, two p_{T}^{V} categories (in the 2-lepton channel), two number-of-jets categories and two number-of-c-tagged-jets categories.

To reduce the background contamination in all channels, the ΔR between the two signal jets is required to be $\Delta R < 2.3$ in events with $75 < p_{\mathrm{T}}^{V} < 150$ GeV, $\Delta R < 1.6$ in

events with $150 < p_{\mathrm{T}}^{V} < 250$ GeV and $\Delta R < 1.2$ in events with $p_{\mathrm{T}}^{V} > 250$ GeV. The ΔR selection criteria, optimised for each p_{T}^{V} range, are approximately 80% efficient for signal events. For each signal region, a corresponding control region is defined as containing events failing the ΔR selection, up to a maximum ΔR of 2.5. These control regions, hereafter referred to as the high-ΔR control regions, are designed to constrain the $V+$jets background normalisations and shapes.

In addition to the high-ΔR control regions, further control regions are defined to constrain the modelling of the most important other background processes. Top control regions, enriched in $t\bar{t}$ and single-top events, are defined in all lepton channels. In the 0- and 1-lepton channels, events with three jets are selected, and in these events exactly one of the signal jets is c-tagged and the non-signal jet is b-tagged, resulting in one control region for each of these lepton channels. In the 2-lepton channel a pure sample of $t\bar{t}$ events is selected by requiring the two leptons to have different flavours ($e\mu$) and opposite electric charges. One control region is defined for each number-of-jets category and p_{T}^{V} region combination, resulting in a total of four 2-lepton top control regions, each containing exactly one c-tagged jet.

Finally, in the 1- and 2-lepton channels, events in which neither of the two signal jets are c-tagged and no non-signal jets are b-tagged are used to constrain the normalisation of the $V+$light-jets backgrounds. One control region is defined for each number-of-jets category and p_{T}^{V} region combination, for a total of six 0-c-tag control regions.

A total of 44 analysis regions are defined: 16 signal regions, 16 high-ΔR control regions, 6 top control regions and 6 0-c-tag control regions. The signal-region selection criteria specific to each channel are described below, and summarised in Table 2.

Table 2 Summary of the signal region event selection in the 0-, 1- and 2-lepton channels. Jet1 and jet2 refer to the two signal jets and H refers to the jet1–jet2 system

Common selections	
Central jets	≥ 2
Signal jet p_{T}	≥ 1 signal jet with $p_{\mathrm{T}} > 45$ GeV
c-jets	One or two c-tagged signal jets
b-jets	No b-tagged non-signal jets
Jets	2, 3 (0- and 1-lepton); 2, ≥ 3 (2-lepton)
p_{T}^{V} regions	75–150 GeV (2-lepton)
	> 150 GeV
ΔR(**jet1**, **jet2**)	$75 < p_{\mathrm{T}}^{V} < 150$ GeV: $\Delta R \leq 2.3$
	$150 < p_{\mathrm{T}}^{V} < 250$ GeV: $\Delta R \leq 1.6$
	$p_{\mathrm{T}}^{V} > 250$ GeV: $\Delta R \leq 1.2$
0-lepton channel	
Trigger	$E_{\mathrm{T}}^{\mathrm{miss}}$
Leptons	No *loose* leptons
$E_{\mathrm{T}}^{\mathrm{miss}}$	> 150 GeV
$p_{\mathrm{T}}^{\mathrm{miss}}$	> 30 GeV
H_{T}	> 120 GeV (2 jets), > 150 GeV (3 jets)
$\min \lvert\Delta\phi(\mathbf{E_T^{miss}}, \mathbf{jet})\rvert$	$> 20°$ (2 jets), $> 30°$ (3 jets)
$\lvert\Delta\phi(\mathbf{E_T^{miss}}, \mathbf{H})\rvert$	$> 120°$
$\lvert\Delta\phi(\mathbf{jet1}, \mathbf{jet2})\rvert$	$< 140°$
$\lvert\Delta\phi(\mathbf{E_T^{miss}}, \mathbf{p_T^{miss}})\rvert$	$< 90°$
1-lepton channel	
Trigger	e sub-channel: single electron
	μ sub-channel: $E_{\mathrm{T}}^{\mathrm{miss}}$
Leptons	One *tight* lepton and no additional *loose* leptons
$E_{\mathrm{T}}^{\mathrm{miss}}$	> 30 GeV (e sub-channel)
m_{T}^{W}	< 120 GeV
2-lepton channel	
Trigger	Single lepton
Leptons	Exactly two *loose* leptons
	Same flavour, opposite charge for $\mu\mu$
$m_{\ell\ell}$	$81 < m_{\ell\ell} < 101$ GeV

0-lepton channel Data were collected using $E_{\mathrm{T}}^{\mathrm{miss}}$ triggers with thresholds ranging from 70 GeV in 2015 to 110 GeV in 2018 [42]. Events must not contain any *loose* electrons or muons, and are required to have $E_{\mathrm{T}}^{\mathrm{miss}} > 150$ GeV. At 150 GeV the $E_{\mathrm{T}}^{\mathrm{miss}}$ triggers are approximately 75–90% efficient, depending on the year, reaching a full efficiency plateau at about 200 GeV. A requirement on the scalar sum of jet transverse momenta, H_{T}, of 120 (150) GeV in 2-jet (3-jet) events is imposed to remove a small region of phase space where the trigger efficiency depends on the number of jets. To remove non-collision backgrounds, $p_{\mathrm{T}}^{\mathrm{miss}}$ is required to exceed 30 GeV. Background multi-jet events with high $E_{\mathrm{T}}^{\mathrm{miss}}$ typically arise from mismeasured jet energies in the calorimeter and can be rejected using angular separation requirements (detailed in Table 2) between the jets, $\boldsymbol{E}_{\mathbf{T}}^{\mathbf{miss}}$ and $\boldsymbol{p}_{\mathbf{T}}^{\mathbf{miss}}$.

1-lepton channel Events must contain exactly one *loose* lepton, that is then required to also be *tight*. If the lepton is an electron (muon), it must have $p_{\mathrm{T}} > 27$ (25) GeV and $|\eta| < 2.47$ (2.5). In the muon sub-channel, data were collected with the same $E_{\mathrm{T}}^{\mathrm{miss}}$ triggers as in the 0-lepton channel. The online $E_{\mathrm{T}}^{\mathrm{miss}}$ calculation does not include muons, so these triggers effectively select on p_{T}^{V} and perform more efficiently than single-muon triggers in the analysis phase space. In the electron sub-channel, single-electron triggers were used to collect data with thresholds starting at 24 GeV for data collected in 2015 and 26 GeV for data collected between 2016 and 2018 [43]. In the electron sub-channel, there is a significant background from events with jets misidentified as electrons at low $E_{\mathrm{T}}^{\mathrm{miss}}$. These events are rejected by requiring $E_{\mathrm{T}}^{\mathrm{miss}} > 30$ GeV. The transverse mass of the

reconstructed W boson,[2] m_{T}^{W}, is required to be less than 120 GeV. The number of multi-jet background events that survive the 1-lepton channel event selection is estimated in each analysis region by performing a template fit to the m_{T}^{W} distribution, which offers good discrimination between multi-jet and simulated backgrounds. The multi-jet m_{T}^{W} templates are extracted from control regions defined by inverting the tight isolation requirements on the leptons, after subtraction of the simulated backgrounds. The shapes of the multi-jet m_{cc} distributions are obtained using the same procedure. More details of the template-fit method can be found in Ref. [9].

2-lepton channel The 2-lepton channel must contain exactly two same-flavour *loose* leptons. At least one of the leptons must have $p_{\mathrm{T}} > 27$ GeV to be consistent with the online single-lepton trigger selection. In the dimuon case, they must have opposite electric charges. This requirement is not imposed in the dielectron subchannel due to a higher probability of charge misidentification. The invariant mass of the two leptons, $m_{\ell\ell}$, is required to be consistent with the mass of the Z boson, $81 < m_{\ell\ell} < 101$ GeV.

Following the event selection, the Z + jets, W + jets and $t\bar{t}$ processes constitute the main backgrounds in the 0-lepton channel. In the 1-lepton channel, the main backgrounds arise from the W + jets and $t\bar{t}$ processes. For both the 0- and 1-lepton channels, the relative background composition depends substantially on the analysis region. In the 2-lepton channel the main background is Z + jets in all regions. The efficiency to select the $VH(\rightarrow c\bar{c})$ signal, in which the V decays to leptons, is $\approx$ 1–2%, and the expected signal-to-background ratio in the mass range 100 GeV $< m_{cc} <$ 150 GeV is (1–7) $\times 10^{-4}$ in the 1-c-tag signal regions and (0.6–8) $\times 10^{-3}$ in the 2-c-tag signal regions.

5 Systematic uncertainties

The sources of systematic uncertainties affecting this analysis can be broadly divided into two groups: those related to experimental effects and those due to the theoretical modelling of signal and background processes. The estimation of these uncertainties closely follows the procedures outlined in Ref. [36].

5.1 Experimental uncertainties

The leading experimental uncertainties in this analysis are due to imperfect calibration of the c-tagging efficiency, jet energy scales and jet energy resolutions. Correction factors for c- and b-tagging are determined from the difference between tagging efficiencies in data and simulation and are derived separately for c-jets, b-jets and light-flavour jets [98–100]. The uncertainties in the correction factors originate from multiple sources and are decomposed into independent components that are correlated between different analysis regions. Two additional uncertainties are included in MC samples where truth-flavour tagging, described in Sect. 4, is used. An uncertainty is included in the V+jets samples, equal to the ΔR correction that is applied to improve agreement between the truth-tagged and direct-tagged simulation samples, and for each MC prediction an uncertainty is included in the overall normalisation correction between direct and truth-flavour tagging.

The uncertainties in the calibration of jet energy scales and resolutions are estimated from multiple measurements [92]. Uncertainties in the jet energy scale and resolution are combined into independent components that are correlated between different analysis regions. An additional uncertainty in the calibration of b- and c-jets is also included.

Uncertainties in the reconstruction, identification, isolation and trigger efficiencies of electrons and muons, and the uncertainties in their energy scale and resolution, have been measured in data and found to be negligible compared to other uncertainties [88,89]. These uncertainties, along with the jet energy scale and resolution uncertainties, are propagated to the calculation of $E_{\mathrm{T}}^{\mathrm{miss}}$ following the method described in Ref. [36]. The $E_{\mathrm{T}}^{\mathrm{miss}}$ calculation has additional uncertainties associated with the p_{T} scale, p_{T} resolution and reconstruction efficiency of the tracks used to build the $E_{\mathrm{T}}^{\mathrm{miss}}$ soft term, and with the modelling of the underlying event [101]. An uncertainty in the $E_{\mathrm{T}}^{\mathrm{miss}}$ trigger efficiency is also included.

The uncertainty in the combined 2015–2018 integrated luminosity is 1.7% [46], obtained using the LUCID-2 detector [104] for the primary luminosity measurements. The average number of interactions per bunch-crossing in simulation is scaled by 1.03 to improve agreement with data, with an uncertainty corresponding to the full size of the correction (±3%).

5.2 Signal and background modelling uncertainties

Modelling uncertainties are evaluated using samples of simulated events. For each process, four categories of uncertainty are considered: cross-section and acceptance uncertainties, which account for the overall normalisation of backgrounds that are not allowed to float freely in the global like-

[2] $m_{\mathrm{T}}^{W} = \sqrt{2p_{\mathrm{T}}^{\ell}p_{\mathrm{T}}^{\nu}(1-\cos(\phi^{\ell}-\phi^{\nu}))}$, where $\boldsymbol{E}_{\mathbf{T}}^{\mathbf{miss}}$ is used as an approximation for $\boldsymbol{p}_{\mathbf{T}}^{\boldsymbol{\nu}}$.

Table 3 Summary of the background modelling systematic uncertainties considered

VH($\rightarrow b\bar{b}$)	
$WH(\rightarrow b\bar{b})$ normalisation	27%
$ZH(\rightarrow b\bar{b})$ normalisation	25%
Diboson	
$WW/ZZ/WZ$ acceptance	10%/5%/12%
p_{T}^{V} acceptance	4%
N_{jet} acceptance	7%–11%
Z + jets	
$Z+hf$ normalisation	Floating
$Z+mf$ normalisation	Floating
$Z+lf$ normalisation	Floating
$Z+bb$ to $Z+cc$ ratio	20%
$Z+bl$ to $Z+cl$ ratio	18%
$Z+bc$ to $Z+cl$ ratio	6%
p_{T}^{V} acceptance	1%–8%
N_{jet} acceptance	10%–37%
High-ΔR CR to SR	12%–37%
0- to 2-lepton ratio	4%–5%
W4+jets	
$W+hf$ normalisation	Floating
$W+mf$ normalisation	Floating
$W+lf$ normalisation	Floating
$W+bb$ to $W+cc$ ratio	4%–10%
$W+bl$ to $W+cl$ ratio	31%–32%
$W+bc$ to $W+cl$ ratio	31%–33%
$W\rightarrow\tau\nu(+c)$ to $W+cl$ ratio	11%
$W\rightarrow\tau\nu(+b)$ to $W+cl$ ratio	27%
$W\rightarrow\tau\nu(+l)$ to $W+l$ ratio	8%
N_{jet} acceptance	8%–14%
High-ΔR CR to SR	15%–29%
$W\rightarrow\tau\nu$ SR to high-ΔR CR ratio	5%–18%
0- to 1-lepton ratio	1%– 6%
Top quark (0- and 1-lepton)	
Top(b) normalisation	Floating
Top(other) normalisation	Floating
N_{jet} acceptance	7%–9%
0- to 1-lepton ratio	4%
SR/top CR acceptance ($t\bar{t}$)	9%
SR/top CR acceptance (Wt)	16%
Wt / $t\bar{t}$ ratio	10%
Top quark (2-lepton)	
Normalisation	Floating
Multi-jet (1-lepton)	
Normalisation	20%–100%

The values given refer to the size of the uncertainty affecting the yield of each background. Where the size of an acceptance systematic uncertainty varies between analysis regions, a range is displayed. Uncertainties in the shapes of the m_{cc} distributions are not shown below, but are taken into account for all backgrounds. CR and SR stand for control region and signal region

lihood fit; flavour-fraction uncertainties, which account for uncertainties in the make-up of subcomponents of each background; relative acceptance uncertainties, which account for the relative normalisations of backgrounds in cases where the overall normalisation is considered correlated across two or more analysis regions; and shape uncertainties, accounting for uncertainties in the shape of the m_{cc} distribution in each region. Unless stated otherwise, normalisation and shape effects of each systematic uncertainty are treated as uncorrelated with one another to ensure that modelling uncertainties are not artificially constrained. The decision to correlate or decorrelate normalisation and shape effects is made for each modelling uncertainty considered and is based on studies of different correlation models, and in cases where the impact of the choice is non-negligible, the model giving the most conservative uncertainty is used. Background modelling uncertainties considered in this analysis are summarised in Table 3.

VH Uncertainties in the $VH(\rightarrow c\bar{c})$ signal are evaluated following the recommendations of the LHC Higgs Working Group [105,106], and include uncertainties in the cross-section of VH production and in the $H\rightarrow c\bar{c}$ branching fraction. In addition, acceptance and shape uncertainties are evaluated by comparing the nominal $VH(\rightarrow c\bar{c})$ samples with alternatives generated using Powheg+Herwig7 [107], and by independently varying the renormalisation (μ_{r}) and factorisation (μ_{f}) scales by factors of one-half and two in the nominal generator. Comparisons are made separately for the three production processes; $q\bar{q}\rightarrow ZH$, $q\bar{q}\rightarrow WH$, and $gg\rightarrow ZH$. Uncertainties in the total acceptance are found to be similar between lepton channels, 4–6% in the quark-initiated processes and 31–35% for $gg\rightarrow ZH$. Similarly, uncertainties in the ratio of 3-jet to 2-jet events are found to be similar between channels for the quark-initiated processes, 6–12%, while uncertainties in the $gg\rightarrow ZH$ processes are larger, 19–56%. In the 2-lepton channel an uncertainty is included to account for differences in acceptance between the two p_{T}^{V} regions, and is 2% for $q\bar{q}\rightarrow ZH$ and 5% for $gg\rightarrow ZH$. Uncertainties in the shapes of the m_{cc} distributions for each of the three production processes are evaluated in a similar way, and good agreement is found between lepton channels, allowing the use of one shape uncertainty per production process. Uncertainties in the normalisation of the $WH(\rightarrow b\bar{b})$ and $ZH(\rightarrow b\bar{b})$ background are taken from the recent ATLAS measurements [36]. Uncertainties in the number of jets and p_{T}^{V} acceptance ratios are set to be the same as those derived for the $H\rightarrow c\bar{c}$ signal. Shape uncertainties in the $H\rightarrow b\bar{b}$ background are evaluated in an equivalent way to the $H\rightarrow c\bar{c}$ signal shape uncertainties.

Diboson Uncertainties in the diboson prediction are evaluated by comparing the nominal diboson MC samples, generated using SHERPA, with alternative samples generated using POWHEG+PYTHIA8 and by independently varying μ_r and μ_f in the nominal samples by factors of one-half and two. Inclusive acceptance uncertainties are assigned to the WW, WZ and ZZ processes, and uncertainties in the ratios of 3-jet to 2-jet events and the ratios of events in different p_T^V regions are also included.
Uncertainties in the m_{cc} shape of the diboson signal, $VW(\to cq)$ and $VZ(\to c\bar{c})$, and background components are evaluated separately by comparing MC events from the two generator set-ups in each lepton channel. These comparisons are made inclusively in the number of jets and, in the 2-lepton channel, split into p_T^V regions. The shape uncertainties are found to be consistent between channels.

V+jets production The largest backgrounds in this analysis originate from $V+$jets, with W + jets and Z + jets being the largest background in the 1-lepton and 2-lepton channels, respectively, and a combination of the two making up the majority of the background in the 0-lepton channel. In all channels, the $V+$jets background is divided into three subsamples based on the flavours of the two signal jets: $V+hf$, $V+mf$ and $V+lf$, where *hf*, *mf* and *lf* stand for heavy-flavour, mixed-flavour and light-flavour, respectively. The $V+hf$ background consists of the $V+bb$ and $V+cc$ contributions, the $V+mf$ background consists of the $V+bl$, $V+cl$ and $V+bc$ contributions, where *l* refers to a *light* jet that doesn't contain a heavy-flavour hadron or τ-lepton, and the $V+lf$ background consists of the remaining contribution where neither of the signal jets contain a heavy-flavour hadron. In the 0-lepton channel a non-negligible component of events contains a $W \to \tau\nu$ decay in which the τ-lepton decays hadronically and is selected as one of the two signal jets. These jets are considered as light jets for the purpose of assigning these events to the $W+mf$ and $W+lf$ background components.
Uncertainties in the $V+$jets backgrounds due to normalisation, acceptance, flavour-fractions and shapes are evaluated using alternative Monte Carlo generator set-ups. These include taking the same SHERPA set-up used to generate the nominal $V+$jets samples but varying μ_r and μ_f by factors of one-half and two independently, and separate samples generated using MADGRAPH5_AMC@NLO [108] at leading order in QCD with up to four additional partons in the matrix element calculation, interfaced to PYTHIA8.
The normalisations of all the W + jets and Z + jets components are free to float in the likelihood fit to data. The $W+lf$ and $Z+lf$ components float independently in the 2-jet and 3-jet signal regions. The $Z+hf$, $Z+mf$ and $Z+lf$ components float independently in the two p_T^V regions. The normalisations of the $V+lf$ backgrounds are constrained by the 0-*c*-tag control regions, while the $V+hf$ and $V+mf$ components are constrained by the signal regions and high-ΔR control regions. Uncertainties are included to account for acceptance effects between number-of-jet categories and lepton channels. Uncertainties in the relative contributions of the components of the $V+hf$, $V+mf$ and $V+lf$ backgrounds are found to be consistent between lepton channels, so one uncertainty per component is used, taken from the lepton channel which offers the most precise estimate.
Shape uncertainties are derived in each analysis region and channel, separately for W + jets and Z + jets, with an uncertainty being included for each of the three comparisons performed, namely the comparisons between the nominal SHERPA sample and the μ_r and μ_f variations, and the comparison with MADGRAPH5_AMC@NLO+PYTHIA8. The comparison between SHERPA and MADGRAPH5_AMC@NLO+PYTHIA8 is performed in a two-step process. First, a comparison is made in the high-ΔR control region, with differences in both the shape and normalisation between the two models propagated to the signal regions in a correlated way. Second, the SHERPA model is weighted such that the two models agree in the high-ΔR control region and any residual difference between the two models in the signal regions is included as a shape-only uncertainty.

Top-quark background The top-quark background comprises $t\bar{t}$ and single-top-quark events. In the 2-lepton channel, the normalisation of this background in each signal region is determined using the corresponding top control region described in Sect. 4.2. Due to the small size of this background, no shape uncertainties are considered.
In the 0- and 1-lepton channels, where this background is larger, $t\bar{t}$ and single-top Wt-channel events are divided into two components based on the flavours of the two signal jets: top(*b*) events, in which at least one of the signal jets originates from a *b*-quark; and top(other) events. For the latter component, the two signal jets are mostly produced in the decay of a *W* boson and therefore their invariant mass peaks at the *W*-boson mass, while for the former component it does not. The normalisations of these two components are free to float separately in the global likelihood fit, with information from the top control regions contributing significantly. The background from *t*- and *s*-channel single-top-quark production is small and is considered separately, with uncertainties in the *t*-channel and *s*-channel production cross-sections included.

Acceptance and shape uncertainties are derived separately for each component by comparing the nominal POWHEG+PYTHIA8 $t\bar{t}$ and single-top MC samples with alternative samples, generated using POWHEG+HERWIG7 and MADGRAPH5_AMC@NLO+PYTHIA8 [108]. In addition, the impact of additional radiation is assessed using POWHEG+PYTHIA8 samples with modified parameter values. Uncertainties are included to cover differences in the normalisation between lepton channels, between number-of-jets categories, and between the signal regions and top control regions. The dominant single-top contribution comes from Wt production. The estimated uncertainty in the relative contributions of $t\bar{t}$ and Wt events to the total top-quark background is included, as is an uncertainty due to the interference between $t\bar{t}$ and Wt events, evaluated using an alternative Wt MC sample in which the $t\bar{t}/Wt$ interference is dealt with using the diagram subtraction scheme instead of the diagram removal scheme used in the nominal Wt sample [109,110].
Shape differences in each of the various MC sample comparisons are considered as separate shape uncertainties. Shape uncertainties are derived for each component of the total top-quark background, top(b) and top(other), separately for $t\bar{t}$ and Wt events.

Multi-jet Uncertainties in the multi-jet background are evaluated separately in the electron and muon subchannels. Normalisation and shape uncertainties are derived by changing the definition of the multi-jet control region and by modifying the normalisation of the $t\bar{t}$ and W+jets backgrounds in this control region by up to 25%. Additionally, the impact of using an alternative variable instead of m_{T}^{W}, namely the azimuthal angle between the charged lepton and $\boldsymbol{E}_{\mathrm{T}}^{\mathrm{miss}}$, $\Delta\phi(\ell, \boldsymbol{E}_{\mathrm{T}}^{\mathrm{miss}})$, in the template fit is considered as an uncertainty.

6 Statistical analysis and results

A binned maximum-likelihood fit to the m_{cc} distribution is performed across the 44 analysis regions to extract three parameters of interest (POI), $\boldsymbol{\mu}$. The parameters of interest, $\mu_{VH(c\bar{c})}$, $\mu_{VW(cq)}$ and $\mu_{VZ(c\bar{c})}$, correspond to signal strengths that multiply the SM cross-sections times branching fractions of the $VH(\to c\bar{c})$, $VW(\to cq)$ and $VZ(\to c\bar{c})$ processes, and are extracted by maximising the likelihood function with respect to both $\boldsymbol{\mu}$ and nuisance parameters, which account for the systematic uncertainties discussed in Sect. 5. Uncertainties are constrained with Gaussian or log-normal distributions in the likelihood function with the exception of the normalisations of the V+jets and top-quark backgrounds, which are allowed to float freely in the fit. The uncertainties due to the limited number of events in the simulated samples used in the fit are included using the Beeston–Barlow technique [111] for the total MC prediction, excluding the $VH(c\bar{c})$ signal. Systematic uncertainties that exhibit large fluctuations are smoothed and uncertainties with negligible impact on the final results are 'pruned' following the procedures outlined in Ref. [112].

The $VH(\to b\bar{b})$ background, expected to be about eight (two) times larger than the SM $H \to c\bar{c}$ signal in the 1-c-tag (2-c-tag) signal regions, is included in the likelihood function with uncertainties; however, at the present level of signal sensitivity it does not significantly impact the search for $VH(\to c\bar{c})$.

The m_{cc} resolution is studied using simulation in the 2-lepton channel and its value is 10–20 GeV depending on the signal region. The resolution is better in the 2-jet signal regions than those with more than two jets, and better in the 2-c-tag signal regions than the 1-c-tag signal regions. In the 2-lepton channel, the resolution in the $p_{\mathrm{T}}^{V} > 150$ GeV signal regions is better than in the 75 GeV $< p_{\mathrm{T}}^{V} < 150$ GeV signal regions. The following m_{cc} ranges and uniform binnings are used in the various signal and control regions:

- 16 bins from 50 to 210 GeV in the signal regions and 0- and 1-lepton top control regions, with the exception of the 2-lepton, 2-c-tag, $p_{\mathrm{T}}^{V} > 150$ GeV signal regions.
- 9 (10) bins from 50 to 185 (200) GeV in the 2-lepton, 2-c-tag, $p_{\mathrm{T}}^{V} > 150$ GeV, 2-jet (3-jet) signal region.
- 13 bins from 80 to 340 GeV in each of the high-ΔR control regions, with the exception of the 2-lepton, 2-c-tag, $p_{\mathrm{T}}^{V} > 150$ GeV high-ΔR regions, where 9 bins from 80 to 350 GeV are used.
- A single bin from 50 to 210 GeV in each of the 0-c-tag control regions and 2-lepton top control regions.

Selected post-fit m_{cc} distributions, where all normalisations and nuisance parameters are adjusted by the likelihood fit, are shown in Fig. 1 for the 0-, 1-, and 2-lepton channels. Post-fit distributions for the remaining analysis regions can be found in the Appendix. Table 4 shows the values of the free-floating background normalisation parameters obtained from the likelihood fit to data. The fitted signal strengths are:

$$\begin{aligned}
\mu_{VH(c\bar{c})} &= -9 \quad \pm 10(\mathrm{stat.}) \quad \pm 12(\mathrm{syst.}) \\
\mu_{VW(cq)} &= 0.83 \pm 0.11(\mathrm{stat.}) \pm 0.21(\mathrm{syst.}) \\
\mu_{VZ(c\bar{c})} &= 1.16 \pm 0.32(\mathrm{stat.}) \pm 0.36(\mathrm{syst.}).
\end{aligned}$$

The correlation between $\mu_{VH(c\bar{c})}$ and $\mu_{VW(cq)}$ ($\mu_{VZ(c\bar{c})}$) is 17% (16%), while $\mu_{VW(cq)}$ and $\mu_{VZ(c\bar{c})}$ are 17% anti-correlated. The probability of compatibility with the SM, defined as all three POIs being equal to unity, is 84%. The observed (expected) significances of the $VW(\to cq)$ and $VZ(\to c\bar{c})$ signals are 3.8 (4.6) and 2.6 (2.2) standard deviations, respectively. For the $\mu_{VH(c\bar{c})}$ signal strength,

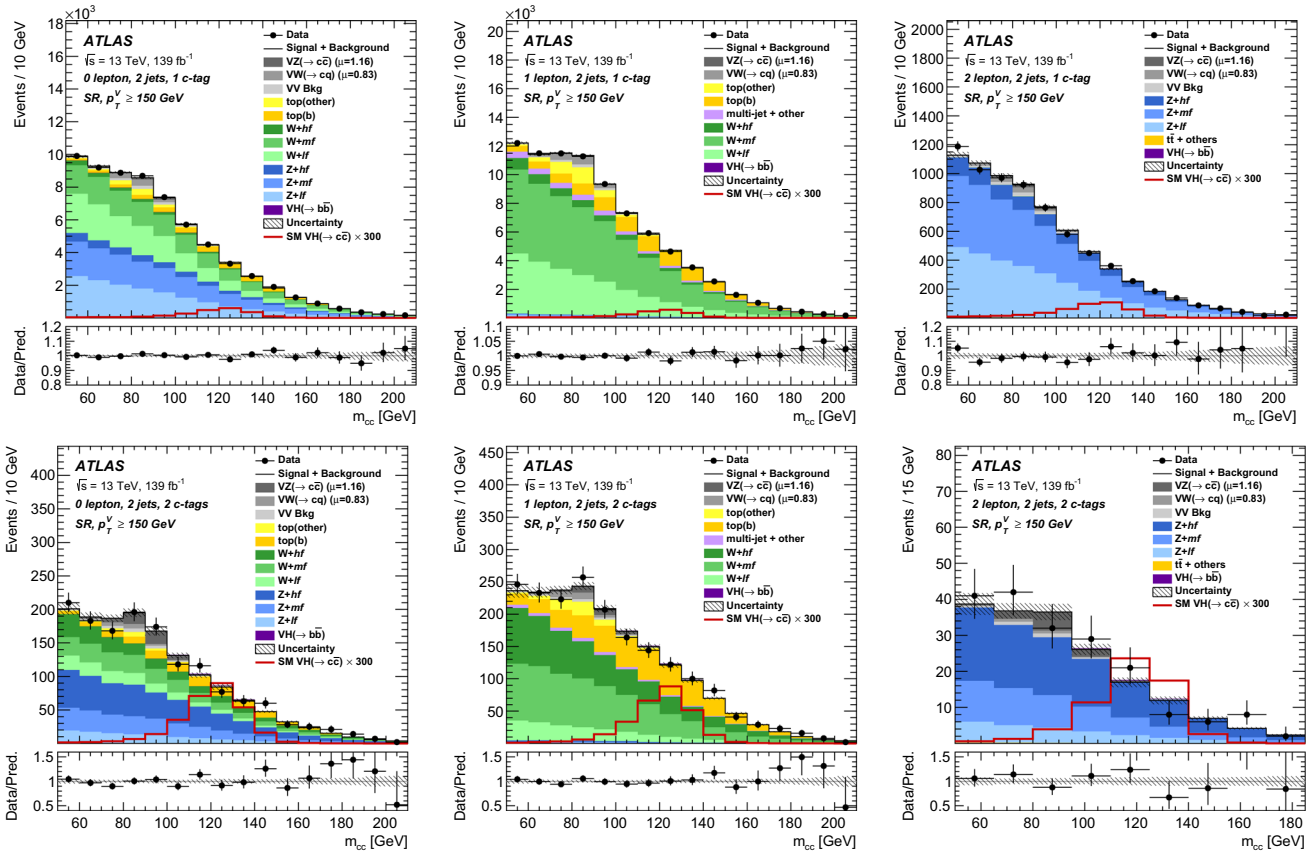

Fig. 1 Post-fit distributions for six selected signal regions out of 44 analysis regions, with two jets and $p_{\mathrm{T}}^{V} > 150$ GeV for the 0-lepton (left), 1-lepton (centre), and 2-lepton (right) channels, with one c-tag (top) and two c-tags (bottom). The total signal-plus-background prediction is shown by the solid black line and includes the $H \to c\bar{c}$ signal scaled to the best-fit value of $\mu_{VH(c\bar{c})} = -9$. The $H \to c\bar{c}$ signal is also shown as an unfilled histogram scaled to 300 times the SM prediction. The post-fit uncertainty is shown as the hatched background. The ratio of the data to the sum of the post-fit signal plus background is shown in the lower panel

an upper limit of 26 (31^{+12}_{-8}) is observed (expected) at 95% CL using a modified frequentist $\mathrm{CL_s}$ method [113], with the profile-likelihood ratio as the test statistic [114], using the RooFit/RooStats framework [115,116]. The limits for the three lepton channels are summarised in Fig. 2.

The effects of systematic uncertainties are summarised in Table 5. For each POI, the statistical uncertainty is obtained from a fit in which all nuisance parameters are fixed to their post-fit values. The total systematic uncertainty is found by subtracting the squared statistical uncertainty from the squared total uncertainty, i.e. $\sigma_{\mathrm{syst.}} = (\sigma^2_{\mathrm{tot.}} - \sigma^2_{\mathrm{stat.}})^{1/2}$. Similarly, the impact of a subset of the systematic uncertainties is assessed by performing the fit with only their nuisance parameters fixed to their post-fit values. For each POI, the impact is then computed as the square root of the decrease in the squared uncertainty of that POI between the nominal fit and the fit with the nuisance parameters fixed. Despite the additional uncertainties it introduces, the use of truth-flavour tagging improves the expected limit on $\mu_{VH(c\bar{c})}$ by about 10% due to the improved statistical precision in the MC predictions.

The improvements in this analysis relative to the previous ATLAS search for ZH, $H \to c\bar{c}$ [16] are quantified by performing a fit in the 2-lepton channel to the 2015–2016 data, corresponding to 36 fb^{-1}. Using the same signal regions as the previous analysis a 36% improvement in the expected limit is found, with most of the improvement due to better flavour-tagging performance. After also including the new 2-lepton signal and control regions introduced in this analysis, a 43% improvement in the expected limit is found. Adding the full Run-2 dataset, along with the 0- and 1-lepton channels, the expected limit is improved by a factor of five in this analysis, relative to the previous ATLAS search.

The m_{cc} distributions for events with either one or two c-tagged jets, summed over all channels and regions, after background subtraction, and using the fitted signal strengths, are shown in Fig. 3.

The best-fit value of the $VH(\to c\bar{c})$ signal strength is interpreted within the kappa framework [37,38], by reparam-

Table 4 Values of the free-floating background normalisation parameters obtained from the likelihood fit to data. The uncertainties represent the combined statistical and systematic uncertainties. Unless otherwise stated, normalisation parameters are correlated across all p_{T}^{V} and number-of-jets analysis regions

Background	p_{T}^{V}	Jets	Value
Top(b)			0.91 ± 0.06
Top(other)			0.94 ± 0.08
$t\bar{t}$ (2-lepton)	$p_{\mathrm{T}}^{V} > 150$ GeV	2	0.76 ± 0.22
		3	0.96 ± 0.13
	$75 < p_{\mathrm{T}}^{V} < 150$ GeV	2	1.08 ± 0.08
		3	1.06 ± 0.07
$W+hf$			1.16 ± 0.35
$W+mf$			1.28 ± 0.14
$W+lf$		2	1.02 ± 0.04
		3	0.97 ± 0.05
$Z+hf$	$p_{\mathrm{T}}^{V} > 150$ GeV		1.19 ± 0.22
	$75 < p_{\mathrm{T}}^{V} < 150$ GeV		1.25 ± 0.25
$Z+mf$	$p_{\mathrm{T}}^{V} > 150$ GeV		1.10 ± 0.15
	$75 < p_{\mathrm{T}}^{V} < 150$ GeV		1.11 ± 0.15
$Z+lf$	$p_{\mathrm{T}}^{V} > 150$ GeV	2	1.07 ± 0.03
		3	1.08 ± 0.05
	$75 < p_{\mathrm{T}}^{V} < 150$ GeV	2	1.12 ± 0.04
		3	1.07 ± 0.06

eterising $\mu_{VH(c\bar{c})}$ in the likelihood function in terms of the Higgs–charm coupling modifier, κ_c, assuming that the coupling modifier only affects the Higgs boson decays. Including effects in both the partial and full width, considering only SM decays and setting all other couplings to their SM predictions, $\mu_{VH(c\bar{c})}$ is parameterised as a function of κ_c

$$\mu_{VH(c\bar{c})}(\kappa_c) = \frac{\kappa_c^2}{1 + B_{H\to c\bar{c}}^{\mathrm{SM}}(\kappa_c^2 - 1)},$$

where $B_{H\to c\bar{c}}^{\mathrm{SM}}$ is the $H \to c\bar{c}$ branching fraction predicted in the SM.

Constraints on κ_c are set using the profile-likelihood ratio test statistic and are shown at 95% CL for each of the three channels and for the combined likelihood fit in Fig. 4. The combination allows an observed (expected) constraint of $|\kappa_c| < 8.5$ (12.4) to be set at the 95% CL.

7 Combination with $VH, H \to b\bar{b}$

A combination of the analysis presented in this paper with the ATLAS $VH, H \to b\bar{b}$ measurement [36] is performed by creating a likelihood function that is the product of the individual likelihood functions of the two analyses. Two parameters of interest are used, $\mu_{VH(c\bar{c})}$ and $\mu_{VH(b\bar{b})}$ for the

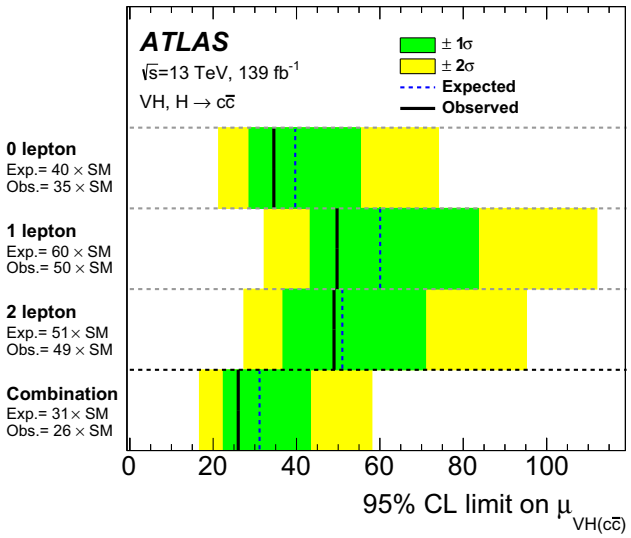

Fig. 2 The observed and expected 95% CL upper limits on the cross-section times branching fraction normalized to its SM prediction in each lepton channel and for the combined fit. The single-channel limits are obtained using a five-POI fit, in which each channel has a separate $VH(\to c\bar{c})$ parameter of interest

$VH, H \to c\bar{c}$ and $VH, H \to b\bar{b}$ signal strengths, respectively, and are included in both of the input likelihood functions. The importance of including both signal strengths in a combined likelihood was pointed out by Refs. [29,30]. Experimental systematic uncertainties that are common to both analyses, detailed in Sect. 5.1, are considered correlated between the two analyses, with the exception of the flavour-tagging systematic uncertainties due to the different calibration procedures used for b- and c-tagging. Background normalisations and modelling uncertainties are considered uncorrelated between the two analyses.

$$\mu_{VH(c\bar{c})} = -9 \quad \pm 10(\mathrm{stat.}) \pm 11(\mathrm{syst.})$$
$$\mu_{VH(b\bar{b})} = 1.06 \pm 0.12(\mathrm{stat.})^{+0.15}_{-0.13}(\mathrm{syst.})$$

with a correlation coefficient of -12%. The fitted signal strengths are consistent with those found in the individual analyses. The expected and observed best-fit values and their 68% and 95% CL contours are shown in Fig. 5.

Although the signal regions of the two analyses are orthogonal due to the b-tagging veto used in the c-tagging definition, a small overlap of events occurs in the control regions used in the two analyses. To test the impact of this, events that appear in both analyses are removed from the $VH, H \to c\bar{c}$ control regions. The results are unchanged. Treating the normalisations of the backgrounds as correlated between the two analyses is also tested and does not affect the expected sensitivity.

The best-fit values of $\mu_{VH(b\bar{b})}$ and $\mu_{VH(c\bar{c})}$ are interpreted in the kappa framework by parameterising the likelihood function in terms of both κ_b and κ_c, while setting all other

Table 5 Breakdown of contributions to the uncertainty in the fitted values of $\mu_{VH(c\bar{c})}$, $\mu_{VW(cq)}$ and $\mu_{VZ(c\bar{c})}$. The sum in quadrature of uncertainties from different sources may differ from the total due to correlations. In cases where the upward and downward systematic variations have different values, the mean of the absolute values is shown

Source of uncertainty		$\mu_{VH(c\bar{c})}$	$\mu_{VW(cq)}$	$\mu_{VZ(c\bar{c})}$
Total		15.3	0.24	0.48
Statistical		10.0	0.11	0.32
Systematic		11.5	0.21	0.36
Statistical uncertainties				
Signal normalisation		7.8	0.05	0.23
Other normalisations		5.1	0.09	0.22
Theoretical and modelling uncertainties				
$VH(\to c\bar{c})$		2.1	< 0.01	0.01
Z + jets		7.0	0.05	0.17
Top quark		3.9	0.13	0.09
W + jets		3.0	0.05	0.11
Diboson		1.0	0.09	0.12
$VH(\to b\bar{b})$		0.8	< 0.01	0.01
Multi-jet		1.0	0.03	0.02
Simulation samples size		4.2	0.09	0.13
Experimental uncertainties				
Jets		2.8	0.06	0.13
Leptons		0.5	0.01	0.01
$E_{\mathrm{T}}^{\mathrm{miss}}$		0.2	0.01	0.01
Pile-up and luminosity		0.3	0.01	0.01
Flavour tagging	c-jets	1.6	0.05	0.16
	b-jets	1.1	0.01	0.03
	light-jets	0.4	0.01	0.06
	τ-jets	0.3	0.01	0.04
Truth-flavour tagging	ΔR correction	3.3	0.03	0.10
	Residual non-closure	1.7	0.03	0.10

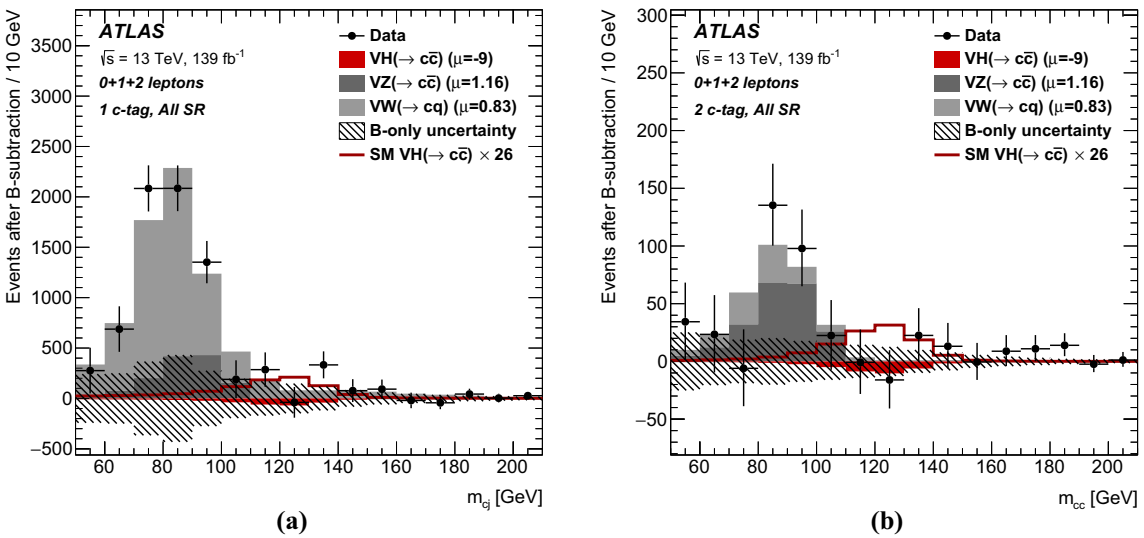

Fig. 3 The post-fit m_{cc} distribution summed over all signal regions after subtracting backgrounds, leaving only the $VH(\to c\bar{c})$, $VW(\to cq)$ and $VZ(\to c\bar{c})$ processes, for events with **a** one c-tag and **b** two c-tags. The red filled histogram corresponds to the $VH, H \to c\bar{c}$ signal for the fitted value of $\mu_{VH(c\bar{c})} = -9$, while the open red histogram corresponds to the signal expected at the 95% CL upper limit on $\mu_{VH(c\bar{c})}$ ($\mu_{VH(c\bar{c})} = 26$). The hatched band shows the uncertainty of the fitted background

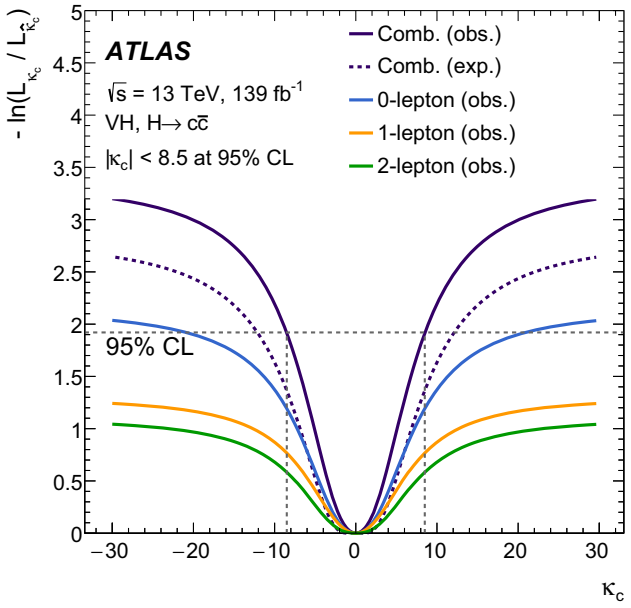

Fig. 4 Expected and observed values of the negative profile log-likelihood ratio as a function of κ_c. The single-channel likelihoods are obtained using a five-POI fit, in which each channel has a separate $VH(\rightarrow c\bar{c})$ parameter of interest. The order of the lines in the plot matches the order of the lines in the legend

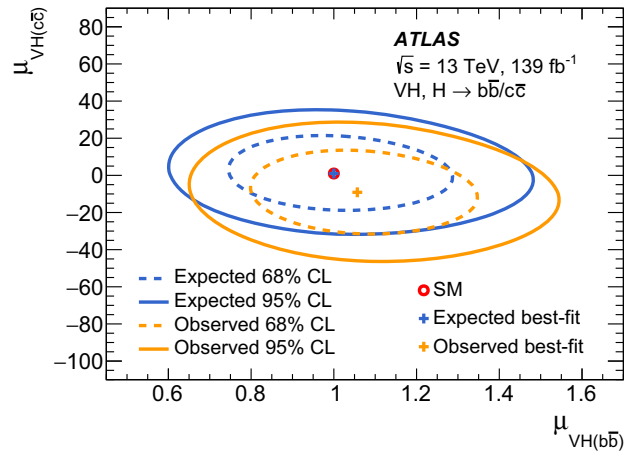

Fig. 5 The observed and expected best fit values of $\mu_{VH(c\bar{c})}$ and $\mu_{VH(b\bar{b})}$ with their 68% and 95% CL contours

couplings to their SM predictions and considering only SM Higgs boson decays. Constraints on κ_b and κ_c are set using the profile-likelihood ratio test statistic. The expected and observed constraints are shown in Fig. 6a and b, respectively. The likelihood function is symmetric relative to the sign of κ_c but not to the sign of κ_b due to the inclusion of κ_b in the parameterisation of $\sigma(gg \rightarrow ZH)$ [117], resulting in two minima in the expected likelihood scan. For most values of κ_b, a value of κ_c is allowed at 95% CL that compensates for the effect of κ_b via the width of the Higgs boson and vice versa. The observed best-fit value is $(\kappa_b, \kappa_c) = (-1.02, 0)$. The difference in the value of the log-likelihood function between the best-fit value and $(\kappa_b, \kappa_c) = (+1.02, 0)$ is 0.02. These constraints complement those from measurements of the Higgs boson p_{T} spectrum [27,118]. The ratio $|\kappa_c/\kappa_b|$ is constrained to be less than 4.5 at 95% CL (5.1 expected). The observed value is smaller than the ratio of the b- and c-quark masses, $m_b/m_c = 4.578 \pm 0.008$ [119], and therefore constrains the coupling of the Higgs boson to the charm quark to be weaker than the coupling of the Higgs boson to the bottom quark at 95% CL. The profile likelihood scan, parameterised in terms of κ_c/κ_b, with κ_b as a free parameter, is shown in Fig. 7.

8 Conclusion

A direct search for the decay of a Higgs boson to a charm quark–antiquark pair has been performed using 139 fb^{-1} of pp collision data recorded at $\sqrt{s} = 13$ TeV by the ATLAS detector at the LHC. The search uses three channels, $ZH \rightarrow \nu\nu c\bar{c}$, $WH \rightarrow \ell\nu c\bar{c}$ and $ZH \rightarrow \ell\ell c\bar{c}$. Signal events are identified using a multivariate charm tagging algorithm.

To enhance the signal sensitivity, events are categorised according to the p_{T} of the reconstructed vector boson, the number of jets and the number of c-tagged jets. The m_{cc} observable is used as the main discriminant in the likelihood fit to extract the signal. The analysis strategy is validated with the study of diboson production, which is found to be consistent with the SM prediction, with observed (expected) significances of 2.6 (2.2) standard deviations for the $VZ(\rightarrow c\bar{c})$ process and 3.8 (4.6) standard deviations for the $VW(\rightarrow cq)$ process.

The analysis yields an observed (expected) limit of 26 (31^{+12}_{-8}) times the predicted SM cross-section times branching fraction for a Higgs boson, with a mass of 125 GeV, decaying into a charm quark–antiquark pair, at the 95% confidence level, the most stringent limit to date. The expected limit is a factor of five more stringent than in the previous ATLAS search for ZH, $H \rightarrow c\bar{c}$, due to the larger dataset, improved c-tagging, and inclusion of the 0- and 1-lepton channels and additional signal and control regions. The result is interpreted in the kappa framework, considering effects on the Higgs boson width and setting all other couplings to their SM values, which results in an observed (expected) constraint on the charm Yukawa coupling modifier strength $|\kappa_c| < 8.5$ (12.4), at the 95% confidence level.

A combination with the ATLAS $H \rightarrow b\bar{b}$ measurement is performed. Interpreted in the kappa framework the combination constrains the observed ratio $|\kappa_c/\kappa_b|$ to be < 4.5 at the 95% confidence level. This is less than the ratio of the b- and c-quark masses, m_b/m_c, and thus constrains the coupling of the Higgs boson to the charm quark to be weaker than the coupling of the Higgs boson to the bottom quark at the 95% confidence level.

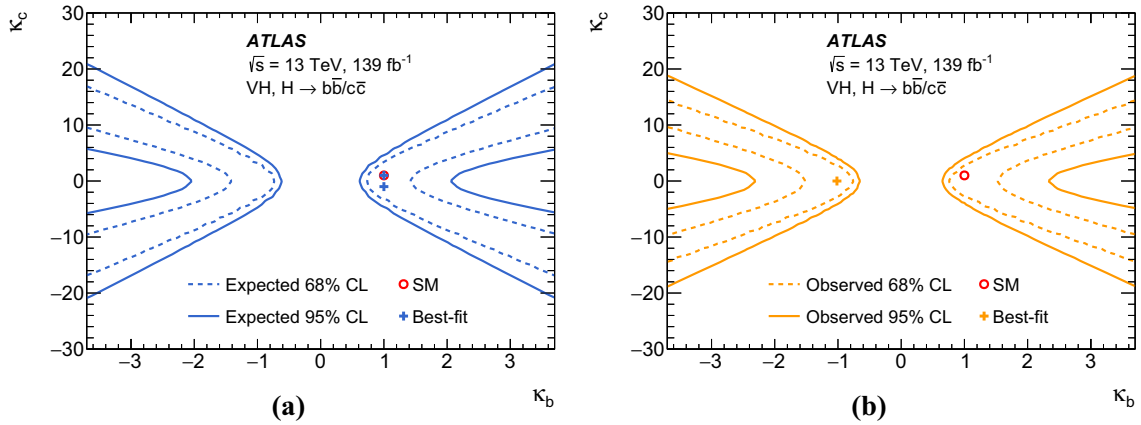

Fig. 6 The **a** expected and **b** observed constraints on κ_c and κ_b at 68% and 95% confidence levels

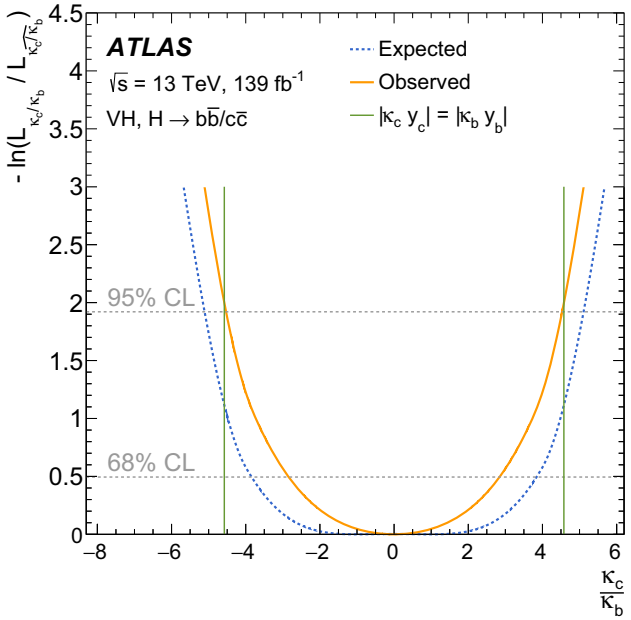

Fig. 7 Expected and observed values of the combined VH, $H \to c\bar{c}$ and VH, $H \to b\bar{b}$ negative profile log-likelihood ratio as a function of κ_c/κ_b, where κ_b is a free parameter. The vertical green lines correspond to the values of $|\kappa_c/\kappa_b|$ for which the Higgs–charm and Higgs–bottom couplings are equal, where each coupling strength $|\kappa_i\, y_i|$ is the product of the κ_i modifier and the Yukawa coupling, y_i, for $i = b, c$, and is equal to $m_b/m_c = 4.578 \pm 0.008$ [119]

Acknowledgements We thank CERN for the very successful operation of the LHC, as well as the support staff from our institutions without whom ATLAS could not be operated efficiently. We acknowledge the support of ANPCyT, Argentina; YerPhI, Armenia; ARC, Australia; BMWFW and FWF, Austria; ANAS, Azerbaijan; SSTC, Belarus; CNPq and FAPESP, Brazil; NSERC, NRC and CFI, Canada; CERN; ANID, Chile; CAS, MOST and NSFC, China; Minciencias, Colombia; MEYS CR, Czech Republic; DNRF and DNSRC, Denmark; IN2P3-CNRS and CEA-DRF/IRFU, France; SRNSFG, Georgia; BMBF, HGF and MPG, Germany; GSRI, Greece; RGC and Hong Kong SAR, China; ISF and Benoziyo Center, Israel; INFN, Italy; MEXT and JSPS, Japan; CNRST, Morocco; NWO, Netherlands; RCN, Norway; MEiN, Poland; FCT, Portugal; MNE/IFA, Romania; JINR; MES of Russia and NRC KI, Russian Federation; MESTD, Serbia; MSSR, Slovakia; ARRS and MIZŠ, Slovenia; DSI/NRF, South Africa; MICINN, Spain; SRC and Wallenberg Foundation, Sweden; SERI, SNSF and Cantons of Bern and Geneva, Switzerland; MOST, Taiwan; TAEK, Turkey; STFC, United Kingdom; DOE and NSF, USA. In addition, individual groups and members have received support from BCKDF, CANARIE, Compute Canada and CRC, Canada; COST, ERC, ERDF, Horizon 2020 and Marie Skłodowska-Curie Actions, European Union; Investissements d'Avenir Labex, Investissements d'Avenir Idex and ANR, France; DFG and AvH Foundation, Germany; Herakleitos, Thales and Aristeia programmes co-financed by EU-ESF and the Greek NSRF, Greece; BSF-NSF and GIF, Israel; Norwegian Financial Mechanism 2014-2021, Norway; NCN and NAWA, Poland; La Caixa Banking Foundation, CERCA Programme Generalitat de Catalunya and PROMETEO and GenT Programmes Generalitat Valenciana, Spain; Göran Gustafssons Stiftelse, Sweden; The Royal Society and Leverhulme Trust, UK. The crucial computing support from all WLCG partners is acknowledged gratefully, in particular from CERN, the ATLAS Tier-1 facilities at TRIUMF (Canada), NDGF (Denmark, Norway, Sweden), CC-IN2P3 (France), KIT/GridKA (Germany), INFN-CNAF (Italy), NL-T1 (Netherlands), PIC (Spain), ASGC (Taiwan), RAL (UK) and BNL (USA), the Tier-2 facilities worldwide and large non-WLCG resource providers. Major contributors of computing resources are listed in Ref. [120].

Data Availability Statement This manuscript has no associated data or the data will not be deposited. [Authors' comment: All ATLAS scientific output is published in journals, and preliminary results are made available in Conference Notes. All are openly available, without restriction on use by external parties beyond copyright law and the standard conditions agreed by CERN. Data associated with journal publications are also made available: tables and data from plots (e.g. cross section values, likelihood profiles, selection efficiencies, cross section limits, ...) are stored in appropriate repositories such as HEPDATA (http://hepdata.cedar.ac.uk/). ATLAS also strives to make additional material related to the paper available that allows a reinterpretation of the data in the context of new theoretical models. For example, an extended encapsulation of the analysis is often provided for measurements in the framework of RIVET (http://rivet.hepforge.org/). This information is taken from the ATLAS Data Access Policy, which is a public document that can be downloaded from http://opendata.cern.ch/record/413 [opendata.cern.ch].]

Funded by SCOAP[3]. SCOAP[3] supports the goals of the International Year of Basic Sciences for Sustainable Development.

Appendix

Post-fit m_{cc} distributions for 34 of the 44 analysis regions used in the statistical analysis of the $VH, H \to c\bar{c}$ search are shown in Figs. 8, 9, 10, 11, 12, 13 and 14. The 0-, 1- and 2-lepton signal regions are shown in Figs. 8, 9 and 10, respectively, with the corresponding high-ΔR control regions shown in Figs. 11, 12 and 13. The 0- and 1-lepton top-quark control regions are shown in Fig. 14. Figures 15, 16 and 17 show the post-fit background composition, including in control regions, for the 0-, 1- and 2-lepton channels, respectively.

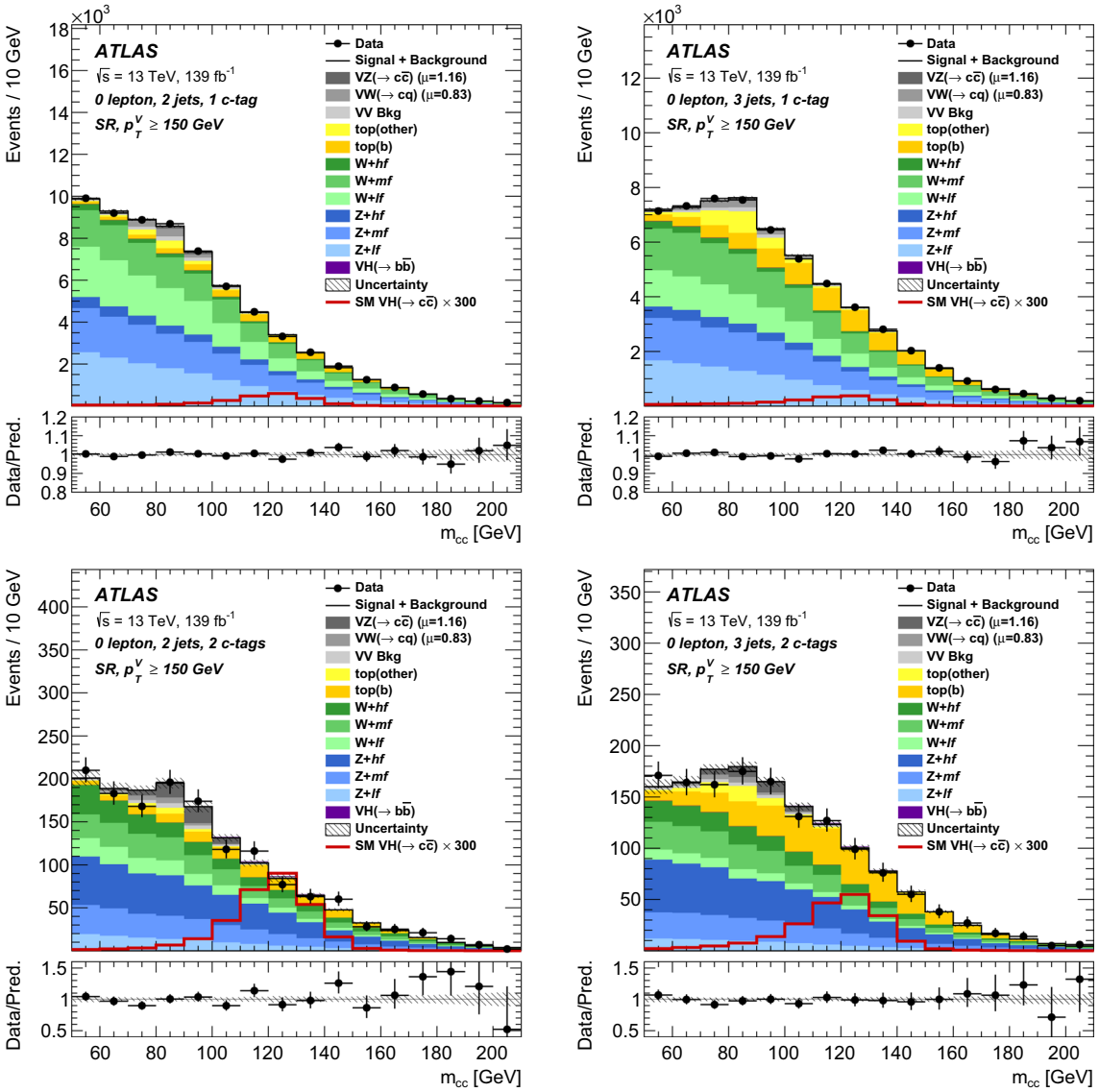

Fig. 8 Post-fit distributions of the four 0-lepton signal regions. The total signal-plus-background prediction is shown by the solid black line and includes the $H \to c\bar{c}$ signal scaled to the best-fit value of $\mu_{VH(c\bar{c})} = -9$. The $H \to c\bar{c}$ signal is also shown as an unfilled histogram scaled to 300 times the SM prediction. The post-fit uncertainty is shown as the hatched background including correlations between uncertainties. The ratio of the data to the sum of the post-fit signal plus background is shown in the lower panel

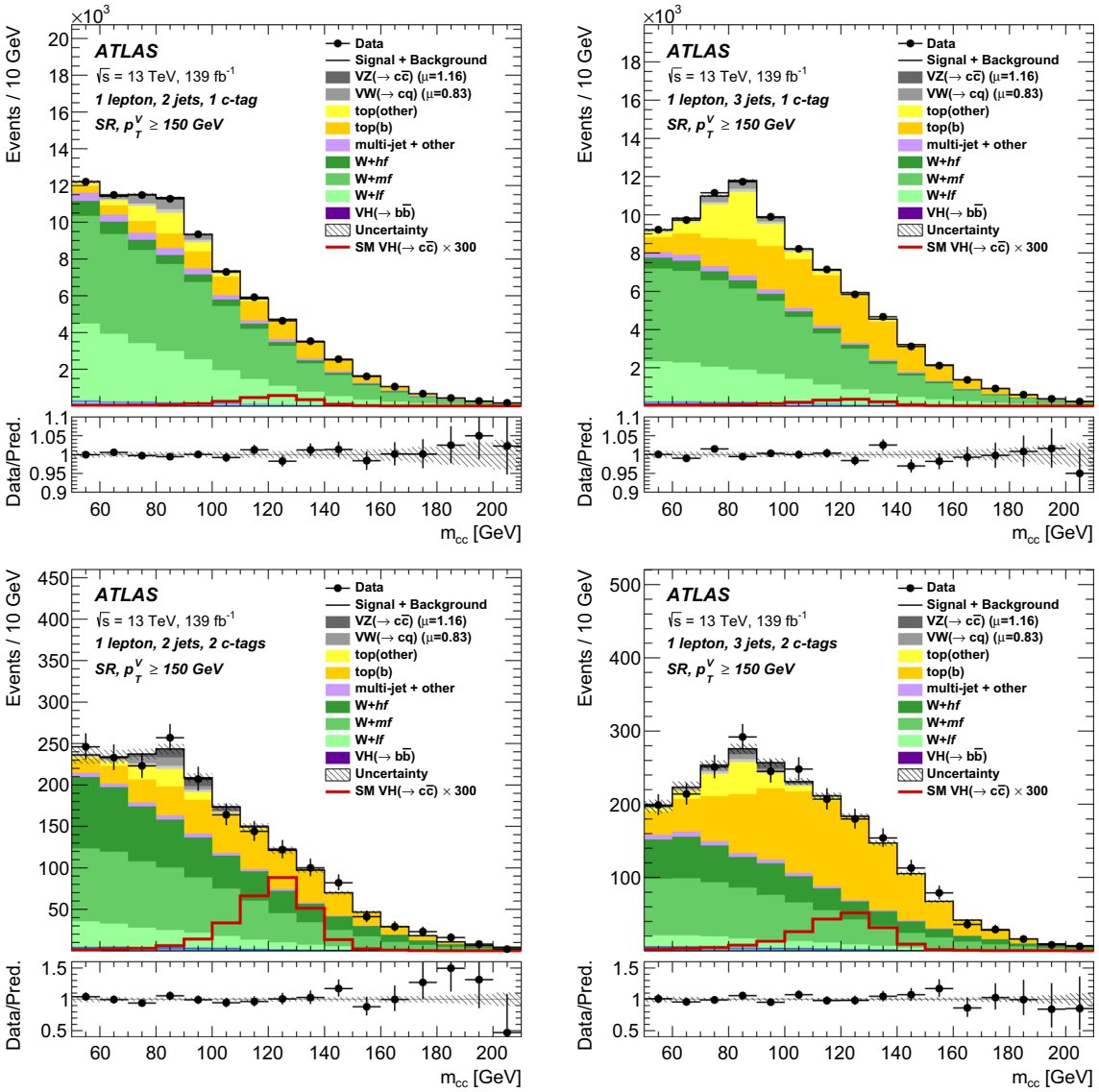

Fig. 9 Post-fit distributions of the four 1-lepton signal regions. The total signal-plus-background prediction is shown by the solid black line and includes the $H \to c\bar{c}$ signal scaled to the best-fit value of $\mu_{VH(c\bar{c})} = -9$. The $H \to c\bar{c}$ signal is also shown as an unfilled histogram scaled to 300 times the SM prediction. The post-fit uncertainty is shown as the hatched background including correlations between uncertainties. The ratio of the data to the sum of the post-fit signal plus background is shown in the lower panel

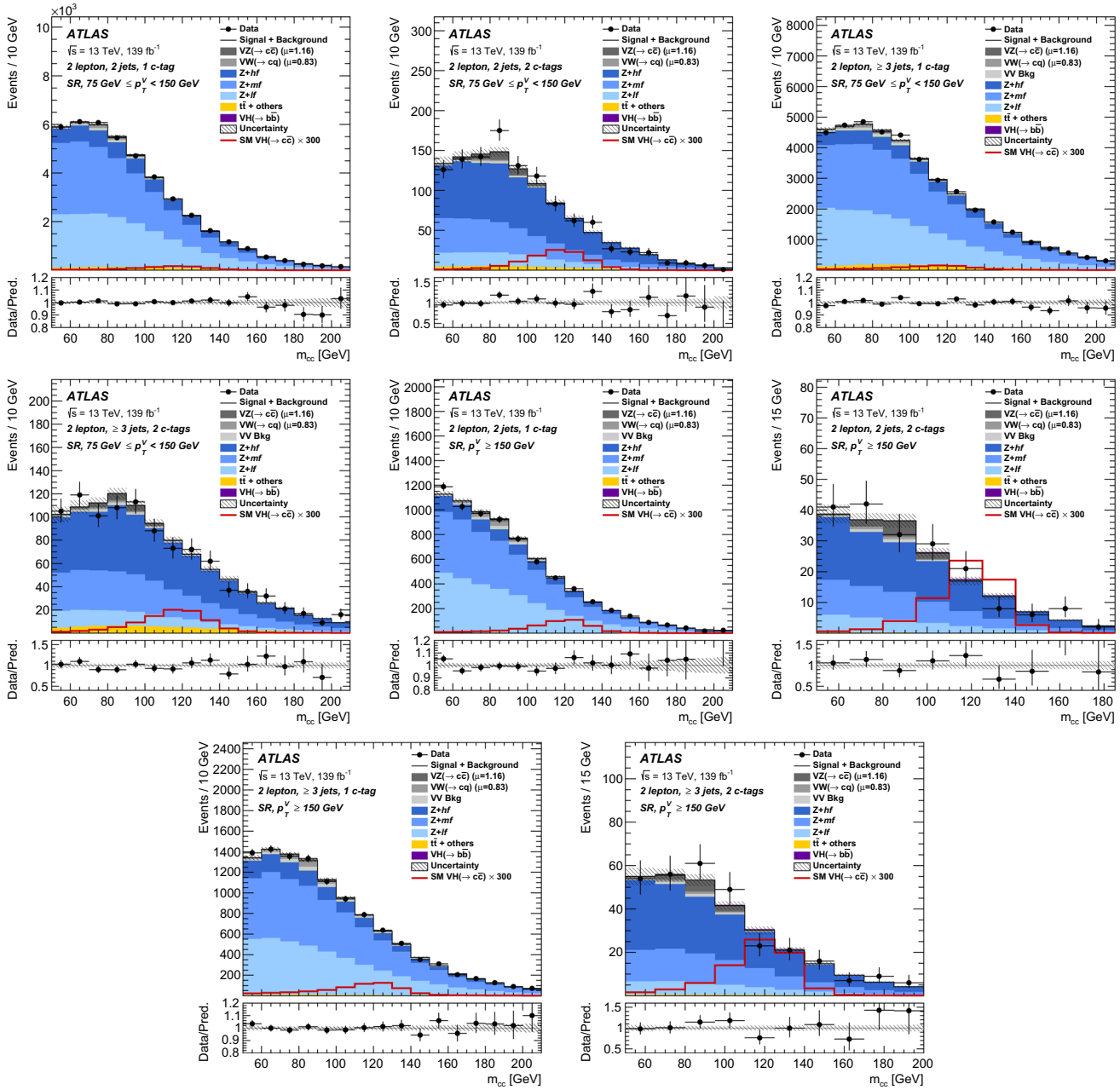

Fig. 10 Post-fit distributions of the eight 2-lepton signal regions. The total signal-plus-background prediction is shown by the solid black line and includes the $H \to c\bar{c}$ signal scaled to the best-fit value of $\mu_{VH(c\bar{c})} = -9$. The $H \to c\bar{c}$ signal is also shown as an unfilled histogram scaled to 300 times the SM prediction. The post-fit uncertainty is shown as the hatched background including correlations between uncertainties. The ratio of the data to the sum of the post-fit signal plus background is shown in the lower panel

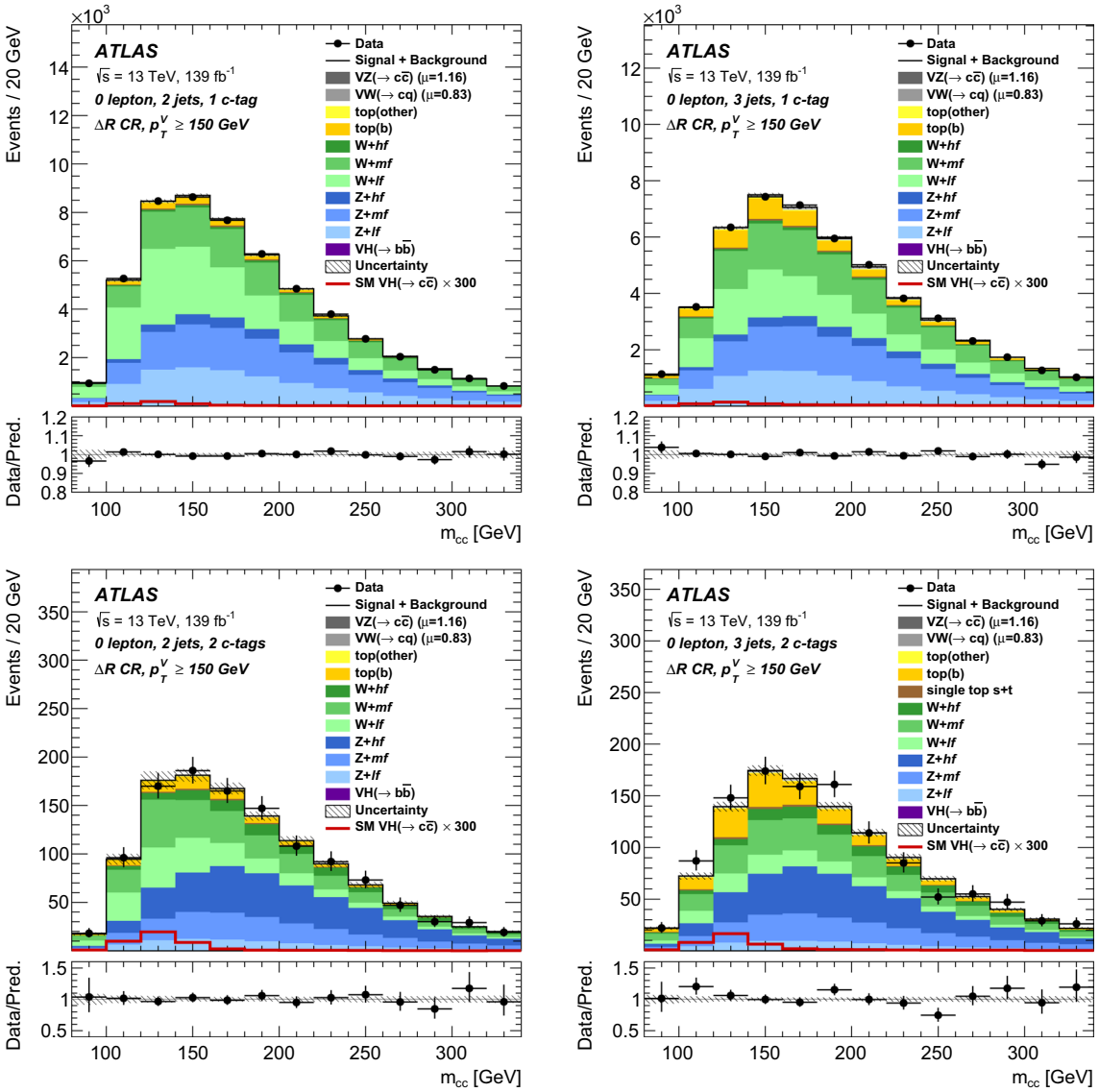

Fig. 11 Post-fit distributions of the four 0-lepton high-ΔR control regions. The total signal-plus-background prediction is shown by the solid black line and includes the $H \to c\bar{c}$ signal scaled to the best-fit value of $\mu_{VH(c\bar{c})} = -9$. The $H \to c\bar{c}$ signal is also shown as an unfilled histogram scaled to 300 times the SM prediction. The post-fit uncertainty is shown as the hatched background including correlations between uncertainties. The ratio of the data to the sum of the post-fit signal plus background is shown in the lower panel

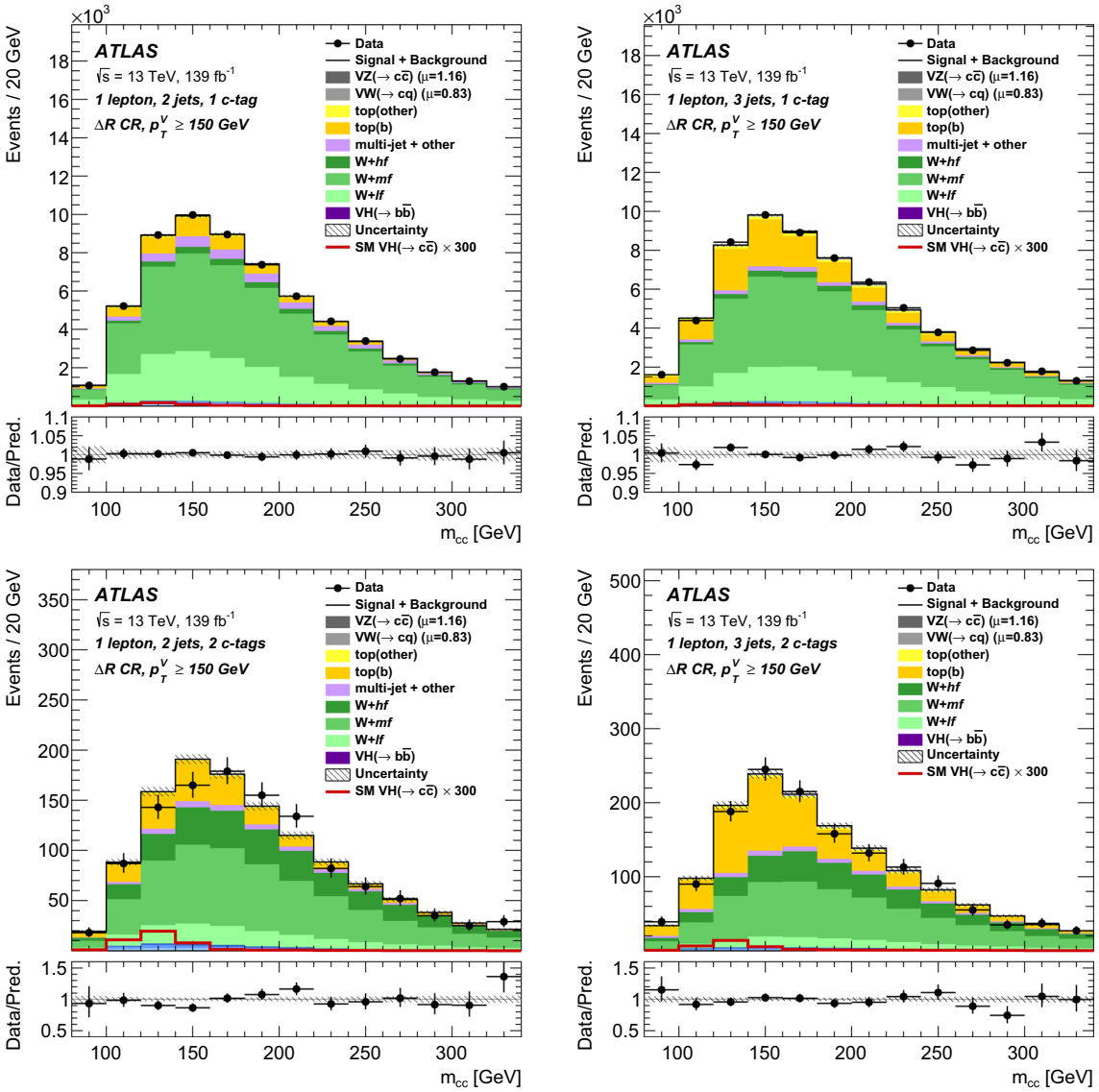

Fig. 12 Post-fit distributions of the four 1-lepton high-ΔR control regions. The total signal-plus-background prediction is shown by the solid black line and includes the $H \to c\bar{c}$ signal scaled to the best-fit value of $\mu_{VH(c\bar{c})} = -9$. The $H \to c\bar{c}$ signal is also shown as an unfilled histogram scaled to 300 times the SM prediction. The post-fit uncertainty is shown as the hatched background including correlations between uncertainties. The ratio of the data to the sum of the post-fit signal plus background is shown in the lower panel

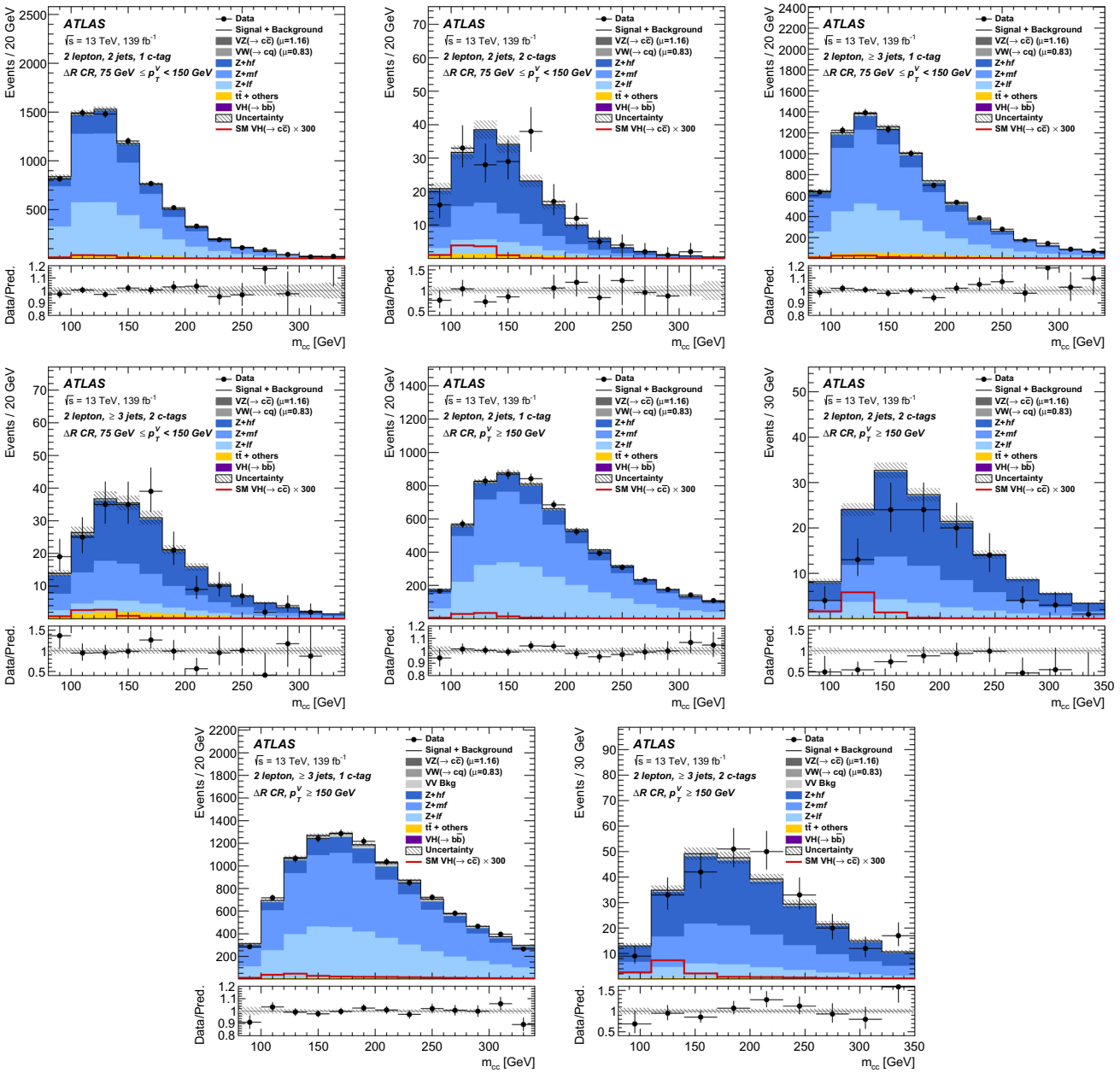

Fig. 13 Post-fit distributions of the eight 2-lepton high-ΔR control regions. The total signal-plus-background prediction is shown by the solid black line and includes the $H \to c\bar{c}$ signal scaled to the best-fit value of $\mu_{VH(c\bar{c})} = -9$. The $H \to c\bar{c}$ signal is also shown as an unfilled histogram scaled to 300 times the SM prediction. The post-fit uncertainty is shown as the hatched background including correlations between uncertainties. The ratio of the data to the sum of the post-fit signal plus background is shown in the lower panel

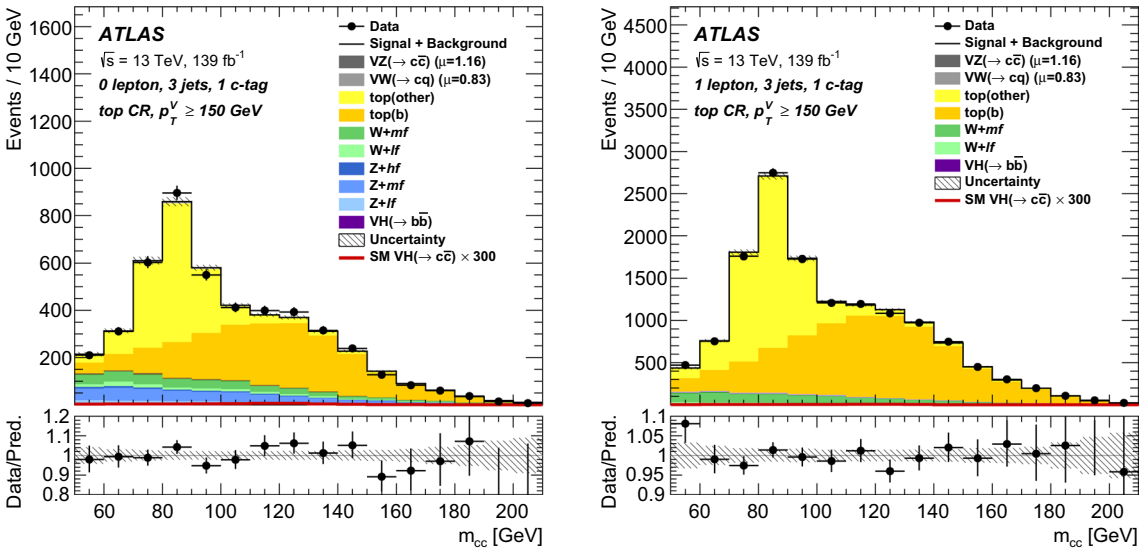

Fig. 14 Post-fit distributions of the 0- and 1-lepton top control regions. The total signal-plus-background prediction is shown by the solid black line and includes the $H \to c\bar{c}$ signal scaled to the best-fit value of $\mu_{VH(c\bar{c})} = -9$. The $H \to c\bar{c}$ signal is also shown as an unfilled histogram scaled to 300 times the SM prediction. The post-fit uncertainty is shown as the hatched background including correlations between uncertainties. The ratio of the data to the sum of the post-fit signal plus background is shown in the lower panel

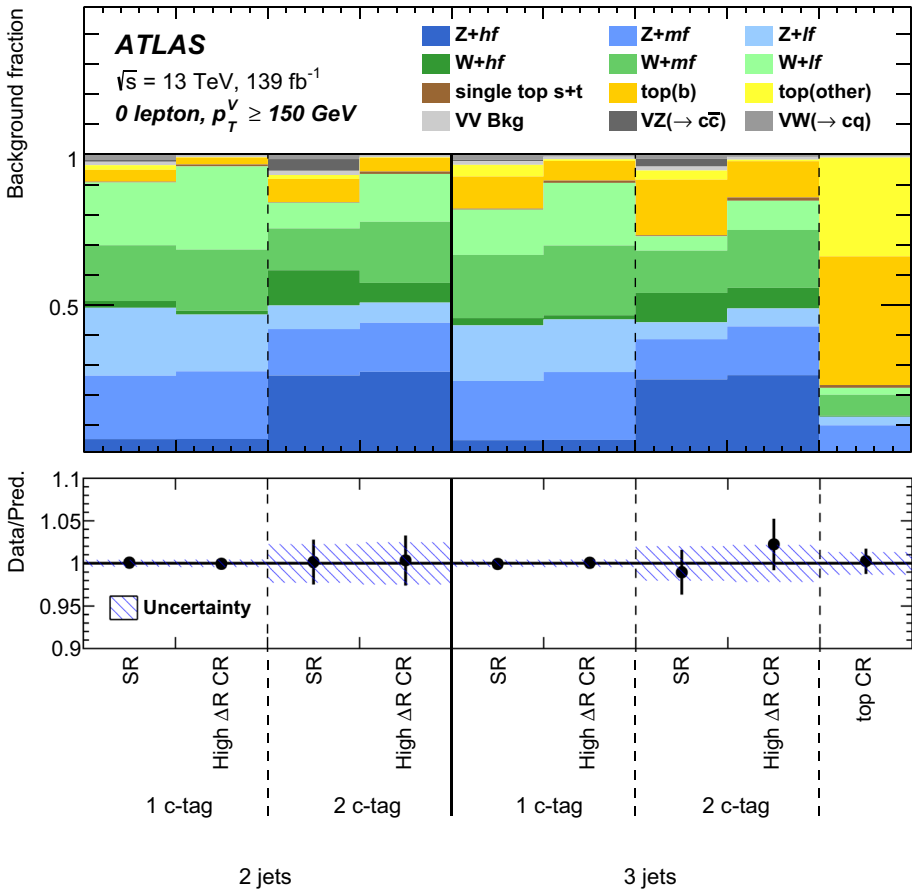

Fig. 15 The background composition in all 0-lepton signal and control regions

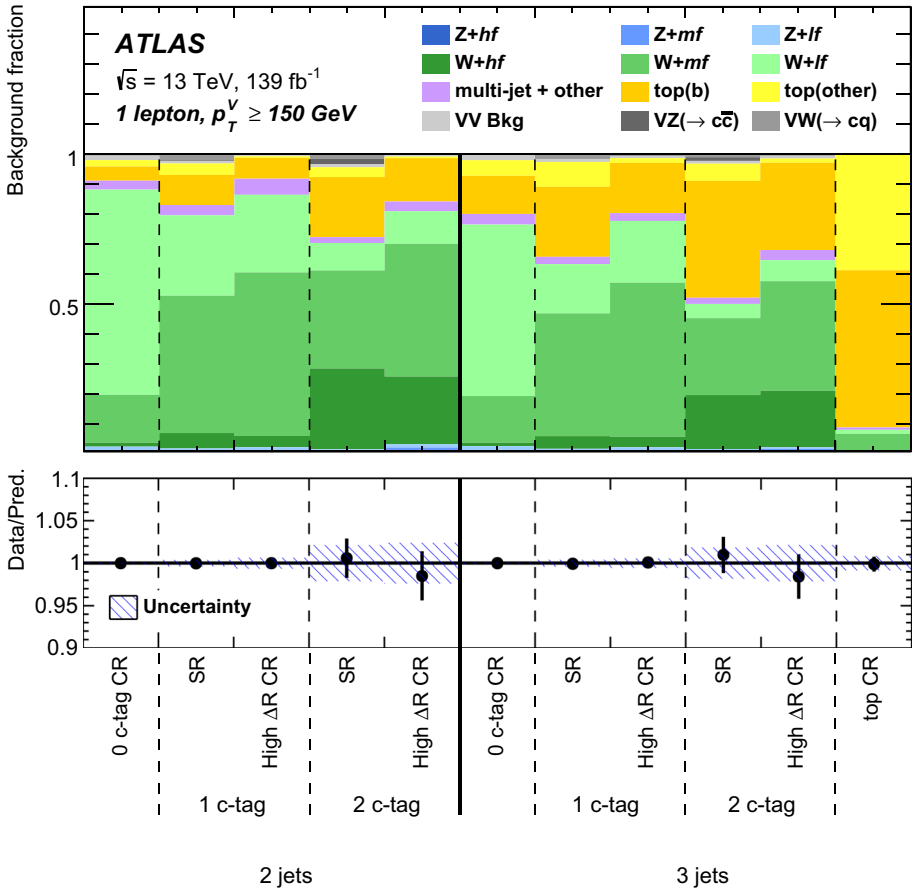

Fig. 16 The background composition in all 1-lepton signal and control regions

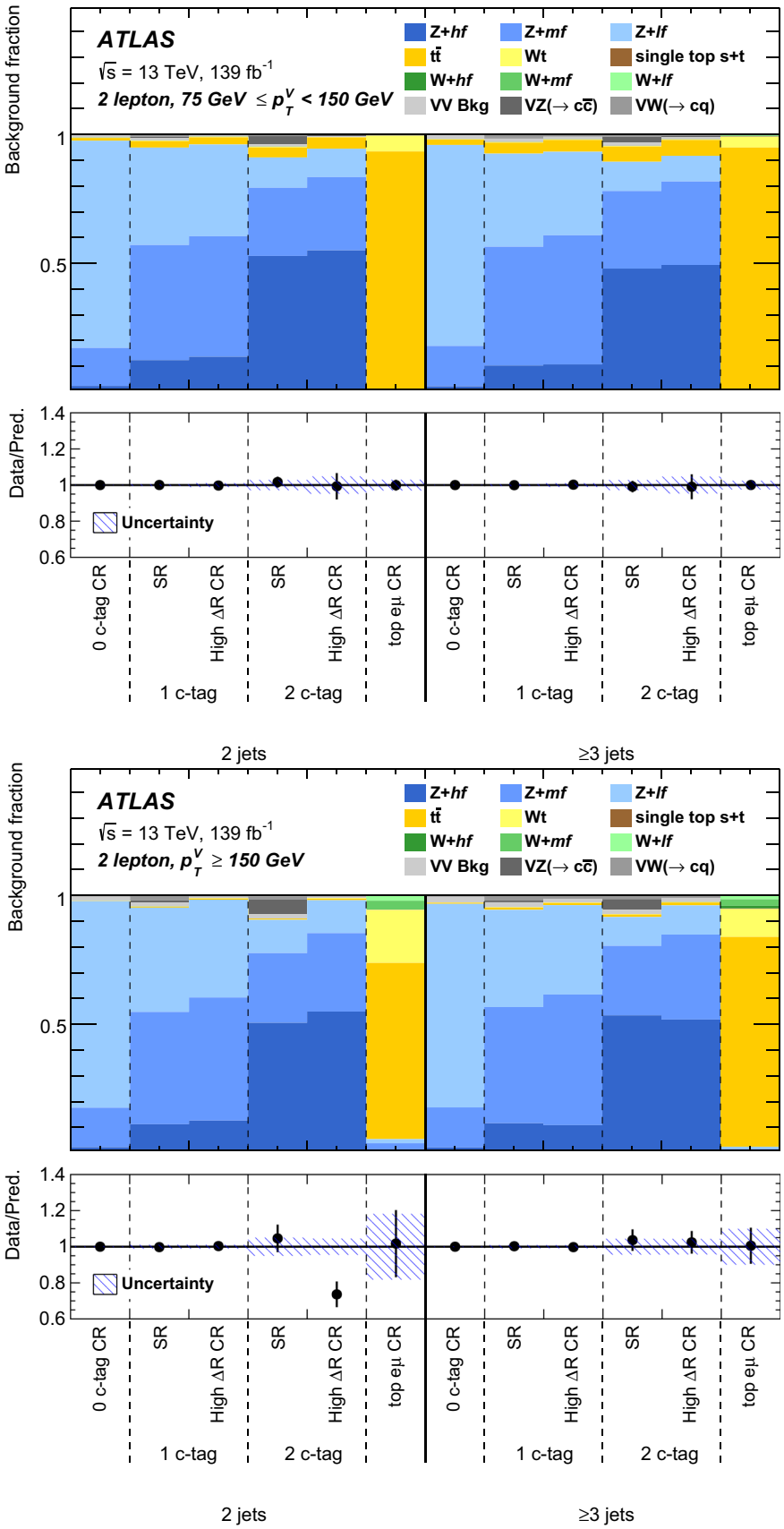

Fig. 17 The background composition in all 2-lepton signal and control regions, for events with $75 < p_{\mathrm{T}}^{V} < 150$ GeV (top) and $p_{\mathrm{T}}^{V} > 150$ GeV (bottom)

References

1. ATLAS Collaboration, Observation of a new particle in the search for the Standard Model Higgs boson with the ATLAS detector at the LHC. Phys. Lett. B **1**, 716 (2012). https://doi.org/10.1016/j.physletb.2012.08.020. arXiv:1207.7214 [hep-ex]
2. CMS Collaboration, Observation of a new boson at a mass of 125 GeV with the CMS experiment at the LHC. Phys. Lett. B **716**, 30 (2012). https://doi.org/10.1016/j.physletb.2012.08.021. arXiv:1207.7235 [hep-ex]
3. L. Evans, P. Bryant, L.H.C. Machine, JINST **3**, S08001 (2008). https://doi.org/10.1088/1748-0221/3/08/S08001
4. F. Englert, R. Brout, Broken symmetry and the mass of gauge vector mesons. Phys. Rev. Lett. **13**, 321 (1964). https://doi.org/10.1103/PhysRevLett.13.321
5. P. Higgs, Broken symmetries, massless particles and gauge fields. Phys. Lett. **12**, 132 (1964). https://doi.org/10.1016/0031-9163(64)91136-9
6. P.W. Higgs, Broken symmetries and the masses of gauge bosons. Phys. Rev. Lett. **13**, 508 (1964). https://doi.org/10.1103/PhysRevLett.13.508
7. G.S. Guralnik, C.R. Hagen, T.W.B. Kibble, Global conservation laws and massless particles. Phys. Rev. Lett. **13**, 585 (1964). https://doi.org/10.1103/PhysRevLett.13.585
8. ATLAS Collaboration, Cross-section measurements of the Higgs boson decaying into a pair of τ-leptons in proton–proton collisions at $\sqrt{s} = 13$ TeV with the ATLAS detector. Phys. Rev. D **99**, 072001 (2019). https://doi.org/10.1103/PhysRevD.99.072001. arXiv:1811.08856 [hep-ex]
9. ATLAS Collaboration, Observation of $H \to b\bar{b}$ decays and VH production with the ATLAS detector. Phys. Lett. B **786**, 59 (2018). https://doi.org/10.1016/j.physletb.2018.09.013. arXiv:1808.08238 [hep-ex]
10. ATLAS Collaboration, Observation of Higgs boson production in association with a top quark pair at the LHC with the ATLAS detector. Phys. Lett. B **784**, 173 (2018). https://doi.org/10.1016/j.physletb.2018.07.035. arXiv:1806.00425 [hep-ex]
11. CMS Collaboration, Observation of the Higgs boson decay to a pair of τ leptons with the CMS detector. Phys. Lett. B **779**, 283 (2018). https://doi.org/10.1016/j.physletb.2018.02.004. arXiv:1708.00373 [hep-ex]
12. CMS Collaboration, Observation of $t\bar{t}H$ production. Phys. Rev. Lett. **120**, 231801 (2018). https://doi.org/10.1103/PhysRevLett.120.231801. arXiv:1804.02610 [hep-ex]
13. CMS Collaboration, Observation of Higgs boson decay to bottom quarks. Phys. Rev. Lett. **121**, 121801 (2018). https://doi.org/10.1103/PhysRevLett.121.121801. arXiv:1808.08242 [hep-ex]
14. CMS Collaboration, Evidence for Higgs boson decay to a pair of muons. JHEP **01**, 148 (2021). https://doi.org/10.1007/JHEP01(2021)148. arXiv:2009.04363 [hep-ex]
15. ATLAS Collaboration, A search for the dimuon decay of the Standard Model Higgs boson with the ATLAS detector. Phys. Lett. B **812**, 135980 (2021). https://doi.org/10.1016/j.physletb.2020.135980. arXiv:2007.07830 [hep-ex]
16. ATLAS Collaboration, Search for the decay of the Higgs boson to charm quarks with the ATLAS experiment. Phys. Rev. Lett. **120**, 211802 (2018). https://doi.org/10.1103/PhysRevLett.120.211802. arXiv:1802.04329 [hep-ex]
17. CMS Collaboration, A search for the standard model Higgs boson decaying to charm quarks. JHEP **03**, 131 (2020). https://doi.org/10.1007/JHEP03(2020)131. arXiv:1912.01662 [hep-ex]
18. ATLAS Collaboration, Search for the Higgs boson decays $H \to ee$ and $H \to e\mu$ in pp collisions at $\sqrt{s} = 13$ TeV with the ATLAS detector. Phys. Lett. B **801**, 135148 (2020). https://doi.org/10.1016/j.physletb.2019.135148. arXiv:1909.10235 [hep-ex]
19. CMS Collaboration, Search for a standard model-like Higgs boson in the $\mu^+\mu^-$ and e^+e^- decay channels at the LHC. Phys. Lett. B **744**, 184 (2015). https://doi.org/10.1016/j.physletb.2015.03.048. arXiv:1410.6679 [hep-ex]
20. ATLAS Collaboration, Search for exclusive Higgs and Z boson decays to $\phi\gamma$ and $\rho\gamma$ with the ATLAS detector. JHEP **07**, 127 (2018). https://doi.org/10.1007/JHEP07(2018)127. arXiv:1712.02758 [hep-ex]
21. ATLAS Collaboration, Searches for exclusive Higgs and Z boson decays into $J/\psi\gamma$, $\psi(2S)\gamma$ and $\gamma(nS)_\gamma$ at $\sqrt{s} = 13$ TeV with the ATLAS detector. Phys. Lett. B **786**, 134 (2018). https://doi.org/10.1016/j.physletb.2018.09.024. arXiv:1807.00802 [hep-ex]
22. CMS Collaboration, Search for decays of the 125 GeV Higgs boson into a Z boson and a ρ or ϕ meson. JHEP **11**, 039 (2020). https://doi.org/10.1016/j.physletb.2018.09.024. arXiv:2007.05122 [hep-ex]
23. CMS Collaboration, Search for rare decays of Z and Higgs bosons to J/ψ and a photon in proton-proton collisions at $\sqrt{s} = 13$ TeV. Eur. Phys. J. C **79**, 94 (2019). https://doi.org/10.1007/JHEP11(2020)039. arXiv:1810.10056 [hep-ex]
24. G. Bodwin, F. Petriello, S. Stoynev, M. Velasco, Higgs boson decays to quarkonia and the $H\bar{c}c$ coupling. Phys. Rev. D **88**, 053003 (2013). https://doi.org/10.1140/epjc/s10052-019-6562-5. arXiv:1306.5770 [hep-ph]
25. A.L. Kagan et al., Exclusive window onto Higgs Yukawa couplings. Phys. Rev. Lett. **114**, 101802 (2015). https://doi.org/10.1103/PhysRevD.88.053003. arXiv:1406.1722 [hep-ph]
26. Y. Soreq, H.X. Zhu, J. Zupan, Light quark Yukawa couplings from Higgs kinematics. JHEP **12**, 045 (2016). https://doi.org/10.1103/PhysRevLett.114.101802. arXiv:1606.09621 [hep-ph]
27. ATLAS Collaboration, Measurements of the Higgs boson inclusive and differential fiducial cross-sections in the diphoton decay channel with 139 fb^{-1} of pp collisions at $\sqrt{s} = 13$ TeV with the ATLAS detector, CERN-EP-2021-227 (2022). arXiv:2202.00487 [hep-ex]
28. A. Djouadi, J. Kalinowski, M. Spira, HDECAY: a program for Higgs boson decays in the Standard Model and its supersymmetric extension. Comput. Phys. Commun. **108**, 56 (1998). https://doi.org/10.1016/S0010-4655(97)00123-9. arXiv:hep-ph/9704448
29. C. Delaunay, T. Golling, G. Perez, Y. Soreq, Enhanced Higgs boson coupling to charm pairs. Phys. Rev. D **89**, 033014 (2014). https://doi.org/10.1103/PhysRevD.89.033014
30. G. Perez, Y. Soreq, E. Stamou, K. Tobioka, Constraining the charm Yukawa and Higgs-quark coupling universality. Phys. Rev. D **92**, 033016 (2015). https://doi.org/10.1103/PhysRevD.92.033016
31. F. Botella, G. Branco, M. Rebelo, J. Silva-Marcos, What if the masses of the first two quark families are not generated by the standard model Higgs boson? Phys. Rev. D **94**, 115031 (2016). https://doi.org/10.1103/PhysRevD.94.115031. arXiv:1602.08011 [hep-ph]
32. S. Bar-Shalom, A. Soni, Universally enhanced light-quarks Yukawa couplings paradigm. Phys. Rev. D **98**, 055001 (2018). https://doi.org/10.1103/PhysRevD.98.055001
33. D. Ghosh, R.S. Gupta, G. Perez, Is the Higgs mechanism of fermion mass generation a fact? A Yukawa-less first-two-generation model. Phys. Lett. B **755**, 504 (2016). https://doi.org/10.1016/j.physletb.2016.02.059. (**issn: 0370-2693**)
34. D. Egana-Ugrinovic, S. Homiller, P.R. Meade, Aligned and spontaneous flavor violation. Phys. Rev. Lett. **123**, 031802 (2019). https://doi.org/10.1103/PhysRevLett.123.031802. arXiv:1811.00017 [hep-ph]
35. D. Egana-Ugrinovic, S. Homiller, P.R. Meade, Higgs bosons with large couplings to light quarks. Phys. Rev. D **100**, 115041 (2019). https://doi.org/10.1103/PhysRevD.100.115041. arXiv:1908.11376 [hep-ph]

36. ATLAS Collaboration, Measurements of WH and ZH production in the $H \to b\bar{b}$ decay channel in pp collisions at 13 TeV with the ATLAS detector. Eur. Phys. J. C **81**, 178 (2021). https://doi.org/10.1140/epjc/s10052-020-08677-2. arXiv:2007.02873 [hep-ex]
37. LHC Higgs Cross Section Working Group, S. Heinemeyer, C. Mariotti, G. Passarino and R. Tanaka (Eds.), Handbook of LHC Higgs Cross Sections: 3. Higgs Properties, CERN-2013-004 (2013). https://doi.org/10.5170/CERN-2013-004. arXiv:1307.1347 [hep-ph]
38. LHC Higgs Cross Section Working Group, D. de Florian, C. Grojean, F. Maltoni, C. Mariotti, A. Nikitenko, M. Pieri, P. Savard, M. Schumacher, R. Tanaka (Eds.), Handbook of LHC Higgs Cross Sections: 4. Deciphering the Nature of the Higgs Sector, CERN-2017-002 (2016). https://doi.org/10.23731/CYRM-2017-002. arXiv:1610.07922 [hep-ph]
39. ATLAS Collaboration, The ATLAS Experiment at the CERN Large Hadron Collider. JINST **3**, S08003 (2008). https://doi.org/10.1088/1748-0221/3/08/S08003
40. ATLAS Collaboration, Operation of the ATLAS trigger system in Run 2. JINST **15**, P10004 (2020). https://doi.org/10.1088/1748-0221/15/10/P10004. arXiv:2007.12539 [hep-ex]
41. ATLAS Collaboration, The ATLAS Collaboration Software and Firmware, ATL-SOFT-PUB-2021-001 (2021). https://cds.cern.ch/record/2767187
42. ATLAS Collaboration, Performance of the missing transverse momentum triggers for the ATLAS detector during Run-2 data taking. JHEP **08**, 080 (2020). https://doi.org/10.1007/JHEP08(2020)080. arXiv:2005.09554 [hep-ex]
43. ATLAS Collaboration, Performance of electron and photon triggers in ATLAS during LHC Run 2. Eur. Phys. J. C **80**, 47 (2020). https://doi.org/10.1140/epjc/s10052-019-7500-2. arXiv:1909.00761 [hep-ex]
44. ATLAS Collaboration, Performance of the ATLAS muon triggers in Run 2. JINST **15**, P09015 (2020). https://doi.org/10.1088/1748-0221/15/09/p09015. arXiv:2004.13447 [hep-ex]
45. ATLAS Collaboration, ATLAS data quality operations and performance for 2015–2018 data-taking. JINST **15**, P04003 (2020). https://doi.org/10.1088/1748-0221/15/04/P04003. arXiv:1911.04632 [physics.ins-det]
46. ATLAS Collaboration, Luminosity determination in pp collisions at $\sqrt{s} = 13$ TeV using the ATLAS detector at the LHC, ATLAS-CONF-2019-021 (2019). https://cds.cern.ch/record/2677054
47. ATLAS Collaboration, The ATLAS Simulation Infrastructure. Eur. Phys. J. C **70**, 823 (2010). https://doi.org/10.1140/epjc/s10052-010-1429-9. arXiv:1005.4568 [physics.ins-det]
48. GEANT4 Collaboration, S. Agostinelli et al., Geant4-a simulation toolkit, Nucl. Instrum. Methods A **506**, 250 (2003). https://doi.org/10.1016/S0168-9002(03)01368-8
49. T. Sjöstrand, S. Mrenna, P. Skands, A brief introduction to PYTHIA 8.1. Comput. Phys. Commun. **178**, 852 (2008). https://doi.org/10.1016/j.cpc.2008.01.036. arXiv:0710.3820 [hep-ph]
50. R.D. Ball et al., Parton distributions with LHC data. Nucl. Phys. B **867**, 244 (2013). https://doi.org/10.1016/j.nuclphysb.2012.10.003. arXiv:1207.1303 [hep-ph]
51. ATLAS Collaboration, The Pythia 8 A3 tune description of ATLAS minimum bias and inelastic measurements incorporating the Donnachie-Landshoff diffractive model, ATL-PHYS-PUB-2016-017 (2016). https://cds.cern.ch/record/2206965
52. D.J. Lange, The EvtGen particle decay simulation package. Nucl. Instrum. Methods A **462**, 152 (2001). https://doi.org/10.1016/S0168-9002(01)00089-4
53. T. Gleisberg et al., Event generation with SHERPA 1.1. JHEP **02**, 007 (2009). https://doi.org/10.1088/1126-6708/2009/02/007. arXiv:0811.4622 [hep-ph]
54. S. Höche, F. Krauss, S. Schumann, F. Siegert, QCD matrix elements and truncated showers. JHEP **05**, 053 (2009). https://doi.org/10.1088/1126-6708/2009/05/053. arXiv:0903.1219 [hep-ph]
55. F. Cascioli, P. Maierhöfer, S. Pozzorini, Scattering amplitudes with open loops. Phys. Rev. Lett. **108**, 111601 (2012). https://doi.org/10.1103/PhysRevLett.108.111601. arXiv:1111.5206 [hep-ph]
56. S. Frixione, P. Nason, C. Oleari, Matching NLO QCD computations with parton shower simulations: the POWHEG method. JHEP **11**, 070 (2007). https://doi.org/10.1088/1126-6708/2007/11/070. arXiv:0709.2092 [hep-ph]
57. S. Alioli, P. Nason, C. Oleari, E. Re, A general framework for implementing NLO calculations in shower Monte Carlo programs: the POWHEG BOX. JHEP **06**, 043 (2010). https://doi.org/10.1007/JHEP06(2010)043. arXiv:1002.2581 [hep-ph]
58. R.D. Ball et al., Parton distributions for the LHC run II. JHEP **04**, 040 (2015). https://doi.org/10.1007/JHEP04(2015)040. arXiv:1410.8849 [hep-ph]
59. T. Sjöstrand et al., An introduction to PYTHIA 8.2. Comput. Phys. Commun. **191**, 159 (2015). https://doi.org/10.1016/j.cpc.2015.01.024. arXiv:1410.3012 [hep-ph]
60. ATLAS Collaboration, Measurement of the Z/γ^* boson transverse momentum distribution in pp collisions at $\sqrt{s} = 7$ TeV with the ATLAS detector. JHEP **09**, 145 (2014). https://doi.org/10.1007/JHEP09(2014)145. arXiv:1406.3660 [hep-ex]
61. M.L. Ciccolini, S. Dittmaier, M. Krämer, Electroweak radiative corrections to associated WH and ZH production at hadron colliders. Phys. Rev. D **68**, 073003 (2003). https://doi.org/10.1103/PhysRevD.68.073003. arXiv:hep-ph/0306234
62. O. Brein, A. Djouadi, R. Harlander, NNLO QCD corrections to the Higgs-strahlung processes at hadron colliders. Phys. Lett. B **579**, 149 (2004). https://doi.org/10.1016/j.physletb.2003.10.112. arXiv:hep-ph/0307206
63. O. Brein, R. Harlander, M. Wiesemann, T. Zirke, Top-quark mediated effects in hadronic Higgs-Strahlung. Eur. Phys. J. C **72**, 1868 (2012). https://doi.org/10.1140/epjc/s10052-012-1868-6. arXiv:1111.0761 [hep-ph]
64. A. Denner, S. Dittmaier, S. Kallweit, A. Mück, HAWK 2.0: a Monte Carlo program for Higgs production in vector-boson fusion and Higgs strahlung at hadron colliders. Comput. Phys. Commun. **195**, 161 (2015). https://doi.org/10.1016/j.cpc.2015.04.021. arXiv:1412.5390 [hep-ph]
65. O. Brein, R.V. Harlander, T.J.E. Zirke, vh@nnlo-Higgs Strahlung at hadron colliders. Comput. Phys. Commun. **184**, 998 (2013). https://doi.org/10.1016/j.cpc.2012.11.002. arXiv:1210.5347 [hep-ph]
66. G. Cullen et al., Automated one-loop calculations with GOSAM. Eur. Phys. J. C **72**, 1889 (2012). https://doi.org/10.1140/epjc/s10052-012-1889-1. arXiv:1111.2034 [hep-ph]
67. K. Hamilton, P. Nason, G. Zanderighi, MINLO: multi-scale improved NLO. JHEP **10**, 155 (2012). https://doi.org/10.1007/JHEP10(2012)155. arXiv:1206.3572 [hep-ph]
68. G. Luisoni, P. Nason, C. Oleari, F. Tramontano, $HW^{\pm}/HZ + 0$ and 1 jet at NLO with the POWHEG BOX interfaced to GoSam and their merging within MiNLO. JHEP **10**, 083 (2013). https://doi.org/10.1007/JHEP10(2013)083. arXiv:1306.2542 [hep-ph]
69. L. Altenkamp, S. Dittmaier, R.V. Harlander, H. Rzehak, T.J.E. Zirke, Gluon-induced Higgs-strahlung at next-to-leading order QCD. JHEP **02**, 078 (2013). https://doi.org/10.1007/JHEP02(2013)078. arXiv:1211.5015 [hep-ph]
70. R.V. Harlander, A. Kulesza, V. Theeuwes, T. Zirke, Soft gluon resummation for gluon-induced Higgs Strahlung. JHEP **11**, 082 (2014). https://doi.org/10.1007/JHEP11(2014)082. arXiv:1410.0217 [hep-ph]
71. S. Frixione, P. Nason, G. Ridolfi, A positive-weight next-to-leading-order Monte Carlo for heavy flavour hadroproduction.

JHEP **09**, 126 (2007). https://doi.org/10.1088/1126-6708/2007/09/126. arXiv:0707.3088 [hep-ph]
72. ATLAS Collaboration, ATLAS Pythia 8 tunes to 7 TeV data, ATL-PHYS-PUB-2014-021 (2014). https://cds.cern.ch/record/1966419
73. M. Beneke, P. Falgari, S. Klein, C. Schwinn, Hadronic top-quark pair production with NNLL threshold resummation. Nucl. Phys. B **855**, 695 (2012). https://doi.org/10.1016/j.nuclphysb.2011.10.021. arXiv:1109.1536 [hep-ph]
74. M. Cacciari, M. Czakon, M. Mangano, A. Mitov, P. Nason, Top-pair production at hadron colliders with next-to-next-to-leading logarithmic soft-gluon resummation. Phys. Lett. B **710**, 612 (2012). https://doi.org/10.1016/j.physletb.2012.03.013. arXiv:1111.5869 [hep-ph]
75. P. Bärnreuther, M. Czakon, A. Mitov, Percent-level-precision physics at the Tevatron: next-to-next-to-leading order QCD corrections to $q\bar{q} \rightarrow t\bar{t} + X$. Phys. Rev. Lett. **109**, 132001 (2012). https://doi.org/10.1103/PhysRevLett.109.132001. arXiv:1204.5201 [hep-ph]
76. M. Czakon, A. Mitov, NNLO corrections to top-pair production at hadron colliders: the all-fermionic scattering channels. JHEP **12**, 054 (2012). https://doi.org/10.1007/JHEP12(2012)054. arXiv:1207.0236 [hep-ph]
77. M. Czakon, A. Mitov, NNLO corrections to top pair production at hadron colliders: the quark–gluon reaction. JHEP **01**, 080 (2013). https://doi.org/10.1007/JHEP01(2013)080. arXiv:1210.6832 [hep-ph]
78. M. Czakon, P. Fiedler, A. Mitov, Total top-quark pair-production cross section at hadron colliders through $O(\alpha_S^4)$. Phys. Rev. Lett. **110**, 252004 (2013). https://doi.org/10.1103/PhysRevLett.110.252004. arXiv:1303.6254 [hep-ph]
79. M. Czakon, A. Mitov, Top++: a program for the calculation of the top-pair cross-section at hadron colliders. Comput. Phys. Commun. **185**, 2930 (2014). https://doi.org/10.1016/j.cpc.2014.06.021. arXiv:1112.5675 [hep-ph]
80. S. Alioli, P. Nason, C. Oleari, E. Re, NLO single-top production matched with shower in POWHEG: s-and t-channel contributions. JHEP **09**, 111 (2009). https://doi.org/10.1088/1126-6708/2009/09/111. arXiv:0907.4076 [hep-ph] (**Erratum: JHEP 02 (2010) 011**)
81. M. Aliev et al., HATHOR-HAdronic top and heavy quarks crOss section calculatoR. Comput. Phys. Commun. **182**, 1034 (2011). https://doi.org/10.1016/j.cpc.2010.12.040. arXiv:1007.1327 [hep-ph]
82. P. Kant et al., HatHor for single top-quark production: Updated predictions and uncertainty estimates for single top-quark production in hadronic collisions. Comput. Phys. Commun. **191**, 74 (2015). https://doi.org/10.1016/j.cpc.2015.02.001. arXiv:1406.4403 [hep-ph]
83. E. Re, Single-top Wt-channel production matched with parton showers using the POWHEG method. Eur. Phys. J. C **71**, 1547 (2011). https://doi.org/10.1140/epjc/s10052-011-1547-z. arXiv:1009.2450 [hep-ph]
84. N. Kidonakis, Two-loop soft anomalous dimensions for single top quark associated production with a W^- or H^-. Phys. Rev. D **82**, 054018 (2010). https://doi.org/10.1103/PhysRevD.82.054018. arXiv:1005.4451 [hep-ph]
85. N. Kidonakis, Top quark production, in *Proceedings, Helmholtz International Summer School on Physics of Heavy Quarks and Hadrons* (HQ 2013) (JINR, Dubna, Russia, 15th-28th July 2013) 139. arXiv:1311.0283 [hep-ph]
86. C. Anastasiou, L.J. Dixon, K. Melnikov, F. Petriello, High precision QCD at hadron colliders: electroweak gauge boson rapidity distributions at next-to-next-to leading order. Phys. Rev. D **69**, 094008 (2004). https://doi.org/10.1103/PhysRevD.69.094008. arXiv:hep-ph/0312266
87. ATLAS Collaboration, Vertex Reconstruction Performance of the ATLAS Detector at $\sqrt{s} = 13$ TeV, ATL-PHYS-PUB-2015-026 (2015). https://cds.cern.ch/record/2037717
88. ATLAS Collaboration, Electron and photon performance measurements with the ATLAS detector using the 2015–2017 LHC proton–proton collision data. JINST **14**, P12006 (2019). https://doi.org/10.1088/1748-0221/14/12/P12006. arXiv:1908.00005 [hep-ex]
89. ATLAS Collaboration, Muon reconstruction and identification efficiency in ATLAS using the full Run 2 pp collision data set at $\sqrt{s} = 13$ TeV. Eur. Phys. J. C **81**, 578 (2021). https://doi.org/10.1140/epjc/s10052-021-09233-2. arXiv:2012.00578 [hep-ex]
90. ATLAS Collaboration, Reconstruction of hadronic decay products of tau leptons with the ATLAS experiment. Eur. Phys. J. C **76**, 295 (2016). https://doi.org/10.1140/epjc/s10052-016-4110-0. arXiv:1512.05955 [hep-ex]
91. ATLAS Collaboration, Measurement of the tau lepton reconstruction and identification performance in the ATLAS experiment using pp collisions at $\sqrt{s} = 13$ TeV, ATLAS-CONF-2017-029 (2017). https://cds.cern.ch/record/2261772
92. ATLAS Collaboration, Jet energy scale measurements and their systematic uncertainties in proton–proton collisions at $\sqrt{s} = 13$ TeV with the ATLAS detector. Phys. Rev. D **96**, 072002 (2017). https://doi.org/10.1103/PhysRevD.96.072002. arXiv:1703.09665 [hep-ex]
93. ATLAS Collaboration, Topological cell clustering in the ATLAS calorimeters and its performance in LHC Run 1. Eur. Phys. J. C **77**, 490 (2017). https://doi.org/10.1140/epjc/s10052-017-5004-5. arXiv:1603.02934 [hep-ex]
94. ATLAS Collaboration, Properties of jets and inputs to jet reconstruction and calibration with the ATLAS detector using proton-proton collisions at $\sqrt{s} = 13$ TeV, ATL-PHYS-PUB-2015-036 (2015). https://cds.cern.ch/record/2044564
95. M. Cacciari, G.P. Salam, G. Soyez, The anti-k_t jet clustering algorithm. JHEP **04**, 063 (2008). https://doi.org/10.1088/1126-6708/2008/04/063. arXiv:0802.1189 [hep-ph]
96. M. Cacciari, G.P. Salam, G. Soyez, FastJet user manual. Eur. Phys. J. C **72**, 1896 (2012). https://doi.org/10.1140/epjc/s10052-012-1896-2. arXiv:1111.6097 [hep-ph]
97. ATLAS Collaboration, Performance of pile-up mitigation techniques for jets in pp collisions at $\sqrt{s} = 8$ TeV using the ATLAS detector. Eur. Phys. J. C **76**, 581 (2016). https://doi.org/10.1140/epjc/s10052-016-4395-z. arXiv:1510.03823 [hep-ex]
98. ATLAS Collaboration, ATLAS b-jet identification performance and efficiency measurement with $t\bar{t}$ events in pp collisions at $\sqrt{s} = 13$ TeV. Eur. Phys. J. C **79**, 970 (2019). https://doi.org/10.1140/epjc/s10052-019-7450-8. arXiv:1907.05120 [hep-ex]
99. ATLAS Collaboration, Measurement of b-tagging efficiency of c-jets in $t\bar{t}$ events using a likelihood approach with the ATLAS detector, ATLAS-CONF-2018-001 (2018). https://cds.cern.ch/record/2306649
100. ATLAS Collaboration, Calibration of light-flavour b-jet mistagging rates using ATLAS proton-proton collision data at $\sqrt{s} = 13$ TeV, ATLAS-CONF-2018-006 (2018). https://cds.cern.ch/record/2314418
101. ATLAS Collaboration, Performance of missing transverse momentum reconstruction with the ATLAS detector using proton-proton collisions at $\sqrt{s} = 13$ TeV. Eur. Phys. J. C **78**, 903 (2018). https://doi.org/10.1140/epjc/s10052-018-6288-9. arXiv:1802.08168 [hep-ex]

102. ATLAS Collaboration, Performance of the ATLAS track reconstruction algorithms in dense environments in LHC Run 2. Eur. Phys. J. C **77**, 673 (2017). https://doi.org/10.1140/epjc/s10052-017-5225-7. arXiv:1704.07983 [hep-ex]
103. J.M. Butterworth, A.R. Davison, M. Rubin, G.P. Salam, Jet substructure as a new Higgs-search channel at the large hadron collider. Phys. Rev. Lett. **100**, 242001 (2008). https://doi.org/10.1103/PhysRevLett.100.242001. arXiv:0802.2470 [hep-ph]
104. G. Avoni et al., The new LUCID-2 detector for luminosity measurement and monitoring in ATLAS. JINST **13**, P07017 (2018). https://doi.org/10.1088/1748-0221/13/07/P07017
105. LHC Higgs Cross Section Working Group, S. Dittmaier, C. Mariotti, G. Passarino and R. Tanaka (Eds.), Handbook of LHC Higgs Cross Sections: 1. Inclusive Observables, CERN-2011-002 (2011). https://doi.org/10.5170/CERN-2011-002. arXiv:1101.0593 [hep-ph]
106. LHC Higgs Cross Section Working Group, S. Dittmaier, C. Mariotti, G. Passarino and R. Tanaka (Eds.), Handbook of LHC Higgs Cross Sections: 2. Differential Distributions, CERN-2012-002 (2012). https://doi.org/10.5170/CERN-2012-002. arXiv:1201.3084 [hep-ph]
107. J. Bellm et al., Herwig 7.0/Herwig++ 3.0 release note. Eur. Phys. J. C **76**, 196 (2016). https://doi.org/10.1140/epjc/s10052-016-4018-8. arXiv:1512.01178 [hep-ph]
108. J. Alwall et al., The automated computation of tree-level and next-to-leading order differential cross sections, and their matching to parton shower simulations. JHEP **07**, 079 (2014). https://doi.org/10.1007/JHEP07(2014)079. arXiv:1405.0301 [hep-ph]
109. S. Frixione, E. Laenen, P. Motylinski, C. White, B.R. Webber, Single-top hadroproduction in association with a W boson. JHEP **07**, 029 (2008). https://doi.org/10.1088/1126-6708/2008/07/029. arXiv:0805.3067 [hep-ph]
110. C.D. White, S. Frixione, E. Laenen, F. Maltoni, Isolating Wt production at the LHC. JHEP **11**, 074 (2009). https://doi.org/10.1088/1126-6708/2009/11/074. arXiv:0908.0631 [hep-ph]
111. R. Barlow, C. Beeston, Fitting using finite Monte Carlo samples. Comput. Phys. Commun. **77**, 219 (1993). https://doi.org/10.1016/0010-4655(93)90005-W
112. ATLAS Collaboration, Search for the $b\bar{b}$ decay of the Standard Model Higgs boson in associated (W/Z)H production with the ATLAS detector. JHEP **01**, 069 (2015). https://doi.org/10.1007/JHEP01(2015)069. arXiv:1409.6212 [hep-ex]
113. A.L. Read, Presentation of search results: the CL_S technique. J. Phys. G **28**, 2693 (2002). https://doi.org/10.1088/0954-3899/28/10/313
114. G. Cowan, K. Cranmer, E. Gross, O. Vitells, Asymptotic formulae for likelihood-based tests of new physics. Eur. Phys. J. C **71**, 1554 (2011). https://doi.org/10.1140/epjc/s10052-011-1554-0 arXiv:1007.1727 [physics.data-an] (**Erratum: Eur. Phys. J. C 73 (2013) 2501**)
115. W. Verkerke, D. Kirkby, The RooFit toolkit for data modeling (2003). arXiv:physics/0306116 [physics.data-an]
116. L. Moneta et al., The RooStats Project (2010). arXiv:1009.1003 [physics.data-an]
117. ATLAS Collaboration, A combination of measurements of Higgs boson production and decay using up to 139 fb^{-1} of proton–proton collision data at $\sqrt{s} = 13$ TeV collected with the ATLAS experiment, ATLAS-CONF-2020-027 (2020). https://cds.cern.ch/record/2725733
118. ATLAS Collaboration, Measurements of the Higgs boson inclusive and differential fiducial cross sections in the 4ℓ decay channel at $\sqrt{s} = 13TeV$. Eur. Phys. J. C **80**, 942 (2020). https://doi.org/10.1140/epjc/s10052-020-8223-0. arXiv:2004.03969 [hep-ex]
119. A. Bazavov et al., Up-, down-, strange-, charm-, and bottom-quark masses from four-flavor lattice QCD. Phys. Rev. D **98**, 054517 (2018). https://doi.org/10.1103/PhysRevD.98.054517
120. ATLAS Collaboration, ATLAS Computing Acknowledgements, ATL-SOFT-PUB-2021-003. https://cds.cern.ch/record/2776662

ATLAS Collaboration*

G. Aad[100], B. Abbott[126], D. C. Abbott[101], A. Abed Abud[36], K. Abeling[53], D. K. Abhayasinghe[93], S. H. Abidi[29], A. Aboulhorma[35e], H. Abramowicz[158], H. Abreu[157], Y. Abulaiti[123], A. C. Abusleme Hoffman[144a], B. S. Acharya[66a,66b,m], B. Achkar[53], L. Adam[98], C. Adam Bourdarios[4], L. Adamczyk[83a], L. Adamek[163], S. V. Addepalli[26], J. Adelman[118], A. Adiguzel[21c], S. Adorni[54], T. Adye[141], A. A. Affolder[143], Y. Afik[36], M. N. Agaras[13], J. Agarwala[70a,70b], A. Aggarwal[98], C. Agheorghiesei[27c], J. A. Aguilar-Saavedra[137a,137f,w], A. Ahmad[36], F. Ahmadov[79], W. S. Ahmed[102], X. Ai[46], G. Aielli[73a,73b], I. Aizenberg[176], M. Akbiyik[98], T. P. A. Åkesson[96], A. V. Akimov[109], K. Al Khoury[39], G. L. Alberghi[23b], J. Albert[172], P. Albicocco[51], M. J. Alconada Verzini[88], S. Alderweireldt[50], M. Aleksa[36], I. N. Aleksandrov[79], C. Alexa[27b], T. Alexopoulos[10], A. Alfonsi[117], F. Alfonsi[23b], M. Alhroob[126], B. Ali[139], S. Ali[155], M. Aliev[162], G. Alimonti[68a], C. Allaire[36], B. M. M. Allbrooke[153], P. P. Allport[20], A. Aloisio[69a,69b], F. Alonso[88], C. Alpigiani[145], E. Alunno Camelia[73a,73b], M. Alvarez Estevez[97], M. G. Alviggi[69a,69b], Y. Amaral Coutinho[80b], A. Ambler[102], L. Ambroz[132], C. Amelung[36], D. Amidei[104], S. P. Amor Dos Santos[137a], S. Amoroso[46], K. R. Amos[170], C. S. Amrouche[54], V. Ananiev[131], C. Anastopoulos[146], N. Andari[142], T. Andeen[11], J. K. Anders[19], S. Y. Andrean[45a,45b], A. Andreazza[68a,68b], S. Angelidakis[9], A. Angerami[39], A. V. Anisenkov[119a,119b], A. Annovi[71a], C. Antel[54], M. T. Anthony[146], E. Antipov[127], M. Antonelli[51], D. J. A. Antrim[17], F. Anulli[72a], M. Aoki[81], J. A. Aparisi Pozo[170], M. A. Aparo[153], L. Aperio Bella[46], C. Appelt[18], N. Aranzabal[36], V. Araujo Ferraz[80a], C. Arcangeletti[51], A. T. H. Arce[49], E. Arena[90], J-F. Arguin[108], S. Argyropoulos[52], J.-H. Arling[46], A. J. Armbruster[36], O. Arnaez[163], H. Arnold[117], Z. P. Arrubarrena Tame[112], G. Artoni[132], H. Asada[114], K. Asai[124], S. Asai[160], N. A. Asbah[59],

E. M. Asimakopoulou[168], J. Assahsah[35d], K. Assamagan[29], R. Astalos[28a], R. J. Atkin[33a], M. Atkinson[169], N. B. Atlay[18], H. Atmani[60b], P. A. Atmasiddha[104], K. Augsten[139], S. Auricchio[69a,69b], V. A. Austrup[178], G. Avner[157], G. Avolio[36], M. K. Ayoub[14c], G. Azuelos[108,ad], D. Babal[28a], H. Bachacou[142], K. Bachas[159], A. Bachiu[34], F. Backman[45a,45b], A. Badea[59], P. Bagnaia[72a,72b], M. Bahmani[18], A. J. Bailey[170], V. R. Bailey[169], J. T. Baines[141], C. Bakalis[10], O. K. Baker[179], P. J. Bakker[117], E. Bakos[15], D. Bakshi Gupta[8], S. Balaji[154], R. Balasubramanian[117], E. M. Baldin[119a,119b], P. Balek[140], E. Ballabene[68a,68b], F. Balli[142], L. M. Baltes[61a], W. K. Balunas[32], J. Balz[98], E. Banas[84], M. Bandieramonte[136], A. Bandyopadhyay[24], S. Bansal[24], L. Barak[158], E. L. Barberio[103], D. Barberis[55a,55b], M. Barbero[100], G. Barbour[94], K. N. Barends[33a], T. Barillari[113], M.-S. Barisits[36], J. Barkeloo[129], T. Barklow[150], R. M. Barnett[17], P. Baron[128], A. Baroncelli[60a], G. Barone[29], A. J. Barr[132], L. Barranco Navarro[45a,45b], F. Barreiro[97], J. Barreiro Guimarães da Costa[14a], U. Barron[158], S. Barsov[135], F. Bartels[61a], R. Bartoldus[150], G. Bartolini[100], A. E. Barton[89], P. Bartos[28a], A. Basalaev[46], A. Basan[98], M. Baselga[47], I. Bashta[74a,74b], A. Bassalat[64,aa], M. J. Basso[163], C. R. Basson[99], R. L. Bates[57], S. Batlamous[35e], J. R. Batley[32], B. Batool[148], M. Battaglia[143], M. Bauce[72a,72b], F. Bauer[142,*], P. Bauer[24], A. Bayirli[21a], J. B. Beacham[49], T. Beau[133], P. H. Beauchemin[166], F. Becherer[52], P. Bechtle[24], H. P. Beck[19,o], K. Becker[174], C. Becot[46], A. J. Beddall[21d], V. A. Bednyakov[79], C. P. Bee[152], L. J. Beemster[15], T. A. Beermann[36], M. Begalli[80b], M. Begel[29], A. Behera[152], J. K. Behr[46], C. Beirao Da Cruz E Silva[36], J. F. Beirer[36,53], F. Beisiegel[24], M. Belfkir[122b], G. Bella[158], L. Bellagamba[23b], A. Bellerive[34], P. Bellos[20], K. Beloborodov[119a,119b], K. Belotskiy[110], N. L. Belyaev[110], D. Benchekroun[35a], Y. Benhammou[158], D. P. Benjamin[29], M. Benoit[29], J. R. Bensinger[26], S. Bentvelsen[117], L. Beresford[36], M. Beretta[51], D. Berge[18], E. Bergeaas Kuutmann[168], N. Berger[4], B. Bergmann[139], J. Beringer[17], S. Berlendis[7], G. Bernardi[5], C. Bernius[150], F. U. Bernlochner[24], T. Berry[93], P. Berta[140], I. A. Bertram[89], O. Bessidskaia Bylund[178], S. Bethke[113], A. Betti[42], A. J. Bevan[92], S. Bhatta[152], D. S. Bhattacharya[173], P. Bhattarai[26], V. S. Bhopatkar[6], R. Bi[136], R. Bi[29], R. M. Bianchi[136], O. Biebel[112], R. Bielski[129], N. V. Biesuz[71a,71b], M. Biglietti[74a], T. R. V. Billoud[139], M. Bindi[53], A. Bingul[21b], C. Bini[72a,72b], S. Biondi[23a,23b], A. Biondini[90], C. J. Birch-sykes[99], G. A. Bird[20,141], M. Birman[176], T. Bisanz[36], J. P. Biswal[2], D. Biswas[177,i], A. Bitadze[99], K. Bjørke[131], I. Bloch[46], C. Blocker[26], A. Blue[57], U. Blumenschein[92], J. Blumenthal[98], G. J. Bobbink[117], V. S. Bobrovnikov[119a,119b], M. Boehler[52], D. Bogavac[13], A. G. Bogdanchikov[119a,119b], C. Bohm[45a], V. Boisvert[93], P. Bokan[46], T. Bold[83a], M. Bomben[5], M. Bona[92], M. Boonekamp[142], C. D. Booth[93], A. G. Borbély[57], H. M. Borecka-Bielska[108], L. S. Borgna[94], G. Borissov[89], D. Bortoletto[132], D. Boscherini[23b], M. Bosman[13], J. D. Bossio Sola[36], K. Bouaouda[35a], J. Boudreau[136], E. V. Bouhova-Thacker[89], D. Boumediene[38], R. Bouquet[5], A. Boveia[125], J. Boyd[36], D. Boye[29], I. R. Boyko[79], J. Bracinik[20], N. Brahimi[60c,60d], G. Brandt[178], O. Brandt[32], F. Braren[46], B. Brau[101], J. E. Brau[129], W. D. Breaden Madden[57], K. Brendlinger[46], R. Brener[176], L. Brenner[36], R. Brenner[168], S. Bressler[176], B. Brickwedde[98], D. Britton[57], D. Britzger[113], I. Brock[24], G. Brooijmans[39], W. K. Brooks[144f], E. Brost[29], P. A. Bruckman de Renstrom[84], B. Brüers[46], D. Bruncko[28b], A. Bruni[23b], G. Bruni[23b], M. Bruschi[23b], N. Bruscino[72a,72b], L. Bryngemark[150], T. Buanes[16], Q. Buat[145], P. Buchholz[148], A. G. Buckley[57], I. A. Budagov[79], M. K. Bugge[131], O. Bulekov[110], B. A. Bullard[59], S. Burdin[90], C. D. Burgard[46], A. M. Burger[38], B. Burghgrave[8], J. T. P. Burr[32], C. D. Burton[11], J. C. Burzynski[149], E. L. Busch[39], V. Büscher[98], P. J. Bussey[57], J. M. Butler[25], C. M. Buttar[57], J. M. Butterworth[94], W. Buttinger[141], C. J. Buxo Vazquez[105], A. R. Buzykaev[119a,119b], G. Cabras[23b], S. Cabrera Urbán[170], D. Caforio[56], H. Cai[136], Y. Cai[14a], V. M. M. Cairo[36], O. Cakir[3a], N. Calace[36], P. Calafiura[17], G. Calderini[133], P. Calfayan[65], G. Callea[57], L. P. Caloba[80b], D. Calvet[38], S. Calvet[38], T. P. Calvet[100], M. Calvetti[71a,71b], R. Camacho Toro[133], S. Camarda[36], D. Camarero Munoz[97], P. Camarri[73a,73b], M. T. Camerlingo[74a,74b], D. Cameron[131], C. Camincher[172], M. Campanelli[94], A. Camplani[40], V. Canale[69a,69b], A. Canesse[102], M. Cano Bret[77], J. Cantero[97], Y. Cao[169], F. Capocasa[26], M. Capua[41a,41b], A. Carbone[68a,68b], R. Cardarelli[73a], J. C. J. Cardenas[8], F. Cardillo[170], G. Carducci[41a,41b], T. Carli[36], G. Carlino[69a], B. T. Carlson[136], E. M. Carlson[164a,172], L. Carminati[68a,68b], M. Carnesale[72a,72b], S. Caron[116], E. Carquin[144f], S. Carrá[46], G. Carratta[23a,23b], J. W. S. Carter[163], T. M. Carter[50], D. Casadei[33c], M. P. Casado[13,f], A. F. Casha[163], E. G. Castiglia[179], F. L. Castillo[61a], L. Castillo Garcia[13], V. Castillo Gimenez[170], N. F. Castro[137a,137e], A. Catinaccio[36], J. R. Catmore[131], V. Cavaliere[29], N. Cavalli[23a,23b], V. Cavasinni[71a,71b], E. Celebi[21a], F. Celli[132], M. S. Centonze[67a,67b], K. Cerny[128], A. S. Cerqueira[80a], A. Cerri[153], L. Cerrito[73a,73b], F. Cerutti[17], A. Cervelli[23b], S. A. Cetin[21d], Z. Chadi[35a], D. Chakraborty[118], M. Chala[137f], J. Chan[177], W. S. Chan[117], W. Y. Chan[90], J. D. Chapman[32], B. Chargeishvili[156b],

D. G. Charlton[20], T. P. Charman[92], M. Chatterjee[19], S. Chekanov[6], S. V. Chekulaev[164a], G. A. Chelkov[79,y], A. Chen[104], B. Chen[158], B. Chen[172], C. Chen[60a], H. Chen[14c], H. Chen[29], J. Chen[60c], J. Chen[26], S. Chen[134], S. J. Chen[14c], X. Chen[60c], X. Chen[14b], Y. Chen[60a], C. L. Cheng[177], H. C. Cheng[62a], A. Cheplakov[79], E. Cheremushkina[46], E. Cherepanova[79], R. Cherkaoui El Moursli[35e], E. Cheu[7], K. Cheung[63], L. Chevalier[142], V. Chiarella[51], G. Chiarelli[71a], G. Chiodini[67a], A. S. Chisholm[20], A. Chitan[27b], Y. H. Chiu[172], M. V. Chizhov[79], K. Choi[11], A. R. Chomont[72a,72b], Y. Chou[101], Y. S. Chow[117], T. Chowdhury[33g], L. D. Christopher[33g], M. C. Chu[62a], X. Chu[14a,14d], J. Chudoba[138], J. J. Chwastowski[84], D. Cieri[113], K. M. Ciesla[84], V. Cindro[91], A. Ciocio[17], F. Cirotto[69a,69b], Z. H. Citron[176,j], M. Citterio[68a], D. A. Ciubotaru[27b], B. M. Ciungu[163], A. Clark[54], P. J. Clark[50], J. M. Clavijo Columbie[46], S. E. Clawson[99], C. Clement[45a,45b], L. Clissa[23a,23b], Y. Coadou[100], M. Cobal[66a,66c], A. Coccaro[55b], R. F. Coelho Barrue[137a], R. Coelho Lopes De Sa[101], S. Coelli[68a], H. Cohen[158], A. E. C. Coimbra[36], B. Cole[39], J. Collot[58], P. Conde Muiño[137a,137g], S. H. Connell[33c], I. A. Connelly[57], E. I. Conroy[132], F. Conventi[69a,ae], H. G. Cooke[20], A. M. Cooper-Sarkar[132], F. Cormier[171], L. D. Corpe[36], M. Corradi[72a,72b], E. E. Corrigan[96], F. Corriveau[102,u], M. J. Costa[170], F. Costanza[4], D. Costanzo[146], B. M. Cote[125], G. Cowan[93], J. W. Cowley[32], K. Cranmer[123], S. Crépé-Renaudin[58], F. Crescioli[133], M. Cristinziani[148], M. Cristoforetti[75a,75b], V. Croft[166], G. Crosetti[41a,41b], A. Cueto[36], T. Cuhadar Donszelmann[167], H. Cui[14a,14d], Z. Cui[7], A. R. Cukierman[150], W. R. Cunningham[57], F. Curcio[41a,41b], P. Czodrowski[36], M. M. Czurylo[61b], M. J. Da Cunha Sargedas De Sousa[60a], J. V. Da Fonseca Pinto[80b], C. Da Via[99], W. Dabrowski[83a], T. Dado[47], S. Dahbi[33g], T. Dai[104], C. Dallapiccola[101], M. Dam[40], G. D'amen[29], V. D'Amico[74a,74b], J. Damp[98], J. R. Dandoy[134], M. F. Daneri[30], M. Danninger[149], V. Dao[36], G. Darbo[55b], S. Darmora[6], A. Dattagupta[129], S. D'Auria[68a,68b], C. David[164b], T. Davidek[140], D. R. Davis[49], B. Davis-Purcell[34], I. Dawson[92], K. De[8], R. De Asmundis[69a], M. De Beurs[117], S. De Castro[23a,23b], N. De Groot[116], P. de Jong[117], H. De la Torre[105], A. De Maria[14c], A. De Salvo[72a], U. De Sanctis[73a,73b], M. De Santis[73a,73b], A. De Santo[153], J. B. De Vivie De Regie[58], D. V. Dedovich[79], J. Degens[117], A. M. Deiana[42], J. Del Peso[97], F. Del Rio[61a], F. Deliot[142], C. M. Delitzsch[47], M. Della Pietra[69a,69b], D. Della Volpe[54], A. Dell'Acqua[36], L. Dell'Asta[68a,68b], M. Delmastro[4], P. A. Delsart[58], S. Demers[179], M. Demichev[79], S. P. Denisov[120], L. D'Eramo[118], D. Derendarz[84], F. Derue[133], P. Dervan[90], K. Desch[24], K. Dette[163], C. Deutsch[24], P. O. Deviveiros[36], F. A. Di Bello[72a,72b], A. Di Ciaccio[73a,73b], L. Di Ciaccio[4], A. Di Domenico[72a,72b], C. Di Donato[69a,69b], A. Di Girolamo[36], G. Di Gregorio[71a,71b], A. Di Luca[75a,75b], B. Di Micco[74a,74b], R. Di Nardo[74a,74b], C. Diaconu[100], F. A. Dias[117], T. Dias Do Vale[149], M. A. Diaz[144a], F. G. Diaz Capriles[24], M. Didenko[170], E. B. Diehl[104], S. Díez Cornell[46], C. Diez Pardos[148], C. Dimitriadi[24,168], A. Dimitrievska[17], W. Ding[14b], J. Dingfelder[24], I.-M. Dinu[27b], S. J. Dittmeier[61b], F. Dittus[36], F. Djama[100], T. Djobava[156b], J. I. Djuvsland[16], D. Dodsworth[26], C. Doglioni[99,96], J. Dolejsi[140], Z. Dolezal[140], M. Donadelli[80c], B. Dong[60c], J. Donini[38], A. D'onofrio[14c], M. D'Onofrio[90], J. Dopke[141], A. Doria[69a], M. T. Dova[88], A. T. Doyle[57], E. Drechsler[149], E. Dreyer[176], A. S. Drobac[166], D. Du[60a], T. A. du Pree[117], F. Dubinin[109], M. Dubovsky[28a], E. Duchovni[176], G. Duckeck[112], O. A. Ducu[27b,36], D. Duda[113], A. Dudarev[36], M. D'uffizi[99], L. Duflot[64], M. Dührssen[36], C. Dülsen[178], A. E. Dumitriu[27b], M. Dunford[61a], S. Dungs[47], K. Dunne[45a,45b], A. Duperrin[100], H. Duran Yildiz[3a], M. Düren[56], A. Durglishvili[156b], B. Dutta[46], B. L. Dwyer[118], G. I. Dyckes[17], M. Dyndal[83a], S. Dysch[99], B. S. Dziedzic[84], B. Eckerova[28a], M. G. Eggleston[49], E. Egidio Purcino De Souza[80b], L. F. Ehrke[54], G. Eigen[16], K. Einsweiler[17], T. Ekelof[168], Y. El Ghazali[35b], H. El Jarrari[35e,155], A. El Moussaouy[35a], V. Ellajosyula[168], M. Ellert[168], F. Ellinghaus[178], A. A. Elliot[92], N. Ellis[36], J. Elmsheuser[29], M. Elsing[36], D. Emeliyanov[141], A. Emerman[39], Y. Enari[160], I. Ene[17], J. Erdmann[47], A. Ereditato[19], P. A. Erland[84], M. Errenst[178], M. Escalier[64], C. Escobar[170], E. Etzion[158], G. Evans[137a], H. Evans[65], M. O. Evans[153], A. Ezhilov[135], S. Ezzarqtouni[35a], F. Fabbri[57], L. Fabbri[23a,23b], G. Facini[174], V. Fadeyev[143], R. M. Fakhrutdinov[120], S. Falciano[72a], P. J. Falke[24], S. Falke[36], J. Faltova[140], Y. Fan[14a], Y. Fang[14a], G. Fanourakis[44], M. Fanti[68a,68b], M. Faraj[60c], A. Farbin[8], A. Farilla[74a], T. Farooque[105], S. M. Farrington[50], F. Fassi[35e], D. Fassouliotis[9], M. Faucci Giannelli[73a,73b], W. J. Fawcett[32], L. Fayard[64], O. L. Fedin[135,n], G. Fedotov[135], M. Feickert[169], L. Feligioni[100], A. Fell[146], D. E. Fellers[129], C. Feng[60b], M. Feng[14b], M. J. Fenton[167], A. B. Fenyuk[120], S. W. Ferguson[43], J. A. Fernandez Pretel[52], J. Ferrando[46], A. Ferrari[168], P. Ferrari[117], R. Ferrari[70a], D. Ferrere[54], C. Ferretti[104], F. Fiedler[98], A. Filipčič[91], E. K. Filmer[1], F. Filthaut[116], M. C. N. Fiolhais[137a,137c,a], L. Fiorini[170], F. Fischer[148], W. C. Fisher[105], T. Fitschen[20,64], I. Fleck[148], P. Fleischmann[104], T. Flick[178], L. Flores[134], M. Flores[33d], L. R. Flores Castillo[62a], F. M. Follega[75a,75b], N. Fomin[16], J. H. Foo[163], B. C. Forland[65], A. Formica[142],

A. C. Forti[99], E. Fortin[100], A. W. Fortman[59], M. G. Foti[17], L. Fountas[9], D. Fournier[64], H. Fox[89], P. Francavilla[71a,71b], S. Francescato[59], M. Franchini[23a,23b], S. Franchino[61a], D. Francis[36], L. Franco[4], L. Franconi[19], M. Franklin[59], G. Frattari[72a,72b], A. C. Freegard[92], P. M. Freeman[20], W. S. Freund[80b], E. M. Freundlich[47], D. Froidevaux[36], J. A. Frost[132], Y. Fu[60a], M. Fujimoto[124], E. Fullana Torregrosa[170], J. Fuster[170], A. Gabrielli[23a,23b], A. Gabrielli[36], P. Gadow[46], G. Gagliardi[55a,55b], L. G. Gagnon[17], G. E. Gallardo[132], E. J. Gallas[132], B. J. Gallop[141], R. Gamboa Goni[92], K. K. Gan[125], S. Ganguly[160], J. Gao[60a], Y. Gao[50], F. M. Garay Walls[144a,144b], B. Garcia[29], C. García[170], J. E. García Navarro[170], J. A. García Pascual[14a], M. Garcia-Sciveres[17], R. W. Gardner[37], D. Garg[77], R. B. Garg[150], S. Gargiulo[52], C. A. Garner[163], V. Garonne[29], S. J. Gasiorowski[145], P. Gaspar[80b], G. Gaudio[70a], P. Gauzzi[72a,72b], I. L. Gavrilenko[109], A. Gavrilyuk[121], C. Gay[171], G. Gaycken[46], E. N. Gazis[10], A. A. Geanta[27b], C. M. Gee[143], J. Geisen[96], M. Geisen[98], C. Gemme[55b], M. H. Genest[58], S. Gentile[72a,72b], S. George[93], W. F. George[20], T. Geralis[44], L. O. Gerlach[53], P. Gessinger-Befurt[36], M. Ghasemi Bostanabad[172], A. Ghosal[148], A. Ghosh[167], A. Ghosh[7], B. Giacobbe[23b], S. Giagu[72a,72b], N. Giangiacomi[163], P. Giannetti[71a], A. Giannini[60a], S. M. Gibson[93], M. Gignac[143], D. T. Gil[83b], B. J. Gilbert[39], D. Gillberg[34], G. Gilles[117], N. E. K. Gillwald[46], L. Ginabat[133], D. M. Gingrich[2,ad], M. P. Giordani[66a,66c], P. F. Giraud[142], G. Giugliarelli[66a,66c], D. Giugni[68a], F. Giuli[73a,73b], I. Gkialas[9,g], P. Gkountoumis[10], L. K. Gladilin[111], C. Glasman[97], G. R. Gledhill[129], M. Glisic[129], I. Gnesi[41b,c], Y. Go[29], M. Goblirsch-Kolb[26], D. Godin[108], S. Goldfarb[103], T. Golling[54], M. G. D. Gololo[33g], D. Golubkov[120], J. P. Gombas[105], A. Gomes[137a,137b], A. J. Gomez Delegido[170], R. Goncalves Gama[53], R. Gonçalo[137a,137c], G. Gonella[129], L. Gonella[20], A. Gongadze[79], F. Gonnella[20], J. L. Gonski[39], S. González de la Hoz[170], S. Gonzalez Fernandez[13], R. Gonzalez Lopez[90], C. Gonzalez Renteria[17], R. Gonzalez Suarez[168], S. Gonzalez-Sevilla[54], G. R. Gonzalvo Rodriguez[170], R. Y. González Andana[50], L. Goossens[36], N. A. Gorasia[20], P. A. Gorbounov[121], H. A. Gordon[29], B. Gorini[36], E. Gorini[67a,67b], A. Gorišek[91], A. T. Goshaw[49], M. I. Gostkin[79], C. A. Gottardo[116], M. Gouighri[35b], V. Goumarre[46], A. G. Goussiou[145], N. Govender[33c], C. Goy[4], I. Grabowska-Bold[83a], K. Graham[34], E. Gramstad[131], S. Grancagnolo[18], M. Grandi[153], V. Gratchev[135], P. M. Gravila[27f], F. G. Gravili[67a,67b], H. M. Gray[17], C. Grefe[24], I. M. Gregor[46], P. Grenier[150], K. Grevtsov[46], C. Grieco[13], A. A. Grillo[143], K. Grimm[31,k], S. Grinstein[13,s], J.-F. Grivaz[64], S. Groh[98], E. Gross[176], J. Grosse-Knetter[53], C. Grud[104], A. Grummer[115], J. C. Grundy[132], L. Guan[104], W. Guan[177], C. Gubbels[171], J. G. R. Guerrero Rojas[170], F. Guescini[113], D. Guest[18], R. Gugel[98], A. Guida[46], T. Guillemin[4], S. Guindon[36], F. Guo[14a], J. Guo[60c], L. Guo[64], Y. Guo[104], R. Gupta[46], S. Gurbuz[24], G. Gustavino[36], M. Guth[54], P. Gutierrez[126], L. F. Gutierrez Zagazeta[134], C. Gutschow[94], C. Guyot[142], C. Gwenlan[132], C. B. Gwilliam[90], E. S. Haaland[131], A. Haas[123], M. Habedank[46], C. Haber[17], H. K. Hadavand[8], A. Hadef[98], S. Hadzic[113], M. Haleem[173], J. Haley[127], J. J. Hall[146], G. D. Hallewell[100], L. Halser[19], K. Hamano[172], H. Hamdaoui[35e], M. Hamer[24], G. N. Hamity[50], J. Han[60b], K. Han[60a], L. Han[14c], L. Han[60a], S. Han[17], Y. F. Han[163], K. Hanagaki[81,q], M. Hance[143], D. A. Hangal[39], M. D. Hank[37], R. Hankache[99], E. Hansen[96], J. B. Hansen[40], J. D. Hansen[40], P. H. Hansen[40], K. Hara[165], D. Harada[54], T. Harenberg[178], S. Harkusha[106], Y. T. Harris[132], P. F. Harrison[174], N. M. Hartman[150], N. M. Hartmann[112], Y. Hasegawa[147], A. Hasib[50], S. Haug[19], R. Hauser[105], M. Havranek[139], C. M. Hawkes[20], R. J. Hawkings[36], S. Hayashida[114], D. Hayden[105], C. Hayes[104], R. L. Hayes[171], C. P. Hays[132], J. M. Hays[92], H. S. Hayward[90], F. He[60a], Y. He[161], Y. He[133], M. P. Heath[50], V. Hedberg[96], A. L. Heggelund[131], N. D. Hehir[92], C. Heidegger[52], K. K. Heidegger[52], W. D. Heidorn[78], J. Heilman[34], S. Heim[46], T. Heim[17], B. Heinemann[46,ab], J. G. Heinlein[134], J. J. Heinrich[129], L. Heinrich[36], J. Hejbal[138], L. Helary[46], A. Held[123], C. M. Helling[143], S. Hellman[45a,45b], C. Helsens[36], R. C. W. Henderson[89], L. Henkelmann[32], A. M. Henriques Correia[36], H. Herde[150], Y. Hernández Jiménez[152], H. Herr[98], M. G. Herrmann[112], T. Herrmann[48], G. Herten[52], R. Hertenberger[112], L. Hervas[36], N. P. Hessey[164a], H. Hibi[82], E. Higón-Rodriguez[170], S. J. Hillier[20], I. Hinchliffe[17], F. Hinterkeuser[24], M. Hirose[130], S. Hirose[165], D. Hirschbuehl[178], B. Hiti[91], O. Hladik[138], J. Hobbs[152], R. Hobincu[27e], N. Hod[176], M. C. Hodgkinson[146], B. H. Hodkinson[32], A. Hoecker[36], J. Hofer[46], D. Hohn[52], T. Holm[24], M. Holzbock[113], L. B. A. H. Hommels[32], B. P. Honan[99], J. Hong[60c], T. M. Hong[136], Y. Hong[53], J. C. Honig[52], A. Hönle[113], B. H. Hooberman[169], W. H. Hopkins[6], Y. Horii[114], L. A. Horyn[37], S. Hou[155], J. Howarth[57], J. Hoya[88], M. Hrabovsky[128], A. Hrynevich[107], T. Hryn'ova[4], P. J. Hsu[63], S.-C. Hsu[145], Q. Hu[39], S. Hu[60c], Y. F. Hu[14a,14d,af], D. P. Huang[94], X. Huang[14c], Y. Huang[60a], Y. Huang[14a], Z. Hubacek[139], M. Huebner[24], F. Huegging[24], T. B. Huffman[132], M. Huhtinen[36], S. K. Huiberts[16], R. Hulsken[58], N. Huseynov[12,x], J. Huston[105], J. Huth[59], R. Hyneman[150], S. Hyrych[28a], G. Iacobucci[54],

G. Iakovidis[29], I. Ibragimov[148], L. Iconomidou-Fayard[64], P. Iengo[36], R. Iguchi[160], T. Iizawa[54], Y. Ikegami[81], A. Ilg[19], N. Ilic[163], H. Imam[35a], T. Ingebretsen Carlson[45a,45b], G. Introzzi[70a,70b], M. Iodice[74a], V. Ippolito[72a,72b], M. Ishino[160], W. Islam[177], C. Issever[18,46], S. Istin[21a,ag], H. Ito[175], J. M. Iturbe Ponce[62a], R. Iuppa[75a,75b], A. Ivina[176], J. M. Izen[43], V. Izzo[69a], P. Jacka[138], P. Jackson[1], R. M. Jacobs[46], B. P. Jaeger[149], C. S. Jagfeld[112], G. Jäkel[178], K. Jakobs[52], T. Jakoubek[176], J. Jamieson[57], K. W. Janas[83a], G. Jarlskog[96], A. E. Jaspan[90], T. Javůrek[36], M. Javurkova[101], F. Jeanneau[142], L. Jeanty[129], J. Jejelava[156a,v], P. Jenni[52,d], S. Jézéquel[4], J. Jia[152], X. Jia[59], Z. Jia[14c], Y. Jiang[60a], S. Jiggins[50], J. Jimenez Pena[113], S. Jin[14c], A. Jinaru[27b], O. Jinnouchi[161], H. Jivan[33g], P. Johansson[146], K. A. Johns[7], C. A. Johnson[65], D. M. Jones[32], E. Jones[174], R. W. L. Jones[89], T. J. Jones[90], J. Jovicevic[15], X. Ju[17], J. J. Junggeburth[36], A. Juste Rozas[13,s], S. Kabana[144e], A. Kaczmarska[84], M. Kado[72a,72b], H. Kagan[125], M. Kagan[150], A. Kahn[39], A. Kahn[134], C. Kahra[98], T. Kaji[175], E. Kajomovitz[157], N. Kakati[176], C. W. Kalderon[29], A. Kamenshchikov[163], N. J. Kang[143], Y. Kano[114], D. Kar[33g], K. Karava[132], M. J. Kareem[164b], E. Karentzos[52], I. Karkanias[159], S. N. Karpov[79], Z. M. Karpova[79], V. Kartvelishvili[89], A. N. Karyukhin[120], E. Kasimi[159], C. Kato[60d], J. Katzy[46], S. Kaur[34], K. Kawade[147], K. Kawagoe[87], T. Kawaguchi[114], T. Kawamoto[142], G. Kawamura[53], E. F. Kay[172], F. I. Kaya[166], S. Kazakos[13], V. F. Kazanin[119a,119b], Y. Ke[152], J. M. Keaveney[33a], R. Keeler[172], G. V. Kehris[59], J. S. Keller[34], A. S. Kelly[94], D. Kelsey[153], J. J. Kempster[20], J. Kendrick[20], K. E. Kennedy[39], O. Kepka[138], S. Kersten[178], B. P. Kerševan[91], S. Ketabchi Haghighat[163], M. Khandoga[133], A. Khanov[127], A. G. Kharlamov[119a,119b], T. Kharlamova[119a,119b], E. E. Khoda[145], T. J. Khoo[18], G. Khoriauli[173], E. Khramov[79], J. Khubua[156b], M. Kiehn[36], A. Kilgallon[129], E. Kim[161], Y. K. Kim[37], N. Kimura[94], A. Kirchhoff[53], D. Kirchmeier[48], C. Kirfel[24], J. Kirk[141], A. E. Kiryunin[113], T. Kishimoto[160], D. P. Kisliuk[163], C. Kitsaki[10], O. Kivernyk[24], M. Klassen[61a], C. Klein[34], L. Klein[173], M. H. Klein[104], M. Klein[90], U. Klein[90], P. Klimek[36], A. Klimentov[29], F. Klimpel[113], T. Klingl[24], T. Klioutchnikova[36], F. F. Klitzner[112], P. Kluit[117], S. Kluth[113], E. Kneringer[76], T. M. Knight[163], A. Knue[52], D. Kobayashi[87], R. Kobayashi[85], M. Kocian[150], T. Kodama[160], P. Kodys[140], D. M. Koeck[153], P. T. Koenig[24], T. Koffas[34], N. M. Köhler[36], M. Kolb[142], I. Koletsou[4], T. Komarek[128], K. Köneke[52], A. X. Y. Kong[1], T. Kono[124], N. Konstantinidis[94], B. Konya[96], R. Kopeliansky[65], S. Koperny[83a], K. Korcyl[84], K. Kordas[159], G. Koren[158], A. Korn[94], S. Korn[53], I. Korolkov[13], N. Korotkova[111], B. Kortman[117], O. Kortner[113], S. Kortner[113], W. H. Kostecka[118], V. V. Kostyukhin[148,162], A. Kotsokechagia[64], A. Kotwal[49], A. Koulouris[36], A. Kourkoumeli-Charalampidi[70a,70b], C. Kourkoumelis[9], E. Kourlitis[6], O. Kovanda[153], R. Kowalewski[172], W. Kozanecki[142], A. S. Kozhin[120], V. A. Kramarenko[111], G. Kramberger[91], P. Kramer[98], M. W. Krasny[133], A. Krasznahorkay[36], J. A. Kremer[98], J. Kretzschmar[90], K. Kreul[18], P. Krieger[163], F. Krieter[112], S. Krishnamurthy[101], A. Krishnan[61b], M. Krivos[140], K. Krizka[17], K. Kroeninger[47], H. Kroha[113], J. Kroll[138], J. Kroll[134], K. S. Krowpman[105], U. Kruchonak[79], H. Krüger[24], N. Krumnack[78], M. C. Kruse[49], J. A. Krzysiak[84], A. Kubota[161], O. Kuchinskaia[162], S. Kuday[3a], D. Kuechler[46], J. T. Kuechler[46], S. Kuehn[36], T. Kuhl[46], V. Kukhtin[79], Y. Kulchitsky[106,x], S. Kuleshov[144b,144d], M. Kumar[33g], N. Kumari[100], M. Kuna[58], A. Kupco[138], T. Kupfer[47], O. Kuprash[52], H. Kurashige[82], L. L. Kurchaninov[164a], Y. A. Kurochkin[106], A. Kurova[110], E. S. Kuwertz[36], M. Kuze[161], A. K. Kvam[145], J. Kvita[128], T. Kwan[102], K. W. Kwok[62a], C. Lacasta[170], F. Lacava[72a,72b], H. Lacker[18], D. Lacour[133], N. N. Lad[94], E. Ladygin[79], B. Laforge[133], T. Lagouri[144e], S. Lai[53], I. K. Lakomiec[83a], N. Lalloue[58], J. E. Lambert[126], S. Lammers[65], W. Lampl[7], C. Lampoudis[159], E. Lançon[29], U. Landgraf[52], M. P. J. Landon[92], V. S. Lang[52], J. C. Lange[53], R. J. Langenberg[101], A. J. Lankford[167], F. Lanni[29], K. Lantzsch[24], A. Lanza[70a], A. Lapertosa[55a,55b], J. F. Laporte[142], T. Lari[68a], F. Lasagni Manghi[23b], M. Lassnig[36], V. Latonova[138], T. S. Lau[62a], A. Laudrain[98], A. Laurier[34], M. Lavorgna[69a,69b], S. D. Lawlor[93], Z. Lawrence[99], M. Lazzaroni[68a,68b], B. Le[99], B. Leban[91], A. Lebedev[78], M. LeBlanc[36], T. LeCompte[150], F. Ledroit-Guillon[58], A. C. A. Lee[94], G. R. Lee[16], L. Lee[59], S. C. Lee[155], L. L. Leeuw[33c], B. Lefebvre[164a], H. P. Lefebvre[93], M. Lefebvre[172], C. Leggett[17], K. Lehmann[149], G. Lehmann Miotto[36], W. A. Leight[101], A. Leisos[159,r], M. A. L. Leite[80c], C. E. Leitgeb[46], R. Leitner[140], K. J. C. Leney[42], T. Lenz[24], S. Leone[71a], C. Leonidopoulos[50], A. Leopold[151], C. Leroy[108], R. Les[105], C. G. Lester[32], M. Levchenko[135], J. Levêque[4], D. Levin[104], L. J. Levinson[176], D. J. Lewis[20], B. Li[14b], B. Li[60b], C. Li[60a], C.-Q. Li[60c,60d], H. Li[60a], H. Li[60b], H. Li[60b], J. Li[60c], K. Li[145], L. Li[60c], M. Li[14a,14d], Q. Y. Li[60a], S. Li[60c,60d,b], T. Li[60b], X. Li[46], Z. Li[60b], Z. Li[132], Z. Li[102], Z. Li[90], Z. Liang[14a], M. Liberatore[46], B. Liberti[73a], K. Lie[62c], J. Lieber Marin[80b], K. Lin[105], R. A. Linck[65], R. E. Lindley[7], J. H. Lindon[2], A. Linss[46], E. Lipeles[134], A. Lipniacka[16], T. M. Liss[169,ac], A. Lister[171], J. D. Little[4], B. Liu[14a], B. X. Liu[149], D. Liu[60c,60d], J. B. Liu[60a], J. K. K. Liu[32], K. Liu[60c,60d],

M. Liu[60a], M. Y. Liu[60a], P. Liu[14a], Q. Liu[60c,60d,145], X. Liu[60a], Y. Liu[46], Y. Liu[14c,14d], Y. L. Liu[104], Y. W. Liu[60a], M. Livan[70a,70b], J. Llorente Merino[149], S. L. Lloyd[92], E. M. Lobodzinska[46], P. Loch[7], S. Loffredo[73a,73b], T. Lohse[18], K. Lohwasser[146], M. Lokajicek[138], J. D. Long[169], I. Longarini[72a,72b], L. Longo[67a,67b], R. Longo[169], I. Lopez Paz[36], A. Lopez Solis[46], J. Lorenz[112], N. Lorenzo Martinez[4], A. M. Lory[112], A. Lösle[52], X. Lou[45a,45b], X. Lou[14a], A. Lounis[64], J. Love[6], P. A. Love[89], J. J. Lozano Bahilo[170], G. Lu[14a], M. Lu[77], S. Lu[134], Y. J. Lu[63], H. J. Lubatti[145], C. Luci[72a,72b], F. L. Lucio Alves[14c], A. Lucotte[58], F. Luehring[65], I. Luise[152], O. Lundberg[151], B. Lund-Jensen[151], N. A. Luongo[129], M. S. Lutz[158], D. Lynn[29], H. Lyons[90], R. Lysak[138], E. Lytken[96], F. Lyu[14a], V. Lyubushkin[79], T. Lyubushkina[79], H. Ma[29], L. L. Ma[60b], Y. Ma[94], D. M. Mac Donell[172], G. Maccarrone[51], J. C. MacDonald[146], R. Madar[38], W. F. Mader[48], J. Maeda[82], T. Maeno[29], M. Maerker[48], V. Magerl[52], J. Magro[66a,66c], D. J. Mahon[39], C. Maidantchik[80b], A. Maio[137a,137b,137d], K. Maj[83a], O. Majersky[28a], S. Majewski[129], N. Makovec[64], V. Maksimovic[15], B. Malaescu[133], Pa. Malecki[84], V. P. Maleev[135], F. Malek[58], D. Malito[41a,41b], U. Mallik[77], C. Malone[32], S. Maltezos[10], S. Malyukov[79], J. Mamuzic[170], G. Mancini[51], J. P. Mandalia[92], I. Mandić[91], L. Manhaes de Andrade Filho[80a], I. M. Maniatis[159], M. Manisha[142], J. Manjarres Ramos[48], D. C. Mankad[176], K. H. Mankinen[96], A. Mann[112], A. Manousos[76], B. Mansoulie[142], S. Manzoni[36], A. Marantis[159,r], G. Marchiori[5], M. Marcisovsky[138], L. Marcoccia[73a,73b], C. Marcon[96], M. Marinescu[20], M. Marjanovic[126], Z. Marshall[17], S. Marti-Garcia[170], T. A. Martin[174], V. J. Martin[50], B. Martin dit Latour[16], L. Martinelli[72a,72b], M. Martinez[13,s], P. Martinez Agullo[170], V. I. Martinez Outschoorn[101], P. Martinez Suarez[13], S. Martin-Haugh[141], V. S. Martoiu[27b], A. C. Martyniuk[94], A. Marzin[36], S. R. Maschek[113], L. Masetti[98], T. Mashimo[160], J. Masik[99], A. L. Maslennikov[119a,119b], L. Massa[23b], P. Massarotti[69a,69b], P. Mastrandrea[71a,71b], A. Mastroberardino[41a,41b], T. Masubuchi[160], T. Mathisen[168], A. Matic[112], N. Matsuzawa[160], J. Maurer[27b], B. Maček[91], D. A. Maximov[119a,119b], R. Mazini[155], I. Maznas[159], M. Mazza[105], S. M. Mazza[143], C. Mc Ginn[29], J. P. Mc Gowan[102], S. P. Mc Kee[104], T. G. McCarthy[113], W. P. McCormack[17], E. F. McDonald[103], A. E. McDougall[117], J. A. Mcfayden[153], G. Mchedlidze[156b], M. A. McKay[42], R. P. Mckenzie[33g], D. J. Mclaughlin[94], K. D. McLean[172], S. J. McMahon[141], P. C. McNamara[103], R. A. McPherson[172,u], J. E. Mdhluli[33g], S. Meehan[36], T. Megy[38], S. Mehlhase[112], A. Mehta[90], B. Meirose[43], D. Melini[157], B. R. Mellado Garcia[33g], A. H. Melo[53], F. Meloni[46], A. Melzer[24], E. D. Mendes Gouveia[137a], A. M. Mendes Jacques Da Costa[20], H. Y. Meng[163], L. Meng[89], S. Menke[113], M. Mentink[36], E. Meoni[41a,41b], C. Merlassino[132], L. Merola[69a,69b], C. Meroni[68a], G. Merz[104], O. Meshkov[109,111], J. K. R. Meshreki[148], J. Metcalfe[6], A. S. Mete[6], C. Meyer[65], J.-P. Meyer[142], M. Michetti[18], R. P. Middleton[141], L. Mijović[50], G. Mikenberg[176], M. Mikestikova[138], M. Mikuž[91], H. Mildner[146], A. Milic[163], C. D. Milke[42], D. W. Miller[37], L. S. Miller[34], A. Milov[176], D. A. Milstead[45a,45b], T. Min[14c], A. A. Minaenko[120], I. A. Minashvili[156b], L. Mince[57], A. I. Mincer[123], B. Mindur[83a], M. Mineev[79], Y. Minegishi[160], Y. Mino[85], L. M. Mir[13], M. Miralles Lopez[170], M. Mironova[132], T. Mitani[175], A. Mitra[174], V. A. Mitsou[170], O. Miu[163], P. S. Miyagawa[92], Y. Miyazaki[87], A. Mizukami[81], J. U. Mjörnmark[96], T. Mkrtchyan[61a], M. Mlynarikova[118], T. Moa[45a,45b], S. Mobius[53], K. Mochizuki[108], P. Moder[46], P. Mogg[112], A. F. Mohammed[14a], S. Mohapatra[39], G. Mokgatitswane[33g], B. Mondal[148], S. Mondal[139], K. Mönig[46], E. Monnier[100], L. Monsonis Romero[170], J. Montejo Berlingen[36], M. Montella[125], F. Monticelli[88], N. Morange[64], A. L. Moreira De Carvalho[137a], M. Moreno Llácer[170], C. Moreno Martinez[13], P. Morettini[55b], S. Morgenstern[174], D. Mori[149], M. Morii[59], M. Morinaga[160], V. Morisbak[131], A. K. Morley[36], L. Morvaj[36], P. Moschovakos[36], B. Moser[117], M. Mosidze[156b], T. Moskalets[52], P. Moskvitina[116], J. Moss[31,l], E. J. W. Moyse[101], S. Muanza[100], J. Mueller[136], R. Mueller[19], D. Muenstermann[89], G. A. Mullier[96], J. J. Mullin[134], D. P. Mungo[68a,68b], J. L. Munoz Martinez[13], F. J. Munoz Sanchez[99], M. Murin[99], W. J. Murray[174,141], A. Murrone[68a,68b], J. M. Muse[126], M. Muškinja[17], C. Mwewa[29], A. G. Myagkov[120,y], A. J. Myers[8], A. A. Myers[136], G. Myers[65], M. Myska[139], B. P. Nachman[17], O. Nackenhorst[47], A. Nag Nag[48], K. Nagai[132], K. Nagano[81], J. L. Nagle[29], E. Nagy[100], A. M. Nairz[36], Y. Nakahama[81], K. Nakamura[81], H. Nanjo[130], R. Narayan[42], E. A. Narayanan[115], I. Naryshkin[135], M. Naseri[34], C. Nass[24], G. Navarro[22a], J. Navarro-Gonzalez[170], R. Nayak[158], P. Y. Nechaeva[109], F. Nechansky[46], T. J. Neep[20], A. Negri[70a,70b], M. Negrini[23b], C. Nellist[116], C. Nelson[102], K. Nelson[104], S. Nemecek[138], M. Nessi[36,e], M. S. Neubauer[169], F. Neuhaus[98], J. Neundorf[46], R. Newhouse[171], P. R. Newman[20], C. W. Ng[136], Y. S. Ng[18], Y. W. Y. Ng[167], B. Ngair[35e], H. D. N. Nguyen[108], R. B. Nickerson[132], R. Nicolaidou[142], D. S. Nielsen[40], J. Nielsen[143], M. Niemeyer[53], N. Nikiforou[11], V. Nikolaenko[120,y], I. Nikolic-Audit[133], K. Nikolopoulos[20], P. Nilsson[29], H. R. Nindhito[54], A. Nisati[72a], N. Nishu[2], R. Nisius[113], S. J. Noacco Rosende[88], T. Nobe[160],

D. L. Noel[32], Y. Noguchi[85], I. Nomidis[133], M. A. Nomura[29], M. B. Norfolk[146], R. R. B. Norisam[94], J. Novak[91], T. Novak[46], O. Novgorodova[48], L. Novotny[139], R. Novotny[115], L. Nozka[128], K. Ntekas[167], E. Nurse[94], F. G. Oakham[34,ad], J. Ocariz[133], A. Ochi[82], I. Ochoa[137a], J. P. Ochoa-Ricoux[144a], S. Oda[87], S. Oerdek[168], A. Ogrodnik[83a], A. Oh[99], C. C. Ohm[151], H. Oide[161], R. Oishi[160], M. L. Ojeda[46], Y. Okazaki[85], M. W. O'Keefe[90], Y. Okumura[160], A. Olariu[27b], L. F. Oleiro Seabra[137a], S. A. Olivares Pino[144e], D. Oliveira Damazio[29], D. Oliveira Goncalves[80a], J. L. Oliver[167], M. J. R. Olsson[167], A. Olszewski[84], J. Olszowska[84], Ö. O. Öncel[52], D. C. O'Neil[149], A. P. O'neill[19], A. Onofre[137a,137e], P. U. E. Onyisi[11], R. G. Oreamuno Madriz[118], M. J. Oreglia[37], G. E. Orellana[88], D. Orestano[74a,74b], N. Orlando[13], R. S. Orr[163], V. O'Shea[57], R. Ospanov[60a], G. Otero y Garzon[30], H. Otono[87], P. S. Ott[61a], G. J. Ottino[17], M. Ouchrif[35d], J. Ouellette[29], F. Ould-Saada[131], M. Owen[57], R. E. Owen[141], K. Y. Oyulmaz[21a], V. E. Ozcan[21a], N. Ozturk[8], S. Ozturk[21d], J. Pacalt[128], H. A. Pacey[32], K. Pachal[49], A. Pacheco Pages[13], C. Padilla Aranda[13], S. Pagan Griso[17], G. Palacino[65], S. Palazzo[50], S. Palestini[36], M. Palka[83b], J. Pan[179], D. K. Panchal[11], C. E. Pandini[117], J. G. Panduro Vazquez[93], P. Pani[46], G. Panizzo[66a,66c], L. Paolozzi[54], C. Papadatos[108], S. Parajuli[42], A. Paramonov[6], C. Paraskevopoulos[10], D. Paredes Hernandez[62b], B. Parida[176], T. H. Park[163], A. J. Parker[31], M. A. Parker[32], F. Parodi[55a,55b], E. W. Parrish[118], V. A. Parrish[50], J. A. Parsons[39], U. Parzefall[52], B. Pascual Dias[108], L. Pascual Dominguez[158], V. R. Pascuzzi[17], F. Pasquali[117], E. Pasqualucci[72a], S. Passaggio[55b], F. Pastore[93], P. Pasuwan[45a,45b], J. R. Pater[99], A. Pathak[177], J. Patton[90], T. Pauly[36], J. Pearkes[150], M. Pedersen[131], R. Pedro[137a], S. V. Peleganchuk[119a,119b], O. Penc[138], C. Peng[62b], H. Peng[60a], M. Penzin[162], B. S. Peralva[80a], A. P. Pereira Peixoto[58], L. Pereira Sanchez[45a,45b], D. V. Perepelitsa[29], E. Perez Codina[164a], M. Perganti[10], L. Perini[68a,68b], H. Pernegger[36], S. Perrella[36], A. Perrevoort[116], O. Perrin[38], K. Peters[46], R. F. Y. Peters[99], B. A. Petersen[36], T. C. Petersen[40], E. Petit[100], V. Petousis[139], C. Petridou[159], A. Petrukhin[148], M. Pettee[17], N. E. Pettersson[36], K. Petukhova[140], A. Peyaud[142], R. Pezoa[144f], L. Pezzotti[36], G. Pezzullo[179], T. Pham[103], P. W. Phillips[141], M. W. Phipps[169], G. Piacquadio[152], E. Pianori[17], F. Piazza[68a,68b], R. Piegaia[30], D. Pietreanu[27b], A. D. Pilkington[99], M. Pinamonti[66a,66c], J. L. Pinfold[2], C. Pitman Donaldson[94], D. A. Pizzi[34], L. Pizzimento[73a,73b], A. Pizzini[117], M.-A. Pleier[29], V. Plesanovs[52], V. Pleskot[140], E. Plotnikova[79], G. Poddar[4], R. Poettgen[96], R. Poggi[54], L. Poggioli[133], I. Pogrebnyak[105], D. Pohl[24], I. Pokharel[53], S. Polacek[140], G. Polesello[70a], A. Poley[149,164a], R. Polifka[139], A. Polini[23b], C. S. Pollard[132], Z. B. Pollock[125], V. Polychronakos[29], D. Ponomarenko[110], L. Pontecorvo[36], S. Popa[27a], G. A. Popeneciu[27d], D. M. Portillo Quintero[164a], S. Pospisil[139], P. Postolache[27c], K. Potamianos[132], I. N. Potrap[79], C. J. Potter[32], H. Potti[1], T. Poulsen[46], J. Poveda[170], G. Pownall[46], M. E. Pozo Astigarraga[36], A. Prades Ibanez[170], P. Pralavorio[100], M. M. Prapa[44], D. Price[99], M. Primavera[67a], M. A. Principe Martin[97], M. L. Proffitt[145], N. Proklova[110], K. Prokofiev[62c], F. Prokoshin[79], G. Proto[73a,73b], S. Protopopescu[29], J. Proudfoot[6], M. Przybycien[83a], D. Pudzha[135], P. Puzo[64], D. Pyatiizbyantseva[110], J. Qian[104], Y. Qin[99], T. Qiu[92], A. Quadt[53], M. Queitsch-Maitland[24], G. Rabanal Bolanos[59], D. Rafanoharana[52], F. Ragusa[68a,68b], J. A. Raine[54], S. Rajagopalan[29], K. Ran[14a,14d], V. Raskina[133], D. F. Rassloff[61a], S. Rave[98], B. Ravina[57], I. Ravinovich[176], M. Raymond[36], A. L. Read[131], N. P. Readioff[146], D. M. Rebuzzi[70a,70b], G. Redlinger[29], K. Reeves[43], D. Reikher[158], A. Reiss[98], A. Rej[148], C. Rembser[36], A. Renardi[46], M. Renda[27b], M. B. Rendel[113], A. G. Rennie[57], S. Resconi[68a], M. Ressegotti[55a,55b], E. D. Resseguie[17], S. Rettie[94], B. Reynolds[125], E. Reynolds[17], M. Rezaei Estabragh[178], O. L. Rezanova[119a,119b], P. Reznicek[140], E. Ricci[75a,75b], R. Richter[113], S. Richter[45a,45b], E. Richter-Was[83b], M. Ridel[133], P. Rieck[123], P. Riedler[36], M. Rijssenbeek[152], A. Rimoldi[70a,70b], M. Rimoldi[46], L. Rinaldi[23a,23b], T. T. Rinn[169], M. P. Rinnagel[112], G. Ripellino[151], I. Riu[13], P. Rivadeneira[46], J. C. Rivera Vergara[172], F. Rizatdinova[127], E. Rizvi[92], C. Rizzi[54], B. A. Roberts[174], B. R. Roberts[17], S. H. Robertson[102,u], M. Robin[46], D. Robinson[32], C. M. Robles Gajardo[144f], M. Robles Manzano[98], A. Robson[57], A. Rocchi[73a,73b], C. Roda[71a,71b], S. Rodriguez Bosca[61a], Y. Rodriguez Garcia[22a], A. Rodriguez Rodriguez[52], A. M. Rodríguez Vera[164b], S. Roe[36], J. T. Roemer[167], A. R. Roepe[126], J. Roggel[178], O. Røhne[131], R. A. Rojas[172], B. Roland[52], C. P. A. Roland[65], J. Roloff[29], A. Romaniouk[110], M. Romano[23b], A. C. Romero Hernandez[169], N. Rompotis[90], M. Ronzani[123], L. Roos[133], S. Rosati[72a], B. J. Rosser[134], E. Rossi[4], E. Rossi[69a,69b], L. P. Rossi[55b], L. Rossini[46], R. Rosten[125], M. Rotaru[27b], B. Rottler[52], D. Rousseau[64], D. Rousso[32], G. Rovelli[70a,70b], A. Roy[169], A. Rozanov[100], Y. Rozen[157], X. Ruan[33g], A. J. Ruby[90], T. A. Ruggeri[1], F. Rühr[52], A. Ruiz-Martinez[170], A. Rummler[36], Z. Rurikova[52], N. A. Rusakovich[79], H. L. Russell[172], L. Rustige[38], J. P. Rutherfoord[7], E. M. Rüttinger[146], K. Rybacki[89], M. Rybar[140], E. B. Rye[131], A. Ryzhov[120], J. A. Sabater Iglesias[54], P. Sabatini[170], L. Sabetta[72a,72b], H.F-W. Sadrozinski[143], R. Sadykov[79],

F. Safai Tehrani[72a], B. Safarzadeh Samani[153], M. Safdari[150], S. Saha[102], M. Sahinsoy[113], A. Sahu[178], M. Saimpert[142], M. Saito[160], T. Saito[160], D. Salamani[36], G. Salamanna[74a,74b], A. Salnikov[150], J. Salt[170], A. Salvador Salas[13], D. Salvatore[41a,41b], F. Salvatore[153], A. Salzburger[36], D. Sammel[52], D. Sampsonidis[159], D. Sampsonidou[60c,60d], J. Sánchez[170], A. Sanchez Pineda[4], V. Sanchez Sebastian[170], H. Sandaker[131], C. O. Sander[46], I. G. Sanderswood[89], J. A. Sandesara[101], M. Sandhoff[178], C. Sandoval[22b], D. P. C. Sankey[141], A. Sansoni[51], C. Santoni[38], H. Santos[137a,137b], S. N. Santpur[17], A. Santra[176], K. A. Saoucha[146], A. Sapronov[79], J. G. Saraiva[137a,137d], J. Sardain[100], O. Sasaki[81], K. Sato[165], C. Sauer[61b], F. Sauerburger[52], E. Sauvan[4], P. Savard[163,ad], R. Sawada[160], C. Sawyer[141], L. Sawyer[95], I. Sayago Galvan[170], C. Sbarra[23b], A. Sbrizzi[23a,23b], T. Scanlon[94], J. Schaarschmidt[145], P. Schacht[113], D. Schaefer[37], U. Schäfer[98], A. C. Schaffer[64], D. Schaile[112], R. D. Schamberger[152], E. Schanet[112], C. Scharf[18], N. Scharmberg[99], V. A. Schegelsky[135], D. Scheirich[140], F. Schenck[18], M. Schernau[167], C. Scheulen[53], C. Schiavi[55a,55b], Z. M. Schillaci[26], E. J. Schioppa[67a,67b], M. Schioppa[41a,41b], B. Schlag[98], K. E. Schleicher[52], S. Schlenker[36], K. Schmieden[98], C. Schmitt[98], S. Schmitt[46], L. Schoeffel[142], A. Schoening[61b], P. G. Scholer[52], E. Schopf[132], M. Schott[98], J. Schovancova[36], S. Schramm[54], F. Schroeder[178], H-C. Schultz-Coulon[61a], M. Schumacher[52], B. A. Schumm[143], Ph. Schune[142], A. Schwartzman[150], T. A. Schwarz[104], Ph. Schwemling[142], R. Schwienhorst[105], A. Sciandra[143], G. Sciolla[26], F. Scuri[71a], F. Scutti[103], C. D. Sebastiani[90], K. Sedlaczek[47], P. Seema[18], S. C. Seidel[115], A. Seiden[143], B. D. Seidlitz[29], T. Seiss[37], C. Seitz[46], J. M. Seixas[80b], G. Sekhniaidze[69a], S. J. Sekula[42], L. Selem[4], N. Semprini-Cesari[23a,23b], S. Sen[49], V. Senthilkumar[170], L. Serin[64], L. Serkin[66a,66b], M. Sessa[74a,74b], H. Severini[126], S. Sevova[150], F. Sforza[55a,55b], A. Sfyrla[54], E. Shabalina[53], R. Shaheen[151], J. D. Shahinian[134], N. W. Shaikh[45a,45b], D. Shaked Renous[176], L. Y. Shan[14a], M. Shapiro[17], A. Sharma[36], A. S. Sharma[1], S. Sharma[46], P. B. Shatalov[121], K. Shaw[153], S. M. Shaw[99], P. Sherwood[94], L. Shi[94], C. O. Shimmin[179], Y. Shimogama[175], J. D. Shinner[93], I. P. J. Shipsey[132], S. Shirabe[54], M. Shiyakova[79], J. Shlomi[176], M. J. Shochet[37], J. Shojaii[103], D. R. Shope[151], S. Shrestha[125], E. M. Shrif[33g], M. J. Shroff[172], P. Sicho[138], A. M. Sickles[169], E. Sideras Haddad[33g], O. Sidiropoulou[36], A. Sidoti[23b], F. Siegert[48], Dj. Sijacki[15], F. Sili[88], J. M. Silva[20], M. V. Silva Oliveira[36], S. B. Silverstein[45a], S. Simion[64], R. Simoniello[36], E. L. Simpson[57], N. D. Simpson[96], S. Simsek[21d], S. Sindhu[53], P. Sinervo[163], V. Sinetckii[111], S. Singh[149], S. Singh[163], S. Sinha[46], S. Sinha[33g], M. Sioli[23a,23b], I. Siral[129], S. Yu. Sivoklokov[111], J. Sjölin[45a,45b], A. Skaf[53], E. Skorda[96], P. Skubic[126], M. Slawinska[84], V. Smakhtin[176], B. H. Smart[141], J. Smiesko[140], S. Yu. Smirnov[110], Y. Smirnov[110], L. N. Smirnova[111,p], O. Smirnova[96], E. A. Smith[37], H. A. Smith[132], R. Smith[150], M. Smizanska[89], K. Smolek[139], A. Smykiewicz[84], A. A. Snesarev[109], H. L. Snoek[117], S. Snyder[29], R. Sobie[172,u], A. Soffer[158], C. A. Solans Sanchez[36], E. Yu. Soldatov[110], U. Soldevila[170], A. A. Solodkov[120], S. Solomon[52], A. Soloshenko[79], K. Solovieva[52], O. V. Solovyanov[120], V. Solovyev[135], P. Sommer[146], H. Son[166], A. Sonay[13], W. Y. Song[164b], A. Sopczak[139], A. L. Sopio[94], F. Sopkova[28b], V. Sothilingam[61a], S. Sottocornola[70a,70b], R. Soualah[122c], A. M. Soukharev[119a,119b], Z. Soumaimi[35e], D. South[46], S. Spagnolo[67a,67b], M. Spalla[113], M. Spangenberg[174], F. Spanò[93], D. Sperlich[52], G. Spigo[36], M. Spina[153], S. Spinali[89], D. P. Spiteri[57], M. Spousta[140], E. J. Staats[34], A. Stabile[68a,68b], R. Stamen[61a], M. Stamenkovic[117], A. Stampekis[20], M. Standke[24], E. Stanecka[84], B. Stanislaus[17], M. M. Stanitzki[46], M. Stankaityte[132], B. Stapf[46], E. A. Starchenko[120], G. H. Stark[143], J. Stark[100], D. M. Starko[164b], P. Staroba[138], P. Starovoitov[61a], S. Stärz[102], R. Staszewski[84], G. Stavropoulos[44], J. Steentoft[168], P. Steinberg[29], A. L. Steinhebel[129], B. Stelzer[149,164a], H. J. Stelzer[136], O. Stelzer-Chilton[164a], H. Stenzel[56], T. J. Stevenson[153], G. A. Stewart[36], M. C. Stockton[36], G. Stoicea[27b], M. Stolarski[137a], S. Stonjek[113], A. Straessner[48], J. Strandberg[151], S. Strandberg[45a,45b], M. Strauss[126], T. Strebler[100], P. Strizenec[28b], R. Ströhmer[173], D. M. Strom[129], L. R. Strom[46], R. Stroynowski[42], A. Strubig[45a,45b], S. A. Stucci[29], B. Stugu[16], J. Stupak[126], N. A. Styles[46], D. Su[150], S. Su[60a], W. Su[60d,145,60c], X. Su[60a,64], K. Sugizaki[160], V. V. Sulin[109], M. J. Sullivan[90], D. M. S. Sultan[75a,75b], L. Sultanaliyeva[109], S. Sultansoy[3b], T. Sumida[85], S. Sun[104], S. Sun[177], O. Sunneborn Gudnadottir[168], M. R. Sutton[153], M. Svatos[138], M. Swiatlowski[164a], T. Swirski[173], I. Sykora[28a], M. Sykora[140], T. Sykora[140], D. Ta[98], K. Tackmann[46,t], A. Taffard[167], R. Tafirout[164a], R. H. M. Taibah[133], R. Takashima[86], K. Takeda[82], E. P. Takeva[50], Y. Takubo[81], M. Talby[100], A. A. Talyshev[119a,119b], K. C. Tam[62b], N. M. Tamir[158], A. Tanaka[160], J. Tanaka[160], R. Tanaka[64], J. Tang[60c], Z. Tao[171], S. Tapia Araya[78], S. Tapprogge[98], A. Tarek Abouelfadl Mohamed[105], S. Tarem[157], K. Tariq[60b], G. Tarna[27b], G. F. Tartarelli[68a], P. Tas[140], M. Tasevsky[138], E. Tassi[41a,41b], G. Tateno[160], Y. Tayalati[35e], G. N. Taylor[103], W. Taylor[164b], H. Teagle[90], A. S. Tee[177], R. Teixeira De Lima[150], P. Teixeira-Dias[93],

J. J. Teoh[163], K. Terashi[160], J. Terron[97], S. Terzo[13], M. Testa[51], R. J. Teuscher[163,u], N. Themistokleous[50], T. Theveneaux-Pelzer[18], O. Thielmann[178], D. W. Thomas[93], J. P. Thomas[20], E. A. Thompson[46], P. D. Thompson[20], E. Thomson[134], E. J. Thorpe[92], Y. Tian[53], V. O. Tikhomirov[109,z], Yu. A. Tikhonov[119a,119b], S. Timoshenko[110], E. X. L. Ting[1], P. Tipton[179], S. Tisserant[100], S. H. Tlou[33g], A. Tnourji[38], K. Todome[23a,23b], S. Todorova-Nova[140], S. Todt[48], M. Togawa[81], J. Tojo[87], S. Tokár[28a], K. Tokushuku[81], R. Tombs[32], M. Tomoto[81,114], L. Tompkins[150], P. Tornambe[101], E. Torrence[129], H. Torres[48], E. Torró Pastor[170], M. Toscani[30], C. Tosciri[37], D. R. Tovey[146], A. Traeet[16], I. S. Trandafir[27b], C. J. Treado[123], T. Trefzger[173], A. Tricoli[29], I. M. Trigger[164a], S. Trincaz-Duvoid[133], D. A. Trischuk[171], W. Trischuk[163], B. Trocmé[58], A. Trofymov[64], C. Troncon[68a], F. Trovato[153], L. Truong[33c], M. Trzebinski[84], A. Trzupek[84], F. Tsai[152], M. Tsai[104], A. Tsiamis[159], P. V. Tsiareshka[106], A. Tsirigotis[159,r], V. Tsiskaridze[152], E. G. Tskhadadze[156a], M. Tsopoulou[159], Y. Tsujikawa[85], I. I. Tsukerman[121], V. Tsulaia[17], S. Tsuno[81], O. Tsur[157], D. Tsybychev[152], Y. Tu[62b], A. Tudorache[27b], V. Tudorache[27b], A. N. Tuna[36], S. Turchikhin[79], I. Turk Cakir[3a], R. Turra[68a], P. M. Tuts[39], S. Tzamarias[159], P. Tzanis[10], E. Tzovara[98], K. Uchida[160], F. Ukegawa[165], P. A. Ulloa Poblete[144c], G. Unal[36], M. Unal[11], A. Undrus[29], G. Unel[167], K. Uno[160], J. Urban[28b], P. Urquijo[103], G. Usai[8], R. Ushioda[161], M. Usman[108], Z. Uysal[21b], V. Vacek[139], B. Vachon[102], K. O. H. Vadla[131], T. Vafeiadis[36], C. Valderanis[112], E. Valdes Santurio[45a,45b], M. Valente[164a], S. Valentinetti[23a,23b], A. Valero[170], A. Vallier[100], J. A. Valls Ferrer[170], T. R. Van Daalen[145], P. Van Gemmeren[6], S. Van Stroud[94], I. Van Vulpen[117], M. Vanadia[73a,73b], W. Vandelli[36], M. Vandenbroucke[142], E. R. Vandewall[127], D. Vannicola[158], L. Vannoli[55a,55b], R. Vari[72a], E. W. Varnes[7], C. Varni[17], T. Varol[155], D. Varouchas[64], K. E. Varvell[154], M. E. Vasile[27b], L. Vaslin[38], G. A. Vasquez[172], F. Vazeille[38], D. Vazquez Furelos[13], T. Vazquez Schroeder[36], J. Veatch[53], V. Vecchio[99], M. J. Veen[117], I. Veliscek[132], L. M. Veloce[163], F. Veloso[137a,137c], S. Veneziano[72a], A. Ventura[67a,67b], A. Verbytskyi[113], M. Verducci[71a,71b], C. Vergis[24], M. Verissimo De Araujo[80b], W. Verkerke[117], J. C. Vermeulen[117], C. Vernieri[150], P. J. Verschuuren[93], M. Vessella[101], M. L. Vesterbacka[123], M. C. Vetterli[149,ad], A. Vgenopoulos[159], N. Viaux Maira[144f], T. Vickey[146], O. E. Vickey Boeriu[146], G. H. A. Viehhauser[132], L. Vigani[61b], M. Villa[23a,23b], M. Villaplana Perez[170], E. M. Villhauer[50], E. Vilucchi[51], M. G. Vincter[34], G. S. Virdee[20], A. Vishwakarma[50], C. Vittori[23a,23b], I. Vivarelli[153], V. Vladimirov[174], E. Voevodina[113], M. Vogel[178], P. Vokac[139], J. Von Ahnen[46], E. Von Toerne[24], B. Vormwald[36], V. Vorobel[140], K. Vorobev[110], M. Vos[170], J. H. Vossebeld[90], M. Vozak[117], L. Vozdecky[92], N. Vranjes[15], M. Vranjes Milosavljevic[15], V. Vrba[139,*], M. Vreeswijk[117], N. K. Vu[100], R. Vuillermet[36], O. V. Vujinovic[98], I. Vukotic[37], S. Wada[165], C. Wagner[101], W. Wagner[178], S. Wahdan[178], H. Wahlberg[88], R. Wakasa[165], M. Wakida[114], V. M. Walbrecht[113], J. Walder[141], R. Walker[112], W. Walkowiak[148], A. M. Wang[59], A. Z. Wang[177], C. Wang[60a], C. Wang[60c], H. Wang[17], J. Wang[62a], P. Wang[42], R.-J. Wang[98], R. Wang[59], R. Wang[6], S. M. Wang[155], S. Wang[60b], T. Wang[60a], W. T. Wang[77], W. X. Wang[60a], X. Wang[14c], X. Wang[169], X. Wang[60c], Y. Wang[60d], Z. Wang[104], Z. Wang[49,60c,60d], Z. Wang[104], A. Warburton[102], R. J. Ward[20], N. Warrack[57], A. T. Watson[20], M. F. Watson[20], G. Watts[145], B. M. Waugh[94], A. F. Webb[11], C. Weber[29], M. S. Weber[19], S. A. Weber[34], S. M. Weber[61a], C. Wei[60a], Y. Wei[132], A. R. Weidberg[132], J. Weingarten[47], M. Weirich[98], C. Weiser[52], T. Wenaus[29], B. Wendland[47], T. Wengler[36], N. S. Wenke[113], N. Wermes[24], M. Wessels[61a], K. Whalen[129], A. M. Wharton[89], A. S. White[59], A. White[8], M. J. White[1], D. Whiteson[167], L. Wickremasinghe[130], W. Wiedenmann[177], C. Wiel[48], M. Wielers[141], N. Wieseotte[98], C. Wiglesworth[40], L. A. M. Wiik-Fuchs[52], D. J. Wilbern[126], H. G. Wilkens[36], D. M. Williams[39], H. H. Williams[134], S. Williams[32], S. Willocq[101], P. J. Windischhofer[132], F. Winklmeier[129], B. T. Winter[52], M. Wittgen[150], M. Wobisch[95], A. Wolf[98], R. Wölker[132], J. Wollrath[167], M. W. Wolter[84], H. Wolters[137a,137c], V. W. S. Wong[171], A. F. Wongel[46], S. D. Worm[46], B. K. Wosiek[84], K. W. Woźniak[84], K. Wraight[57], J. Wu[14a,14d], S. L. Wu[177], X. Wu[54], Y. Wu[60a], Z. Wu[142,60a], J. Wuerzinger[132], T. R. Wyatt[99], B. M. Wynne[50], S. Xella[40], L. Xia[14c], M. Xia[14b], J. Xiang[62c], X. Xiao[104], M. Xie[60a], X. Xie[60a], I. Xiotidis[153], D. Xu[14a], H. Xu[60a], H. Xu[60a], L. Xu[60a], R. Xu[134], T. Xu[60a], W. Xu[104], Y. Xu[14b], Z. Xu[60b], Z. Xu[150], B. Yabsley[154], S. Yacoob[33a], N. Yamaguchi[87], Y. Yamaguchi[161], H. Yamauchi[165], T. Yamazaki[17], Y. Yamazaki[82], J. Yan[60c], S. Yan[132], Z. Yan[25], H. J. Yang[60c,60d], H. T. Yang[17], S. Yang[60a], T. Yang[62c], X. Yang[60a], X. Yang[14a], Y. Yang[42], Z. Yang[104,60a], W.-M. Yao[17], Y. C. Yap[46], H. Ye[14c], J. Ye[42], S. Ye[29], X. Ye[60a], I. Yeletskikh[79], M. R. Yexley[89], P. Yin[39], K. Yorita[175], C. J. S. Young[52], C. Young[150], M. Yuan[104], R. Yuan[60b,h], X. Yue[61a], M. Zaazoua[35e], B. Zabinski[84], G. Zacharis[10], E. Zaid[50], A. M. Zaitsev[120,y], T. Zakareishvili[156b], N. Zakharchuk[34], S. Zambito[36], D. Zanzi[52], O. Zaplatilek[139], S. V. Zeißner[47], C. Zeitnitz[178], J. C. Zeng[169], D. T. Zenger Jr[26], O. Zenin[120], T. Ženiš[28a], S. Zenz[92], S. Zerradi[35a], D. Zerwas[64], B. Zhang[14c],

D. F. Zhang[146], G. Zhang[14b], J. Zhang[6], K. Zhang[14a], L. Zhang[14c], M. Zhang[169], R. Zhang[177], S. Zhang[104], X. Zhang[60c], X. Zhang[60b], Z. Zhang[64], H. Zhao[145], P. Zhao[49], T. Zhao[60b], Y. Zhao[143], Z. Zhao[60a], A. Zhemchugov[79], Z. Zheng[150], D. Zhong[169], B. Zhou[104], C. Zhou[177], H. Zhou[7], N. Zhou[60c], Y. Zhou[7], C. G. Zhu[60b], C. Zhu[14a,14d], H. L. Zhu[60a], H. Zhu[14a], J. Zhu[104], Y. Zhu[60a], X. Zhuang[14a], K. Zhukov[109], V. Zhulanov[119a,119b], D. Zieminska[65], N. I. Zimine[79], S. Zimmermann[52,*], J. Zinsser[61b], M. Ziolkowski[148], L. Živković[15], A. Zoccoli[23a,23b], K. Zoch[54], T. G. Zorbas[146], O. Zormpa[44], W. Zou[39], L. Zwalinski[36]

[1] Department of Physics, University of Adelaide, Adelaide, Australia
[2] Department of Physics, University of Alberta, Edmonton, AB, Canada
[3] [(a)]Department of Physics, Ankara University, Ankara, Turkey; [(b)]Division of Physics, TOBB University of Economics and Technology, Ankara, Turkey
[4] LAPP, Univ. Savoie Mont Blanc, CNRS/IN2P3, Annecy , France
[5] Université de Paris, CNRS/IN2P3, AstroParticule et Cosmologie, Paris, France
[6] High Energy Physics Division, Argonne National Laboratory, Argonne, IL, USA
[7] Department of Physics, University of Arizona, Tucson, AZ, USA
[8] Department of Physics, University of Texas at Arlington, Arlington, TX, USA
[9] Physics Department, National and Kapodistrian University of Athens, Athens, Greece
[10] Physics Department, National Technical University of Athens, Zografou, Greece
[11] Department of Physics, University of Texas at Austin, Austin, TX, USA
[12] Institute of Physics, Azerbaijan Academy of Sciences, Baku, Azerbaijan
[13] Institut de Física d'Altes Energies (IFAE), Barcelona Institute of Science and Technology, Barcelona, Spain
[14] [(a)]Institute of High Energy Physics, Chinese Academy of Sciences, Beijing, China; [(b)]Physics Department, Tsinghua University, Beijing, China; [(c)]Department of Physics, Nanjing University, Nanjing, China; [(d)]University of Chinese Academy of Science (UCAS), Beijing, China
[15] Institute of Physics, University of Belgrade, Belgrade, Serbia
[16] Department for Physics and Technology, University of Bergen, Bergen, Norway
[17] Physics Division, Lawrence Berkeley National Laboratory and University of California, Berkeley, CA, USA
[18] Institut für Physik, Humboldt Universität zu Berlin, Berlin, Germany
[19] Albert Einstein Center for Fundamental Physics and Laboratory for High Energy Physics, University of Bern, Bern, Switzerland
[20] School of Physics and Astronomy, University of Birmingham, Birmingham, UK
[21] [(a)]Department of Physics, Bogazici University, Istanbul, Turkey; [(b)]Department of Physics Engineering, Gaziantep University, Gaziantep, Turkey; [(c)]Department of Physics, Istanbul University, Istanbul, Turkey; [(d)]Istinye University, Sariyer, Istanbul, Turkey
[22] [(a)]Facultad de Ciencias y Centro de Investigaciónes, Universidad Antonio Nariño, Bogotá, Colombia; [(b)]Departamento de Física, Universidad Nacional de Colombia, Bogotá, Colombia
[23] [(a)]Dipartimento di Fisica e Astronomia A. Righi, Universitá di Bologna, Bologna, Italy; [(b)]INFN Sezione di Bologna, Bologna, Italy
[24] Physikalisches Institut, Universität Bonn, Bonn, Germany
[25] Department of Physics, Boston University, Boston, MA, USA
[26] Department of Physics, Brandeis University, Waltham, MA, USA
[27] [(a)]Transilvania University of Brasov, Brasov, Romania; [(b)]Horia Hulubei National Institute of Physics and Nuclear Engineering, Bucharest, Romania; [(c)]Department of Physics, Alexandru Ioan Cuza University of Iasi, Iasi, Romania; [(d)]National Institute for Research and Development of Isotopic and Molecular Technologies, Physics Department, Cluj-Napoca, Romania; [(e)]University Politehnica Bucharest, Bucharest, Romania; [(f)]West University in Timisoara, Timisoara, Romania
[28] [(a)]Faculty of Mathematics, Physics and Informatics, Comenius University, Bratislava, Slovak Republic; [(b)]Department of Subnuclear Physics, Institute of Experimental Physics of the Slovak Academy of Sciences, Kosice, Slovak Republic
[29] Physics Department, Brookhaven National Laboratory, Upton, NY, USA
[30] Departamento de Física (FCEN) and IFIBA, Universidad de Buenos Aires and CONICET, Buenos Aires, Argentina
[31] California State University, Long Beach, CA, USA
[32] Cavendish Laboratory, University of Cambridge, Cambridge, UK

[33] [(a)]Department of Physics, University of Cape Town, Cape Town, South Africa; [(b)]iThemba Labs, Johannesburg, Western Cape, South Africa; [(c)]Department of Mechanical Engineering Science, University of Johannesburg, Johannesburg, South Africa; [(d)]National Institute of Physics, University of the Philippines Diliman (Philippines), Quezon City, Philippines; [(e)]Department of Physics, University of South Africa, Pretoria, South Africa; [(f)]University of Zululand, KwaDlangezwa, South Africa; [(g)]School of Physics, University of the Witwatersrand, Johannesburg, South Africa
[34] Department of Physics, Carleton University, Ottawa, ON, Canada
[35] [(a)]Faculté des Sciences Ain Chock, Réseau Universitaire de Physique des Hautes Energies-Université Hassan II, Casablanca, Morocco; [(b)]Faculté des Sciences, Université Ibn-Tofail, Kenitra, Morocco; [(c)]Faculté des Sciences Semlalia, Université Cadi Ayyad, LPHEA-Marrakech, Marrakech, Morocco; [(d)]LPMR, Faculté des Sciences, Université Mohamed Premier, Oujda, Morocco; [(e)]Faculté des sciences, Université Mohammed V, Rabat, Morocco; [(f)]Mohammed VI Polytechnic University, Ben Guerir, Morocco
[36] CERN, Geneva, Switzerland
[37] Enrico Fermi Institute, University of Chicago, Chicago, IL, USA
[38] LPC, Université Clermont Auvergne, CNRS/IN2P3, Clermont-Ferrand, France
[39] Nevis Laboratory, Columbia University, Irvington, NY, USA
[40] Niels Bohr Institute, University of Copenhagen, Copenhagen, Denmark
[41] [(a)]Dipartimento di Fisica, Università della Calabria, Rende, Italy; [(b)]INFN Gruppo Collegato di Cosenza, Laboratori Nazionali di Frascati, Frascati, Italy
[42] Physics Department, Southern Methodist University, Dallas, TX, USA
[43] Physics Department, University of Texas at Dallas, Richardson, TX, USA
[44] National Centre for Scientific Research "Demokritos", Agia Paraskevi, Greece
[45] [(a)]Department of Physics, Stockholm University, Sweden; [(b)]Oskar Klein Centre, Stockholm, Sweden
[46] Deutsches Elektronen-Synchrotron DESY, Hamburg and Zeuthen, Germany
[47] Fakultät Physik , Technische Universität Dortmund, Dortmund, Germany
[48] Institut für Kern- und Teilchenphysik, Technische Universität Dresden, Dresden, Germany
[49] Department of Physics, Duke University, Durham, NC, USA
[50] SUPA-School of Physics and Astronomy, University of Edinburgh, Edinburgh, UK
[51] INFN e Laboratori Nazionali di Frascati, Frascati, Italy
[52] Physikalisches Institut, Albert-Ludwigs-Universität Freiburg, Freiburg, Germany
[53] II. Physikalisches Institut, Georg-August-Universität Göttingen, Göttingen, Germany
[54] Département de Physique Nucléaire et Corpusculaire, Université de Genève, Geneva, Switzerland
[55] [(a)]Dipartimento di Fisica, Università di Genova, Genoa, Italy; [(b)]INFN Sezione di Genova, Genoa, Italy
[56] II. Physikalisches Institut, Justus-Liebig-Universität Giessen, Giessen, Germany
[57] SUPA-School of Physics and Astronomy, University of Glasgow, Glasgow, UK
[58] LPSC, Université Grenoble Alpes, CNRS/IN2P3, Grenoble INP, Grenoble, France
[59] Laboratory for Particle Physics and Cosmology, Harvard University, Cambridge, MA, USA
[60] [(a)]Department of Modern Physics and State Key Laboratory of Particle Detection and Electronics, University of Science and Technology of China, Hefei, China; [(b)]Institute of Frontier and Interdisciplinary Science and Key Laboratory of Particle Physics and Particle Irradiation (MOE), Shandong University, Qingdao, China; [(c)]School of Physics and Astronomy, Shanghai Jiao Tong University, Key Laboratory for Particle Astrophysics and Cosmology (MOE), SKLPPC, Shanghai, China; [(d)]Tsung-Dao Lee Institute, Shanghai, China
[61] [(a)]Kirchhoff-Institut für Physik, Ruprecht-Karls-Universität Heidelberg, Heidelberg, Germany; [(b)]Physikalisches Institut, Ruprecht-Karls-Universität Heidelberg, Heidelberg, Germany
[62] [(a)]Department of Physics, Chinese University of Hong Kong, Shatin, N.T., Hong Kong, China; [(b)]Department of Physics, University of Hong Kong, Hong Kong, China; [(c)]Department of Physics and Institute for Advanced Study, Hong Kong University of Science and Technology, Clear Water Bay, Kowloon, Hong Kong, China
[63] Department of Physics, National Tsing Hua University, Hsinchu, Taiwan
[64] IJCLab, Université Paris-Saclay, CNRS/IN2P3, 91405 Orsay, France
[65] Department of Physics, Indiana University, Bloomington, IN, USA
[66] [(a)]INFN Gruppo Collegato di Udine, Sezione di Trieste, Udine, Italy; [(b)]ICTP, Trieste, Italy; [(c)]Dipartimento Politecnico di Ingegneria e Architettura, Università di Udine, Udine, Italy
[67] [(a)]INFN Sezione di Lecce, Lecce, Italy; [(b)]Dipartimento di Matematica e Fisica, Università del Salento, Lecce, Italy
[68] [(a)]INFN Sezione di Milano, Milan, Italy; [(b)]Dipartimento di Fisica, Università di Milano, Milan, Italy

[69] [(a)]INFN Sezione di Napoli, Naples, Italy; [(b)]Dipartimento di Fisica, Università di Napoli, Naples, Italy
[70] [(a)]INFN Sezione di Pavia, Pavia, Italy; [(b)]Dipartimento di Fisica, Università di Pavia, Pavia, Italy
[71] [(a)]INFN Sezione di Pisa, Pisa, Italy; [(b)]Dipartimento di Fisica E. Fermi, Università di Pisa, Pisa, Italy
[72] [(a)]INFN Sezione di Roma, Rome, Italy; [(b)]Dipartimento di Fisica, Sapienza Università di Roma, Rome, Italy
[73] [(a)]INFN Sezione di Roma Tor Vergata, Rome, Italy; [(b)]Dipartimento di Fisica, Università di Roma Tor Vergata, Rome, Italy
[74] [(a)]INFN Sezione di Roma Tre, Rome, Italy; [(b)]Dipartimento di Matematica e Fisica, Università Roma Tre, Rome, Italy
[75] [(a)]INFN-TIFPA, Rome, Italy; [(b)]Università degli Studi di Trento, Trento, Italy
[76] Institut für Astro- und Teilchenphysik, Leopold-Franzens-Universität, Innsbruck, Austria
[77] University of Iowa, Iowa City, IA, USA
[78] Department of Physics and Astronomy, Iowa State University, Ames, IA, USA
[79] Joint Institute for Nuclear Research, Dubna, Russia
[80] [(a)]Departamento de Engenharia Elétrica, Universidade Federal de Juiz de Fora (UFJF), Juiz de Fora, Brazil; [(b)]Universidade Federal do Rio De Janeiro COPPE/EE/IF, Rio de Janeiro, Brazil; [(c)]Instituto de Física, Universidade de São Paulo, São Paulo, Brazil; [(d)]Rio de Janeiro State University, Rio de Janeiro, Brazil
[81] KEK, High Energy Accelerator Research Organization, Tsukuba, Japan
[82] Graduate School of Science, Kobe University, Kobe, Japan
[83] [(a)]AGH University of Science and Technology, Faculty of Physics and Applied Computer Science, Kraków, Poland; [(b)]Marian Smoluchowski Institute of Physics, Jagiellonian University, Kraków, Poland
[84] Institute of Nuclear Physics Polish Academy of Sciences, Kraków, Poland
[85] Faculty of Science, Kyoto University, Kyoto, Japan
[86] Kyoto University of Education, Kyoto, Japan
[87] Research Center for Advanced Particle Physics and Department of Physics, Kyushu University, Fukuoka , Japan
[88] Instituto de Física La Plata, Universidad Nacional de La Plata and CONICET, La Plata, Argentina
[89] Physics Department, Lancaster University, Lancaster, UK
[90] Oliver Lodge Laboratory, University of Liverpool, Liverpool, UK
[91] Department of Experimental Particle Physics, Jožef Stefan Institute and Department of Physics, University of Ljubljana, Ljubljana, Slovenia
[92] School of Physics and Astronomy, Queen Mary University of London, London, UK
[93] Department of Physics, Royal Holloway University of London, Egham, UK
[94] Department of Physics and Astronomy, University College London, London, UK
[95] Louisiana Tech University, Ruston, LA, USA
[96] Fysiska institutionen, Lunds universitet, Lund, Sweden
[97] Departamento de Física Teorica C-15 and CIAFF, Universidad Autónoma de Madrid, Madrid, Spain
[98] Institut für Physik, Universität Mainz, Mainz, Germany
[99] School of Physics and Astronomy, University of Manchester, Manchester, UK
[100] CPPM, Aix-Marseille Université, CNRS/IN2P3, Marseille, France
[101] Department of Physics, University of Massachusetts, Amherst, MA, USA
[102] Department of Physics, McGill University, Montreal, QC, Canada
[103] School of Physics, University of Melbourne, Victoria, Australia
[104] Department of Physics, University of Michigan, Ann Arbor, MI, USA
[105] Department of Physics and Astronomy, Michigan State University, East Lansing, MI, USA
[106] B.I. Stepanov Institute of Physics, National Academy of Sciences of Belarus, Minsk, Belarus
[107] Research Institute for Nuclear Problems of Byelorussian State University, Minsk, Belarus
[108] Group of Particle Physics, University of Montreal, Montreal, QC, Canada
[109] P.N. Lebedev Physical Institute of the Russian Academy of Sciences, Moscow, Russia
[110] National Research Nuclear University MEPhI, Moscow, Russia
[111] D.V. Skobeltsyn Institute of Nuclear Physics, M.V. Lomonosov Moscow State University, Moscow, Russia
[112] Fakultät für Physik, Ludwig-Maximilians-Universität München, Munich, Germany
[113] Max-Planck-Institut für Physik (Werner-Heisenberg-Institut), Munich, Germany
[114] Graduate School of Science and Kobayashi-Maskawa Institute, Nagoya University, Nagoya, Japan
[115] Department of Physics and Astronomy, University of New Mexico, Albuquerque, NM, USA
[116] Institute for Mathematics, Astrophysics and Particle Physics, Radboud University/Nikhef, Nijmegen, The Netherlands

[117] Nikhef National Institute for Subatomic Physics and University of Amsterdam, Amsterdam, The Netherlands
[118] Department of Physics, Northern Illinois University, DeKalb, IL, USA
[119] [(a)]Budker Institute of Nuclear Physics and NSU, SB RAS, Novosibirsk, Russia; [(b)]Novosibirsk State University, Novosibirsk, Russia
[120] Institute for High Energy Physics of the National Research Centre Kurchatov Institute, Protvino, Russia
[121] Institute for Theoretical and Experimental Physics named by A.I. Alikhanov of National Research Centre "Kurchatov Institute", Moscow, Russia
[122] [(a)]New York University Abu Dhabi, Abu Dhabi, United Arab Emirates; [(b)]United Arab Emirates University, Al Ain, United Arab Emirates; [(c)]University of Sharjah, Sharjah, United Arab Emirates
[123] Department of Physics, New York University, New York, NY, USA
[124] Ochanomizu University, Otsuka, Bunkyo-ku, Tokyo, Japan
[125] Ohio State University, Columbus, OH, USA
[126] Homer L. Dodge Department of Physics and Astronomy, University of Oklahoma, Norman, OK, USA
[127] Department of Physics, Oklahoma State University, Stillwater, OK, USA
[128] Palacký University, Joint Laboratory of Optics, Olomouc, Czech Republic
[129] Institute for Fundamental Science, University of Oregon, Eugene, OR, USA
[130] Graduate School of Science, Osaka University, Osaka, Japan
[131] Department of Physics, University of Oslo, Oslo, Norway
[132] Department of Physics, Oxford University, Oxford, UK
[133] LPNHE, Sorbonne Université, Université de Paris, CNRS/IN2P3, Paris, France
[134] Department of Physics, University of Pennsylvania, Philadelphia, PA, USA
[135] Konstantinov Nuclear Physics Institute of National Research Centre "Kurchatov Institute", PNPI, St. Petersburg, Russia
[136] Department of Physics and Astronomy, University of Pittsburgh, Pittsburgh, PA, USA
[137] [(a)]Laboratório de Instrumentação e Física Experimental de Partículas - LIP, Lisbon, Portugal; [(b)]Departamento de Física, Faculdade de Ciências, Universidade de Lisboa, Lisbon, Portugal; [(c)]Departamento de Física, Universidade de Coimbra, Coimbra, Portugal; [(d)]Centro de Física Nuclear da Universidade de Lisboa, Lisbon, Portugal; [(e)]Departamento de Física, Universidade do Minho, Braga, Portugal; [(f)]Departamento de Física Teórica y del Cosmos, Universidad de Granada, Granada, Spain; [(g)]Instituto Superior Técnico, Universidade de Lisboa, Lisbon, Portugal
[138] Institute of Physics of the Czech Academy of Sciences, Prague, Czech Republic
[139] Czech Technical University in Prague, Prague, Czech Republic
[140] Faculty of Mathematics and Physics, Charles University, Prague, Czech Republic
[141] Particle Physics Department, Rutherford Appleton Laboratory, Didcot, UK
[142] IRFU, CEA, Université Paris-Saclay, Gif-sur-Yvette, France
[143] Santa Cruz Institute for Particle Physics, University of California Santa Cruz, Santa Cruz, CA, USA
[144] [(a)]Departamento de Física, Pontificia Universidad Católica de Chile, Santiago, Chile; [(b)]Millennium Institute for Subatomic Physics at High Energy Frontier (SAPHIR), Santiago, Chile; [(c)]Instituto de Investigación Multidisciplinario en Ciencia y Tecnología y Departamento de Física, Universidad de La Serena, La Serena, Chile; [(d)]Universidad Andres Bello, Department of Physics, Santiago, Chile; [(e)]Instituto de Alta Investigación, Universidad de Tarapacá, Arica, Chile; [(f)]Departamento de Física, Universidad Técnica Federico Santa María, Valparaiso, Chile
[145] Department of Physics, University of Washington, Seattle, WA, USA
[146] Department of Physics and Astronomy, University of Sheffield, Sheffield, UK
[147] Department of Physics, Shinshu University, Nagano, Japan
[148] Department Physik, Universität Siegen, Siegen, Germany
[149] Department of Physics, Simon Fraser University, Burnaby, BC, Canada
[150] SLAC National Accelerator Laboratory, Stanford, CA, USA
[151] Department of Physics, Royal Institute of Technology, Stockholm, Sweden
[152] Departments of Physics and Astronomy, Stony Brook University, Stony Brook, NY, USA
[153] Department of Physics and Astronomy, University of Sussex, Brighton, UK
[154] School of Physics, University of Sydney, Sydney, Australia
[155] Institute of Physics, Academia Sinica, Taipei, Taiwan
[156] [(a)]E. Andronikashvili Institute of Physics, Iv. Javakhishvili Tbilisi State University, Tbilisi, Georgia; [(b)]High Energy Physics Institute, Tbilisi State University, Tbilisi, Georgia
[157] Department of Physics, Technion, Israel Institute of Technology, Haifa, Israel

[158] Raymond and Beverly Sackler School of Physics and Astronomy, Tel Aviv University, Tel Aviv, Israel
[159] Department of Physics, Aristotle University of Thessaloniki, Thessaloniki, Greece
[160] International Center for Elementary Particle Physics and Department of Physics, University of Tokyo, Tokyo, Japan
[161] Department of Physics, Tokyo Institute of Technology, Tokyo, Japan
[162] Tomsk State University, Tomsk, Russia
[163] Department of Physics, University of Toronto, Toronto, ON, Canada
[164] [(a)]TRIUMF, Vancouver, BC, Canada; [(b)]Department of Physics and Astronomy, York University, Toronto, ON, Canada
[165] Division of Physics and Tomonaga Center for the History of the Universe, Faculty of Pure and Applied Sciences, University of Tsukuba, Tsukuba, Japan
[166] Department of Physics and Astronomy, Tufts University, Medford, MA, USA
[167] Department of Physics and Astronomy, University of California Irvine, Irvine, CA, USA
[168] Department of Physics and Astronomy, University of Uppsala, Uppsala, Sweden
[169] Department of Physics, University of Illinois, Urbana, IL, USA
[170] Instituto de Física Corpuscular (IFIC), Centro Mixto Universidad de Valencia-CSIC, Valencia, Spain
[171] Department of Physics, University of British Columbia, Vancouver, BC, Canada
[172] Department of Physics and Astronomy, University of Victoria, Victoria, BC, Canada
[173] Fakultät für Physik und Astronomie, Julius-Maximilians-Universität Würzburg, Würzburg, Germany
[174] Department of Physics, University of Warwick, Coventry, UK
[175] Waseda University, Tokyo, Japan
[176] Department of Particle Physics and Astrophysics, Weizmann Institute of Science, Rehovot, Israel
[177] Department of Physics, University of Wisconsin, Madison, WI, USA
[178] Fakultät für Mathematik und Naturwissenschaften, Fachgruppe Physik, Bergische Universität Wuppertal, Wuppertal, Germany
[179] Department of Physics, Yale University, New Haven, CT, USA

[a] Also at Borough of Manhattan Community College, City University of New York, New York, NY, USA
[b] Also at Center for High Energy Physics, Peking University, China
[c] Also at Centro Studi e Ricerche Enrico Fermi, Fermi, Italy
[d] Also at CERN, Geneva, Switzerland
[e] Also at Département de Physique Nucléaire et Corpusculaire, Université de Genève, Geneva, Switzerland
[f] Also at Departament de Fisica de la Universitat Autonoma de Barcelona, Barcelona, Spain
[g] Also at Department of Financial and Management Engineering, University of the Aegean, Chios, Greece
[h] Also at Department of Physics and Astronomy, Michigan State University, East Lansing, MI, USA
[i] Also at Department of Physics and Astronomy, University of Louisville, Louisville, KY, USA
[j] Also at Department of Physics, Ben Gurion University of the Negev, Beer Sheva, Israel
[k] Also at Department of Physics, California State University, East Bay, Long Beach, USA
[l] Also at Department of Physics, California State University, Sacramento, USA
[m] Also at Department of Physics, King's College London, London, UK
[n] Also at Department of Physics, St. Petersburg State Polytechnical University, St. Petersburg, Russia
[o] Also at Department of Physics, University of Fribourg, Fribourg, Switzerland
[p] Also at Faculty of Physics, M.V. Lomonosov Moscow State University, Moscow, Russia
[q] Also at Graduate School of Science, Osaka University, Osaka, Japan
[r] Also at Hellenic Open University, Patras, Greece
[s] Also at Institucio Catalana de Recerca i Estudis Avancats, ICREA, Barcelona, Spain
[t] Also at Institut für Experimentalphysik, Universität Hamburg, Hamburg, Germany
[u] Also at Institute of Particle Physics (IPP), Victoria, Canada
[v] Also at Institute of Theoretical Physics, Ilia State University, Tbilisi, Georgia
[w] Also at Instituto de Fisica Teorica, IFT-UAM/CSIC, Madrid, Spain
[x] Also at Joint Institute for Nuclear Research, Dubna, Russia
[y] Also at Moscow Institute of Physics and Technology State University, Dolgoprudny, Russia
[z] Also at National Research Nuclear University MEPhI, Moscow, Russia
[aa] Also at Physics Department, An-Najah National University, Nablus, Palestine
[ab] Also at Physikalisches Institut, Albert-Ludwigs-Universität Freiburg, Freiburg, Germany

[ac] Also at The City College of New York, New York, NY, USA
[ad] Also at TRIUMF, Vancouver, BC, Canada
[ae] Also at Universita di Napoli Parthenope, Napoli, Italy
[af] Also at University of Chinese Academy of Sciences (UCAS), Beijing, China
[ag] Also at Yeditepe University, Physics Department, Istanbul, Turkey
* Deceased